universität wien

MASTERARBEIT / MASTER'S THESIS

Titel der Masterarbeit / Title of the Master's thesis

Planktic Foraminifera Stratigraphy along the Oceanic Anoxic Event II of the Tunisian Tethys

verfasst von / submitted by

Theobald Hazod, BSc

angestrebter akademischer Grad / in partial fulfillment of the requirements for the degree of

Master of Science (MSc)

Wien, 2023 / Vienna, 2023

Studienkennzahl lt. Studienblatt / degree programme code as it appears on the student record sheet:	UA 066 815
Studienrichtung lt. Studienblatt / degree programme as it appears on the student record sheet:	Masterstudium Erdwissenschaften
Betreut von / Supervisor	Univ.-Prof. Dr. Michael Wagreich

Acknowledgements

I would like to express my sincere gratitude to my supervisor Prof. Dr. Michael Wagreich, for his continuous support and help throughout the time working on this thesis. Furthermore, I would like to thank Dr. Benjamin Sames, who granted me access to the Scanning Electron Microscope, helped me greatly with its usage and gave me important insights in imaging of microfossils and beyond. Thanks to Sabine Hruby-Nichtenberger for the help in the laboratory and use of the sample splitter. Also, thanks to my workplace colleagues Christoph, Lukas, Sonja for their moral support, coffee breaks and delightful keyboard noises. Finally, I would like to thank my family.

Abbreviations

BF	Benthic Foraminifera
C/T	Cenomanian/Turonian
Fm	Formation
FO	First Occurrence
HST	Highstand Systems Tract
LO	Last Occurrence
OAE	Oceanic Anoxic Event
OK	Oued Kharroub
OMZ	Oxygen Minimum Zone
OM	Organic Matter
PCE	Plenus Cold Event
P-CIE	Plenus Carbon Isotope Excursion
PF	Planktic Foraminifera
SEM	Scanning Electron Microscope
TOC	Total Organic Carbon
TST	Transgressive Systems Tract
WIS	Western Interior Seaway

Abstract

Northern-Central Tunisia is well known for its Upper Cretaceous Tethyan black shale deposits. They constitute an important part of the research on Cretaceous stratigraphy and Oceanic Anoxic Events in particular. The Bahloul Formation of Tunisia comprises deep water deposits rich in organic matter, that span over the Cenomanian-Turonian boundary and the Oceanic Anoxic Event 2 (CTBE). Black shale samples from a ~38m thick section in Oued Kharroub (northern-central Tunisia) have been studied for their microfossil content, focusing on planktic foraminifera, in order to obtain a biostratigraphical zonation of the section and thus the OAE-2 event at the southern Tethyan margin. Moreover, the characteristics of the assemblages were studied in detail, to gain insight into paleoenvironmental conditions and paleoecological dynamics that prevailed at this specific locality. The outcrop yielded 12 samples containing microfossils, that have been studied, counted and classified. In addition to the faunal study, geochemical data, including carbonate content ($CaCO_3$), total organic carbon content (TOC), and Stable Carbon Isotope data ($\delta^{13}C_{carb}$), have been used to further enhance stratigraphic and paleoenvironmental understanding of the Oued Kharroub section.

Three planktic foraminifera biozones and several secondary associated bioevents could be identified. The base of the section, including the first 2-3 meters represents the *Rotalipora cushmani* zone (*Dicarinella algeriana* subzone). The assemblages in this zone reflect relatively stable environmental conditions, with at least partly oxygenated bottom waters and abundant and diverse large keeled planktic foraminifera (*Rotalipora, Praeglobotruncana*). The LO of *R. cushmani*, along with the extinction of the genus *Rotalipora* is reported at -0.70, just below the first $\delta^{13}C_{carb}$ - peak. It marks the beginning of the faunal turnover and the *W. archaeocretacea* zone, which spans over ~20m in this section. With the extinction of *Rotalipora*, a crisis for keeled, deep dwelling foraminifera could be observed, that persists until the top of the section. One minor return of keeled taxa is reported in the middle of the *W. archaeocretacea* zone just above a ~3m silica interval with an acme of radiolaria. Here, transitional forms between *H. praehelvetica* and *H. helvetica* occur, as well as large *Dicarinella*. This has been interpreted as a temporary upward movement of the oxygen minimum zone, which allowed larger keeled species to exist. A prominent development recorded for the OAE-2 section at Oued Kharroub is the proliferation of

Heterohelix (*Heterohelix* shift). Generally, the planktic foraminifera assemblages of the *W. archaeocretacea* zone in this section are clearly dominated by opportunists and surface dwellers. *Heterohelix*, *Whiteinella* and *Muricohedbergella* make out the vast majority of the PF assemblages. The FO of *H. helvetica* in this section coincides with a slight return of keeled genera (*Dicarinella*, *Marginotruncana*), the marker species however remains very rare. The paleoenvironmental situation during the OAE-2 at the OK section can be defined as highly stressed, with continuous oxygen deficient waters, which preclude the proliferation or even at times rare presence of larger complex morphotypes within the planktic foraminifera genera. The stable isotope excursion lasts from the LO of *R. cushmani* until slightly below the FO of *H. helvetica*, which suggests a record of a little under 20 meters representing the Oceanic Anoxic Event 2. TOC values are elevated with a delay compared to the isotope excursion. They correlate with a general decrease of microfossils per gram sediment and a reduction in carbonate in the respective interval especially in the middle part of the *W. archaeocreatea* zone. Benthic foraminifera remain rare and low in diversity throughout the section, although small infaunal forms become more frequent in the upper part of the section (upper *W. archaeocretacea* zone and *H. helvetica* zone). The faunal assemblages remaining OAE-typical until the top of the section, where a *Guembelitria cenomana* acme and highest occurrence of *Heterohelix* occur, raise questions about the local environmental conditions after the OAE-2 and the stratigraphical position of the top of the section.

Zusammenfassung

Der Norden Tunesiens ist weithin bekannt für Tethys-Ablagerungen aus der Oberkreide. Die Schwarzschiefer (Black Shale) der Cenomanium-Turonium-Grenze stellen einen wichtigen Teil der Kreide-Stratigraphie Forschung sowie der Erforschung von globalen Sauerstoffkrisen im Ozean (Oceanic Anoxic Events) dar. Die Bahloul Formation in Tunesien ist aufgebaut aus Tiefwasserablagerungen rund um das OAE-2, welche reich an organischem Material sind. Im Rahmen dieser Arbeit wurden Schwarzschiefer - Proben aus einem ~39m mächtigen Aufschluss in Oued Kharroub (Nördl. Tunesien) auf ihren Gehalt an Mikrofossilien analysiert, wobei der Fokus auf planktischen Foraminiferen lag. Das Ziel dieser Arbeit war es, eine biostratigraphische Analyse, eine Biozonierung des Profils und somit des OAE-2 durchzuführen. Die Charakteristika der verschiedenen Fossil-Vergemeinschaftungen wurden im Detail analysiert, um Informationen über paläoökologische Dynamiken, sowie Paläoumweltbedingungen zu erlangen. 12 Proben wurden analysiert, gezählt (>300 Individuen), und klassifiziert. Zusätzlich zu der Studie der Mikrofossilien wurden geochemische Parameter untersucht, um ein erweitertes Verständnis des OAE-2 in dieser Lokalität zu erlangen. Diese umfassten den Karbonat-Gehalt, den Gehalt an organischem Kohlenstoff (Total Organic Carbon) sowie stabile Kohlenstoffisotopen Verhältnisse ($\delta^{13}C_{carb}$).

Drei planktische Foraminiferen Zonen und einige sekundäre Bio-Events wurden entlang des OK-Profils identifiziert. Die Basis des Profils, die ersten 2-3 m, repräsentieren die *Rotalipora cushmani* Zone (*Dicainella algeriana* Subzone). Die Mikrofossilien-Vergesellschaftungen reflektieren stabile Umweltbedingungen, mit sauerstoffreichem tieferem Wasser und einer hohen Diversität an großen, gekielten planktischen Foraminiferen (*Rotalipora, Praeglobotruncana*). Das letzte Vorkommen von *R. cushmani* geht einher mit dem Aussterben des Genus *Rotalipora* bei Meter -0.70, etwas unterhalb des ersten $\delta^{13}C_{carb}$ - Peaks.

Dies markiert den Beginn der OAE-2 und einen abrupten Wandel in der Verteilung planktischer Foraminiferen Spezies (*W. archaeocretacea* Zone). Das Aussterben von *Rotalipora* leitet eine Krise der gekielten Morphotypen unter den planktischen Foraminiferen ein, die, mit temporären Ausnahmen, bis zum oberen Ende des Profils anhält. Eine dieser kurzen Phasen mit erhöhtem Auftreten von K-Strategen ist in der Mitte der *W.*

archaeocretacea Zone, direkt über einem ~3m Silica-Intervall mit einem Höhepunkt an Radiolarien-Vorkommen gelegen, und eine zweite liegt am Beginn der *H. helvetica* Zone. Die Erstere sieht Mischformen von *H. praehelvetica* und *H. helvetica,* sowie große Formen des Genus *Dicarinella*. Die Vergesellschaftungen von planktischen Foraminiferen entlang des Profils sind durchwegs dominiert von Opportunisten und Bewohnern des oberflächennahen Teils der Wassersäule. Die häufigsten Genera sind *Heterohelix*, *Whiteinella* und *Muricohedbergella*. Der immense Anstieg im prozentuellen Anteil von *Heterohelix* im Vergleich zu den anderen PF-Spezies (*Heterohelix* shift) ist ein wichtiges Bio-Event dieses Profils. Das erste Vorkommen von *H. helvetica* geht mit dem zweiten Radiolaria Höhepunkt sowie dem zweiten Wiederauftreten von gekielten Formen (*Dicarinella, Marginotruncana*) einher. *H. helvetica* selbst ist hier jedoch äußerst rar und konnte in der obersten Probe des Profils nicht gefunden werden.

Die Umweltbedingungen während des OAE-2 in Oued Kharroub können als hoch angespannt in Bezug auf Sauerstoffverfügbarkeit und Eutrophie bezeichnet werden. Bedingungen, die es großen gekielten, komplexen Morphotypen, mit den genannten Ausnahmen, nicht erlauben, sich auszubreiten. Die stabile Kohlenstoff-Isotopen Exkursion reicht vom letzten Auftreten von *R. cushmani* bis direkt unter dem ersten Auftreten von *H. helvetica*. Dies ergibt in etwa 20m des Profils, welche das OAE-2 repräsentieren. TOC-Werte kulminieren in einem Plateau, welches dem Isotopen-Signal gegenüber verspätet auftritt (9.50-20.00). Kalziumkarbonat-Werte sind reduziert im mittleren Teil des Profils und korrelieren mit der Isotopenkurve und dem Rückgang der Anzahl an Mikrofossilien pro Gramm Sediment. Benthische Foraminiferen sind durchwegs selten und zeigen geringe Diversität, wobei kleine infaunale Formen zum oberen Ende des Profils hin häufiger werden. Generell bleiben die Faunen-Vergesellschaftungen bis zum oberen Ende des Profils OAE-typisch. Dort findet sich auch ein Höhepunkt des Vorkommens von *Guembelitria,* sowie die größten Exemplare von *Heterohelix*. Dies wirft Fragen bezüglich der Umweltbedingungen, sowie der stratigraphischen Position in dieser obersten Probe auf.

TABLE OF CONTENTS

1. INTRODUCTION

Oceanic Anoxic Events (OAEs; Schlanger & Jenkyns, 1976) have, eversince the term was first coined by Schlanger & Jenkyns in 1976, been an important part of Cretaeous geological research. They were then described as "*the result of widespread and thick O_2-minimum zones in the world ocean*", meaning that these anoxic conditions transcended local phenomena, related to specific basin topographies (Schlanger & Jenkyns, 1976). OAEs are associated with a significant, globally synchronous, accumulation of organic matter (OM) on the ocean floor, resulting in widespread occurrences of dark-coloured calcareous marls and shales (Black shales, Wignall, 1994) with a total organic content (TOC) of >1% up to 30% (Khain & Polykova, 2010). Black shales constitute the bulk source of available hydrocarbons (Wignall, 1994; Soua, 2016) of the world and therefore are of enormous economic value in petroleum exploration, which thus, naturally, has been strongly interwoven with the scientific work on these sediments in the last century. Their scientific significance extends over different fields in geosciences like sedimentology, paleoceanography, paleoecology and stratigraphy among others (Wignall, 1994).

The Cretaceous is well known for its greenhouse climate, with high atmospheric CO_2-levels and a major transgression, that reached its peak in the lower Turonian (Zhang et al. 2008). Simultaneous intense endogenic activity, resulting in submarine volcanism on a massive scale is likely to be a major cause for these conditions (see Chapter 3) (Zhang et al. 2008, Petrizzo et al. 2022, Jenkyns et al. 2017). Global warm-periods and transgressions constitute crucial preconditions for the development of widespread anoxic conditions in the open ocean (Parrish, 1998) during the Cretaceous. Although OAEs and their associated organic rich sediments are known from earlier geological periods as well, the Cretaceous period with its exceptional climatic and geological features has yielded several of the most prominent and most studied (Khain & Polyakova, 2010). Various black shale horizons are known from the Berriasian to the Turonian. The most prominent ones are the OAE 1 in the Aptian-Albian (OAE1a, 1b, 1c, (Schlanger & Jenkyns, 1976), Selli-Event (Coccioni, 1989)) and the OAE

2 just below the Cenomanian-Turonian boundary (C/T-boundary event (Schlanger & Jenkyns, 1976; Arthur et al. 1990), Bonarelli-event (Schlanger et al. 1987)). These events constitute major perturbations in the oceanic realm and coincide with geochemical anomalies as well as faunal turnovers and extinction events among marine organisms (Coccioni & Luciani, 2004; Caron et al. 2006). An estimated 20% of marine organisms became extinct during the OAE-2, which is considered the most severe of OAEs in the Cretaceous (Soua et al, 2022; Takashima et al. 2009).

Considering the assemblages found in the deposits associated with OAEs, planktic organisms are of great significance and therefore constitute a viable point of interest when studying them (Coccioni & Luciani, 2004). This is especially due to the highly reduced presence of benthos in anoxic bottom waters. Among the most abundant and stratigraphically useful planktic organisms in the Cretaceous and beyond are planktic foraminifera (BouDhager-Fadhel, 2015). From the Late Triassic to Early Jurassic, when foraminifera first adopted a planktic lifestyle, up to today, they constitute a major group of plankton in the modern oceans (Boudagher-Fadel 2015). Their high diversity and abundance, the fact that they are, due to their planktic lifestyle, not regionally restricted, as well as their relatively fast evolutionary rates make them ideal biostratigraphic markers and crucial for global-scale zonations (Jones, 2014). Planktic foraminifera are highly sensitive to changes in water chemistry and temperature, as well as trophic structure and density gradient (Coccioni & Luciani, 2004). Thus, their assemblages are highly controlled by these factors, which makes them viable indicators for oceanic environmental conditions (Reolid, et al. 2015).

The respective turnovers and bioevents at the C/T-boundary specifically include the temporary disappearance of keeled taxa and the extinction of the genus *Rotalipora* Brotzen, 1942, including the marker species *Rotalipora cushmani* (Morrow, 1934) as well as the proliferation of *Heterohelix* Ehrenberg, 1843 (*Heterohelix* shift), and other opportunistic genera and species (e.g. *Guembelitria* Cushman, 1940, *Schackoina* Thalmann, 1932), the first occurrence of *Helvetoglobotruncana helvetica* Bolli, 1945 in the Lower Turonian, the eventual return of other larger, keeled taxa like *Marginotruncana* Hofker, 1956 (Hart, 1999; Premoli Silva & Verga 2004, i.a.). Alongside the faunal changes in the geological record, these events are also characterized by certain geochemical properties. For one, the TOC of the OAE-type sediments (Black Shales) is expected to be significantly higher than in normal

pelagic shales like calcareous marls, while at the same time $CaCO_3$-content is reduced. TOC values can vary significantly in different OAE sites depending on the respective locality (Soua et al. 2011). Furthermore, these events show a positive excursion of $\delta^{13}C$ (referring the ratio of ^{13}C to ^{12}C isotopes), that is associated with enhanced burial OM, which is richer in the light ^{12}C isotope (Soua et al. 2011). Whether the causes of this enhanced burial of OM are to be seen in the higher productivity, or the increased preservation of OM, is still highly debated (See Chapter 3). The duration of the $\delta^{13}C$-excursion marks the beginning and end of the OAE-2. Its total duration is still a matter of debate and ranges from about ~950 kyr (Petrizzo et al. 2022) to ~500kyr (Soua et al. 2022).
During the OAE-2, the prevailing greenhouse conditions are interrupted by a short cold-temperature-period, called the Plenus Cold event (Petrizzo et al. 2021), which was first recognized by Gale & Christensen in 1996 (Jenkyns et al. 2017). This event is thought to have occurred as a negative feedback effect of the climate as pCO2-levels were lowered significantly by the intense burial of OM during the OAE-2 (Petrizzo et al. 2021). It occurred between the peaks 'a' and 'b' of the $\delta^{13}C$-excursion of the OAE-2 (O'Connor et al. 2020) and is characterized by migration of boreal macro-fauna into lower latitudes as well as a trough in the $\delta^{13}C$ excursion and two positive $\delta^{18}O$ shifts (Petrizzo et al. 2021).

Among other important localities of the Cenomanian-Turonian boundary and the Oceanic Anoxic Event II (OAE 2), like the type section in Pueblo, Colorado in the Western Interior Seaway (WIS), low-latitude localities of the Tethys Ocean have been important in the understanding of this event. A lot of work has been done on C/T-deposits and the OAE-2 of northern Africa, especially eastern Maghreb area in the last decades (Caron et al. 2006, Lüning et al. 2004, Ben Fadhel et al, 2015, Reolid et al. 2015, Soua, 2011, Robaszynski et al. 2010; Soua et al. 2009, 2011, 2013, 2022; Zagrarni et al. 2008; Nederbragt & Fiorentino, 1999 i.a.). The basis for this study has been pelagic C/T deposits from Oued Kharroub, a locality in northern central Tunisia, which represents the southern margin of the Upper Cretaceous western Tethys Ocean.

The aim of this master's thesis is to achieve a detailed and coherent biostratigraphy of a ~39m thick section in central northern Tunisia based on planktic foraminifera. Counting and classification of planktic foraminifera shall yield an image of the faunal turnover that took place during the event. In addition to the biostratigraphic data obtained from microfossils,

relevant geochemical properties (total organic carbon, stable carbon isotope and carbonate content) of the section have been obtained and shall be discussed and analyzed in regard of their contained stratigraphic and paleoenvironmental information. Finally, the combination of biostratigraphic, micropaleontological and geochemical data shall yield insight to the conditions that prevailed during this environmental crisis at this locality

2. PLANKTIC FORAMINIFERA STRATIGRAPHY

2.1 Historical Background

The first documentation of foraminifera dates back to Herodot in the fifth century BC, who mentioned the components of the rocks comprising the Pyramids of Giza (BouDhager-Fadhel, 2015). Later in the first century BC, Strabo took up the idea, that these large benthic foraminifera (*Nummulites),* were lentils, left behind by the workers that have built the pyramids (Jones, 2014). Most foraminifera, however, especially planktic forms, are not visible or recognizable with the naked eye. Accounts of description of smaller foraminifera began about two millennia later, in the 16th and 17th century A.D., when the invention of microscope and its use as a tool for studying small structures made the study of microfossils such as foraminifera possible. They were initially placed within Molluscs in the Class Cephalopoda, due to their superficial resemblance in the coiling shape (Haq, Boersma 1978). In 1825, Alcide D'Orbigny recognized the difference in the septa of some of these minute forms compared to the other species in this genus and introduced the name Foraminifera (Carpenter 1862). The name is derived from Greek and Latin respectively and basically means "bearing holes", referring to the pores that cover their tests (BouDagher-Fadel 2015). In 1846, D'Orbigny published a first classification of foraminifera, based on morphology. D'Orbigny also made important stratigraphic contributions in the 1840s, separating the Cretaceous into five "étages": Neocomian, Aptian, Albian, Turonian and Senonian on the basis of fossils. A division which he later updated by introducing the Cenomanian and the Urgonian. In today's division of the Cretaceous the Barremian has replaced the Urgonian and the Senonian has been further divided into Coniacian, Santonian, Campian and Maastrichtian (Gale et al. 2020).

The extensive industrial search for oil in the early to mid-20th century made use of microfossils, especially foraminifera, and thus stimulated the scientific progress in this field (Haq & Boersma 1978). First applications of foraminifera for stratigraphic purposes are known already from the late 19th century. However, the importance of planktic foraminifera

in that matter was not recognized until the 1930s, when first biostratigraphic zonation schemes of the Late Cretaceous and Paleogene based on planktic foraminifera were done. Subbotina published the first PF-zonation scheme for Caucasus sections in the 1950s (Haq & Boersma, 1978). Simultaneously, planktic foraminiferal biostratigraphy was done in Trinidad by Hans Bolli (1957), which served as an important basis for later work in the field (Haq & Boersma, 1978). A globally correlated planktic foraminifera zonation for the Cretaceous and Cenozoic that also included higher latitude sites was achieved in the following years. Not least through the help of the DSDP (Deep Sea Drilling Project) that started in the 1960s (Bolli, Saunders et al. 1989). The global planktic foraminifer biozonation of the Cretaceous, specifically a division into 19 zones from the Aptian to the Maastrichtian, proposed by Bolli (1966), has not changed significantly since then (Bolli et al. 1989). Robaszynski & Caron (1976, 1984) provided a Cretaceous planktic foraminifera atlas including detailed description of index species. Bolli et al. (1989) proposed a zonation scheme for the Cretaceous from the Hauterivian to the Maastrichtian including 28 zones, which are correlated to ammonite-zones. Though phylogenetics within Foraminifera are still highly debated, biostratigraphic marker species of the Cretaceous used by Bolli in 1966 are still widely agreed on (Bolli et al. 1989). Further work on planktic foraminifera zonations, including their correlation with ammonite zones, has been done by Robaszynski & Caron (1995). This work has been an important basis for further zonation schemes, including the one used in this study (Premoli-Silva & Verga, 2004; Mikrotax.org).

Projects like the DSDP, as well as subsequent projects like the ODP (Ocean Drilling Project), and the CLIMAP project, proved to be of great value for the globalization of zones and combination of tropical and boreal zonation schemes. They also led to the first discovery of black shales and the subsequent work on Oceanic Anoxic Events (Schlanger & Jenkyns, 1976), where planktic foraminifera have proven to be viable tools for biostratigraphy. Apart from deep sea borehole samples, locations in the Tethys (Northern Africa, Tibet, Europe, Middle East) as well as the WIS (C/T type locality, Pueblo, USA) have been important for the biostratigraphic work on OAEs in the Cretaceous. The C/T-Boundary and OAE-2 in particular, a lot of biostratigraphical work has been done in low-latitude Tethys localities in the last decades (see introduction). These are mostly based on planktic foraminifera, radiolaria and nannofossils combined with geochemical and stable isotope data.

Upper Cretaceous stratigraphy is today defined on the basis of ammonoids, inoceramid bivalves, planktic foraminifers, crinoids and magnetic polarity chrons. The C/T-boundary in particular, previously defined by ammonite occurrence, is now defined by the FO of the ammonite *Watinoceras devonense*, with the GSSP in Pueblo, USA. The age of the boundary is defined by $^{40}Ar/^{39}Ar$ at 94Ma (Gale et al., 2020). Global correlations of OAE-2 (C/T-boundary) sections including isotope data and bioevents are still very much in progress and continuously being reevaluated (Falzoni et al. 2018). Planktic foraminifera play a vital role in this endeavor. Issues concerning diachrony of bioevents, classification schemes of planktic foraminifera and differing approaches in sample sizing i.a. remain matters of debate, and further work in the field is surely needed.

2.2 Planktic Foraminifera in the Cretaceous

The oldest foraminifera thought to have had a planktic mode of living was *Sphaerogerina* Korchagin & Kutznezova, 2003 from the Late Triassic period, which did not survive the extinction event at the end of the Triassic. The second planktic foraminifer group to have evolved from their benthic relatives were *Conoglobigerina* Morozova, 1961 in the Mid Jurassic (Bajocian) (BouDhager-Fadel 1997, 2015). The evolution from benthic to meroplanktonic, an intermediate step towards the evolution to a fully planktic lifestyle, may likely be linked to widespread anoxia, as well as sea regression (Haq & Boersma, 1998). Conditions which appeared similarly in the Late Triassic as well as the Mid-Jurassic and constituted an advantage for a planktic mode of living. In the Jurassic, planktic foraminifera are still relatively rare, compared to their benthic relatives (Haq & Boersma, 1998).

By the time of the Early Cretaceous, planktic foraminifera experienced a major radiation and diversification. Praehedbergellidae, a descendant family of the Jurassic Conoglobigerinidae that appears in the Valanginian, are the first geographically widespread planktic foraminifera family. They eventually give rise to Schackoinidae and Hedbergellidae. All Cretaceous trochospiral taxa are descendant from Hedbergellids (Bou-Dhager Fadel, 2015). A first major radiation is incised by the Oceanic Anoxic Event 1a in the Aptian, a significant extinction event for planktic foraminifera, where a majority of species (~82%) become extinct (Bou-Dhager Fadel 2015). From the Albian onwards, another radiation and diversification of planktic foraminifera occurs. The bi- and multiserial Heterohelicida,

including the biserial Heterohelicidae and the triserial Guembelitridae appear. Within trochospiral families, the first keeled forms occur in the Albian (Genus *Rotalipora*; Haq & Boersma, 1998). The OAE-2 at the Cenomanian-Turonian boundary again leads to a major reduction of planktic foraminifera diversity with ~47% of the species going extinct (Bou-Dhager Fadel, 2015). Keeled morphotypes experience a major recession with rotaliporids going extinct just below the C/T boundary. Simple morphotypes, species living in shallow water and ones thriving in eutrophic conditions dominate the assemblages during the oxygen-crisis that characterizes the OAE-2. After re-stabilisation of the climate and recovery of the diversity of planktic foraminifera in the Turonian, the continuous radiation and diversification with the mentioned incisions eventually led to a peak in diversity in the Maastrichtian at the end of the Cretaceous (Premoli Silva & Verga 2004). At the Cretaceous-Paleogene boundary at 66 Ma, most planktic foraminifera species (95%) go extinct. After this dramatic incision, with only few planktic foraminifera species surviving (including *Guembelitria* and Hedbergellids) they recovered during the Paleocene, and subsequently constituted, throughout the Cenozoic and until the present day, a major component of oceanic plankton, from tropical to boreal realms (BouDhager-Fadhel, 2015).

Considering the timeframe of the OAE-2, some genera of planktic foraminifera are typical. OAE deposits are typically characterized by a dominance of species that could adapt to stressed and oxygen deficient environments and those who dwelled near the water surface. Around the C/T-boundary, typical planktic foraminifera genera included *Muricohedbergella*, *Macroglobigerinelloides*, *Praeglobotruncana*, *Dicarinella*, *Rotalipora* (before their extinction just below the C/T-boundary) and *Whiteinella.* Furthermore, *Heterohelix* is known to thrive in stressed conditions and therefore is found in high numbers in upper Cenomanian / lower Turonian open marine deposits. Towards the end of the event, the keeled *Marginotruncana* began to diversify and proliferate.

3. CRETACEOUS OCEANIC ANOXIC EVENTS

3.1 The Upper Cretaceous World

The Cretaceous period is generally known to exhibit two major exceptional features: (1) exceptionally warm climate and (2) high sea levels. The Cretaceous' exceptional greenhouse climate and high CO_2-levels were, as is widely agreed on, evoked by intense volcanic activity following the breakup of Gondwana (Zhang et al. 2008). Extensive submarine basalt outflow led to the formation of vast submarine igneous provinces. Oceanic crust in these areas is several times thicker than average, and in some areas formed oceanic plateaus (Ontong Java Plateau, Manihiki, Kerguelen, and Caribbean) (Zhang et al. 2008). Furthermore, the ocean spreading rate in the mid-Cretaceous was much higher than it is known today. The opening of the Atlantic Ocean among other ocean spreading events, together with submarine volcanism led to the reduction of ocean basin volume, which in turn led to a massive eustatic sea level rise (Zhang et al. 2008). With no ice stored on the poles, this major transgressive phase reached its estimated peak at around 240-250 m (Haq, 2014; Lüning et al. 2004) to 300 m (Keller, 2008) above modern sea level[1], at the beginning of the Turonian stage. Endogenic activity in the Cretaceous is thought to have had its peak around the same time, between 120-80 Ma (Zhang et al. 2008). This intense volcanic activity was naturally accompanied by high emissions of CO_2, a strong greenhouse gas. Atmospheric CO_2-levels in the mid-Cretaceous reached their peak at about 9 times higher than modern (pre-industrial) levels according to Zhang et al. (2008) and 4 times higher according to Gebhart et a. (2010). The flooding of vast areas of continents, and development of large shelf areas and large epicontinental seas around 300m deep, like the Western Interior Seaway (WIS) in North America or the Trans-Saharan seaway in Africa (see fig. 3) meant a much smaller total area of exposed landmass. That is to say a significant reduction of anorganic

[1] Estimates of the sea level values differ quite a lot between authors. The paleogeographic map given in this work (Fig.3) is based on sea level projections of only about 160m above today's levels.

weathering and reduction of areas inhabited by terrestrial plants, both being important CO_2 sinks (Zhang et al. 2008).

Furthermore, the flooding of land led to an increased input of terrestrial plant material into the ocean system, which is recorded in the isotopic signal of carbon atoms in organic rich layers of this period. This, as well as iron-rich hydrothermal fluids that occured at mid ocean ridges, constituted major nutrient sources in the oceans (Zhang et al. 2008). The high nutrient supply causing phytoplankton blooms and the high sea-surface temperature, which is estimated at around 36°C at low latitudes (Petrizzo et al. 2020) and 20°C or higher in polar regions (Ohkouchi et al. 2015) led to the widespread development of stagnant, oxygen deficient waters. Due to the climatic preconditions, the development of oceanic deficient zones or oceanic minimum zones (OMZ) spread beyond typical areas (e.g. upwelling areas) on a global scale.

3.2 OAEs and Black Shales

Tyson (1987) defined black shales as "dark-coloured, fine grained mudrocks having the sedimentological, palaeoecological and geochemical characteristics associated with deposition under oxygen-deficient or oxygen-free bottom waters." In the course of the DSDP (Deep Sea Drilling Project), in the early 1970s, organic rich carbonaceous sediments were found in the Pacific Ocean floor. Earlier interpretations of these sediments attributed them only to being local phenomena, resulting from structural-topographic isolation (Schlanger & Jenkyns 1976). Schlanger and Jenkyns proposed in 1976, that, as these sediments occur worldwide, they were to be interpreted as global events, in which the oxygen minimum zone in the ocean expanded vastly. They then coined the term Oceanic Anoxic Events (OAEs) as the cause of the globally spread occurrence of these organic rich sediments. By combining different DSDP data and also outcrop data, the conclusion arose, that two of these OAEs occurred in the Cretaceous period, one in the Aptian - Albian and the other one in the late Cenomanian and possibly overlapping the Cenomanian-Turonian boundary. In the following decades, (I)ODP-data, as well as outcrop data from the Tethys, have enabled to the discovery of more Cretaceous black shale deposits (Soua, 2016). A more detailed division for Cretaceous OAEs defines the Weissert Event (Valanginian), Faraoni Event (late

Hauterivian, OAE 1a / Selli Event (early Aptian), OAE 1b / Paquier Event (early Albian), OAE 1d Breistroffer Event (late Albian) and OAE 2 / Bonarelli Event (Cenomanian-Turonian boundary interval) (Soua, 2016).

The TOC content of black shales can vary significantly. Some black shales from DSDP sites show a TOC content of over 50% (Ohkouchi et al. 2015), while in some north African Tethys sites of the OAE-2, 2-13% are typical values for TOC content of black shales (Lüning et al. 2004). Black shales typically display a variation in $^{13}C/^{12}C$ ratio compared to other deep-sea sediments. This property is known to reflect the amount of dissolved CO_2 in the ocean. The relative enrichment in ^{13}C in black shales is thought to represent increased burial of the ^{13}C-depleted organic matter at the time (Ohkouchi et al. 2015). This signal can be used as detection of OAEs and stratigraphic correlation of Cretaceous sediments (Ohkouchi et al. 2015).

As stated in Tyson's definition, black shale deposition occurs in oxygen-deficient or oxygen-free bottom waters. Two hypotheses concerning black shale deposition and OAEs are prevalent in the literature today. One is stressing the importance of preservation and burial of organic matter, while the other focusses on the primary productivity as a main cause (Ohkouchi et al. 2015). Khain & Polyakova (2010) suggest a clear connection between oceanic anoxic events and times of increased endogenic activity, be it in the form of island-arc volcanism, LIPs or ocean spreading. The climatic developments in the Cretaceous associated with intense volcanism mentioned in chapter 3.1 surely provide a clear connection and the significance of it concerning environmental change at the time.

4. LOCATION AND GEOLOGICAL SETTING

4.1 Location

The studied section of this thesis at Oued Kharroub lies in northern Tunisia, some 100 kilometers southwest of the capital Tunis (Fig.1) within the northern folded part of the Tunisian Atlas. It constitutes a hill slope of inclined strata of pelagic sediments, namely calcareous marls and black shales with some chert layers in-between (Fig.2). The samples at the base lie on the horizontal part, marked with a "-", OK 0.00 lies at the toe of the slope and the majority of the samples lie on the slope. The section is part of the Bargou area, a known locality for CTBE- deposits in Tunisia.

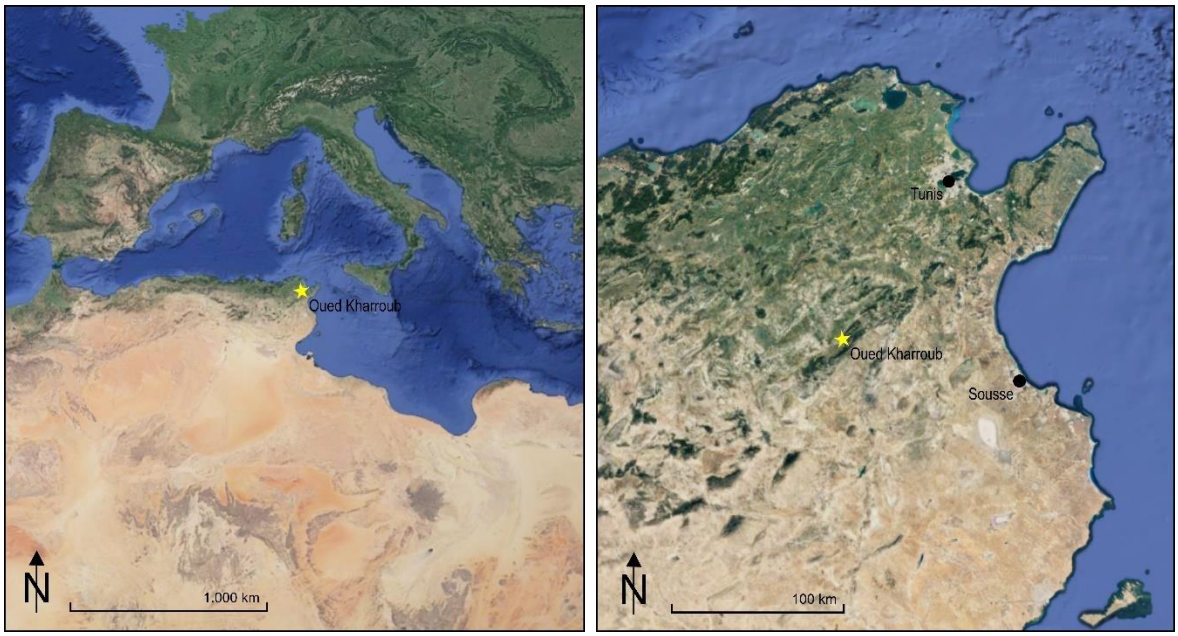

Figure 1 *Maps showing the location of Oued Kharroub in northern Tunisia. Scalebars: 1.000 km (left) and 100 km (right) Source: Google Earth (© Google 2022).*

4.2 Geology of Tunisia

Tunisia is located at the eastern edge of the Atlas Mountains, which stretch all across the northern Maghreb from Morocco to Tunisia. The Tunisian Atlas borders the Pelagian Block to the east, the Saharan Platform to the south and the Tellian Units in the Northwest (Bocalletti et al. 1989). The geological structure of Tunisia can be seen in a north-south divide, where Mesozoic and Cenozoic layers in the north are deformed by Alpine tectonic movements, and southern strata are thinner and less deformed. The tectonic activity in Tunisia, as in the whole of north Africa, was characterized by extension throughout the Mesozoic. This is in association with the opening of the Neotethys to the north and the opening of the southern/equatorial Atlantic to the west / south-west. (Soua et al. 2009). Two major Mesozoic rifting events are recorded in Tunisia. One Late Jurassic to early Aptian, and one from the late Aptian to the early Cenomanian (Lüning et al. 2005). They resulted in E-W trending and NW-SE trending half graben systems. In addition, diapiric movements of

Figure 2 *Outcrop at Oued Kharroub. (Photo by M. Wagreich)*

Triassic evaporites occurred from the Albian to the Eocene (Lüning et al. 2005). Both, the structure and thickness of half graben systems and diapir tectonics, have been the main controlling factors on the thickness of C/T-organic rich deposits in Tunisia (Soua 2016). The resulting regionally different tectonic environments led to significant variations in facies characteristics and thickness of the C/T-strata (Lüning et al. 2004). In the mid-Cretaceous, Tunisia generally was characterized by a northward dipping slope where facies differences range from terrestrial in the south, to bathyal in the north. South of the Tunisian Atlas, Cretaceous strata of the Saharan Platform are rather thin and barely affected by the named tectonic activities (Soua et al. 2009).

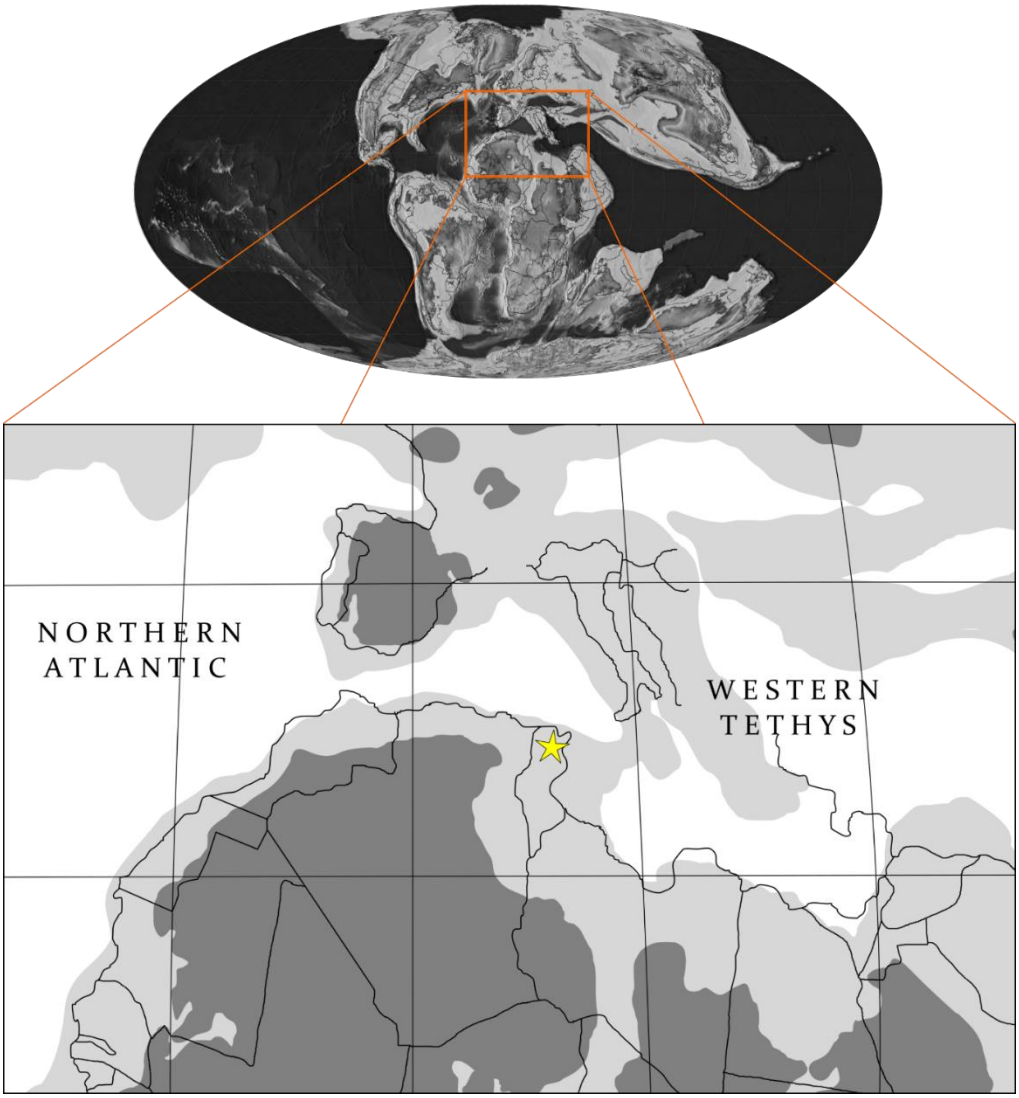

Figure 3 *Paleogeographic map, Early Turonian (91,1 Ma), redrawn after Scotese PALEOMAP PaleoAtlas (2014). Dark grey = landmass; light grey = shelf; white = deep sea. The two latitude lines represent 15° and 30° N respectively. Estimated sea level for this map is 160m above modern level. Yellow star = Location of Oued Kharroub.*

The organic-rich C/T-strata of Tunisia are grouped into the Bahloul Formation. The Bahloul Formation is made up of black and greyish limestones and calcareous marls and shales (black shales) with TOC values up to 13% (Lüning et al. 2004). They represent a large transgressive systems tract (TST). Eustatic sea level rise and subsidence had a higher rate than carbonate production, which led to platform drowning (Touir et al. 2017). It therefore represents a drowned carbonate platform with low carbonate production, a deep-water shelf lying on a northward dipping basement (Touir et al. 2017). The organic rich facies represent a depositional environment of intermediate water depth, where the OMZ impinged onto the southern Tethyan margin. The Bahloul Formation is subdivided into the organic-poor Bahloul and the organic-rich Bahloul. Out of the three different parts of the organic-rich Bahloul in Tunisia, the central-north region of onshore Tunisia is where the Bahloul Fm. is the largest and thickest (Lüning et al. 2004). It is usually a few tens of meters thick, although as mentioned above, the thickness varies significantly depending on the respective locality. The Bahloul Formation generally represents the late Cenomanian but can in some areas reach into the early Turonian. It overlies the Fahdène Formation and is overlain by the Annaba member of the Kef Formation in the north (Soua et al. 2009). The deposition of the Bahloul Formation is to be seen in the context of the structural features of the area, i.e. half-graben systems and associated subsidence and deformation through halotectonic movements, as well as the simultaneous global eustatic flooding event, that occurred at the time. During the deposition of the Bahloul Fm., the Tethys was connected to the Atlantic through the Trans-Sahararan Seaway. This is also still valid for the overlying Annaba Member (HST), which is constituted of hemipelagic marls and assigned to the lower Turonian (Zagrarni et al. 2008). The Annaba Member is followed by the Gattar Member (Zagrarni et al. 2008) southwards, which represents a northward dipping carbonate ramp (Touir et al. 2017).

4.3 Biostratigraphical Framework

The Bahloul Formation has been assigned a late Cenomanian to early Turonian age on account of ammonite biozones *Pseudaspidoceras pseudonodosoides* and *Watinoceras* sp. and *Fagesia* sp., respectively (Zagrarni et al. 2008). The lowest part of the Bahloul Fm. represents the uppermost part of the *Rotalipora cushmani* Zone (see fig.4). The onset of the OAE-2, which is accompanied by a positive $\delta^{13}C$ excursion, is typically marked with the extinction of the genus *Rotalipora*. The LO of *R. cushmani* is reported globally and a good stratigraphic marker (Huber & Petrizzo, 2014). Although its last occurrence is also diachronic within the WIS, its distinct morphology and sudden extinction makes it a very good marker (Falzoni et al. 2018). The Cenomanian-Turonian boundary lies within the *Whiteinella archaeocretacea* zone, the partial range zone between the LO of *R. cushmani* and the FO of *H. helvetica* (Premoli Silva & Verga, 2004). The biomarkers for the C/T-boundary are the FO of *Quadrum gartneri* among nannofossils, and the LO of *Anaticinella planoconvexa* for foraminifera respectively. The age for the boundary has been defined at 93.5 Ma in Pueblo (Kennedy et al. 2005). The middle of the Bahloul Formation is characterized by a dominance of heterohelicids and a reduction of larger planktic foraminifera. The rise of *Heterohelix* is coined "*Heterohelix* shift" (Leckie, 1985) or "*Heterohelix* dominated assemblage" and usually occurs in the upper part of the *W. archaeocretacea* zone. The onset of this shift is defined at the point where specimens of *Heterohelix* exceed 50% of total planktic foraminifera assemblage

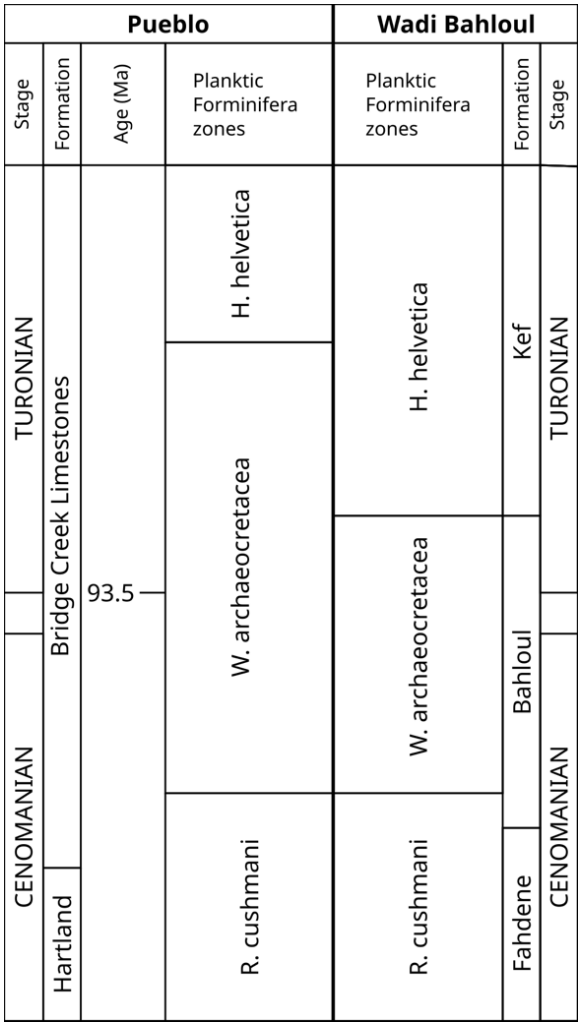

Figure 4 *Stratigraphic scheme showing the diachronism in biozones of the GSSP type section of Pueblo (Colorado, USA) and Tunisian section Wadi Bahloul. Modified after Caron et al. 2006. The FO of H. helvetica differs in high latitude (Pueblo) versus low latitude (Wadi Bahloul) sites, whereas the LO of R. cushmani is relatively synchronous, as is displayed here. (Caron et al. 2006)*

(Falzoni et al. 2018). The upper part of the Bahloul Fm. includes the *Helvetoglobotruncana helvetica* zone, which spans the total stratigraphic range of *H. helvetica*. The first occurrence of *H. helvetica* is known to be diachronous depending on latitude (Caron et al. 2006). In Tunisia, it may occur within the Bahloul Fm. (upper part) (Reolid et al., 2015; Zaghbib-Turki et al., 2013) or at the base of the Kef Formation, as in Wadi Bahloul (Fig.4). The FO of *H. helvetica* coincides typically with a general return of larger keeled genera (i.e. *Dicarinella, Marginotruncana*), although stratigraphic occurrences of these secondary markers vary significantly considering different locations and publications (Falzoni et al. 2018). The top of the Bahloul Fm. typically lies in the early Turonian (Touir et al. 2017).

Various C/T-locations in Tunisia are known to contain silica-layers around the C/T boundary (Ben Fadhel et al. 2012), which are attributed to a significant peak in abundance of radiolaria. Radiolaria themselves display a shift, where nasselarian species are declining and spumellarian species become more abundant along the OAE-2 and C/T transition. The Annaba Member / Gattar Member (Kef) contain the following biozones (*M. schneegansi* /*D. concavata, D. primitiva*), that represent post-OAE conditions and a return to a more stable environment.

5. MATERIAL & METHODS

5.1 Site and Samples

16 samples of the succession in Oued Kharroub have been collected. They are spaced over the range of about 38 meters along a creek slope. The samples are labelled and numbered as follows: OK -2.40, OK, -1.50, OK -0.70, OK 0.00, OK 5.00, OK 7.55, OK 9.50, OK 10.40, OK 11.70, OK 13.50, OK 15.00, OK 16.00, OK 18.60, OK 20.00, OK 25.00, OK 36.00. This numbering is due to the morphology of the site, 0.00 being at the base of the slope. The samples below 0.00 are in the horizontal part of the outcrop and represent the base of the section, the ones above 0.00 are situated on the slope (see fig. 2). The outcrop represents a sequence of thin-layered black shales and calcareous marls. They are macroscopically quite similar, with slight differences in colour from brownish-grey to dark grey. Four samples, 5.00, 7.55, 10.40 and 25.00, differ significantly in structure, hardness and colour from the darker coloured black shales. Within two of these light-coloured intervals (7.55 and 10.40), chert accretions appear. All these light-coloured samples including the chert accretions which could not be dissolved with the applied methods are excluded from present microfossil study.

5.2 Sample Treatment

Around 30 to 60 grams per sample have been crushed into ~5mm pieces with a hammer. After weighing, the crushed sample was put in a beaker filled with Rewoquat tenside until properly dissolved, which took about 3-4 days. The samples were then washed through 1mm, >125µm and >63µm sieves. The 1mm sieve was used to sort out possible larger components, that would complicate the subsequent counting. The >125µm and >63µm sieves split the microfossil components into two size fractions to again facilitate counting. The < 63µm fraction was not used, as it is not significant for the foraminifera component of the sample. After the wet sieving process, all fractions of the samples were collected and dried at 80°C. After 1-2 days, the fractions were again weighed. Considering the weight-% of the samples, an average of around 94% of the sample was <63µm in grainsize and the rest fell into the

63-1000µm fraction. The weight-percentage of >1mm components is 0.06% on average. The two samples OK 11.70 and OK 18.60 differ significantly from the average, where the >1mm fraction makes out ~20% and ~8% respectively. Thus, the dissolution with Rewoquat did not work equally well in all samples. Larger, not disintegrated, fragments of the sample were caught in the >1mm sieve, as is the case for the samples OK 11.70 and OK 18.60. There, these aggregates account for most of the >1mm fractions, and also make out a good part of the >125µm fraction. This result has been the same in two separate runs of the process. The data for the microfossil individuals/g sediment per sample have therefore been corrected with the mean values of nearby samples that do not differ in other aspects. These values are marked red, as they are impaired by the incomplete disintegration of a significant percentage of the sample and therefore not representative. Nevertheless, corrected data has been included, as it may represent a close approximation to the real weight-distribution. The >1mm fraction of all samples has been subtracted from the total weight for the individual per gram data (see chapter 6, tab.1).

5.3 Subsampling

The sample fractions yielded by sieving were still too large to allow proper counting on the tray. They were split with a sample splitter several times until small enough for the counting process on the tray. In this process, the respective sample fraction is filled into a sample splitter, in which the grains run through a grid that divides the sample into two equal fractions. Having done the splitting to a certain point, it was concluded, that the inaccuracy of the device gets higher the smaller the sample gets. Hence, further fractioning of the sample was done on the picking tray to eventually end up with the desired amount of at least 300 counted specimens per sample fraction. This was done by distributing the sample on the tray and picking in randomly chosen squares on the tray. The percentage of the counted squares on the tray combined with the percentage of the subsample compared to the sample achieved by splitting was extrapolated afterwards to obtain the specimen per gram sediment value. (see appendix – tables)

5.4 Microfossil Counting

The counting comprised all biotic components in the samples. These included the microfossils of planktic foraminifera, benthic foraminifera, radiolaria and ostracoda. The samples yielded predominantly planktic foraminifera, which are the focus of the study and

the only group further classified in genera and species. When counting microfossils, one has to consider that not all specimens present in the sample can be classified. Incomplete or partly dissoluted specimens, as well as ones that experienced higher taphonomic stress will quite possibly not display the features necessary for a proper classification. Naturally, these just named specimens were excluded from counting. The threshold for counting was a potential classification at genus-niveau, in order to obtain useful data for the study. This, however counts for planktic foraminifera, which make out the vast majority of the sample. All other biogenic components in the assemblage were counted, but not further classified than to the family-niveau.

The counting process was as follows. The subsample was put on a picking-tray with a grid of 45 squares. The subsample still being too large to be counted in total, it was then evenly distributed throughout the grid on the tray. Then, single squares were chosen for counting. This was done randomly across the grid to minimize the error that is caused by a not perfectly even distribution of the different sized microfossils on the grid. The decision of counting this way, rather than splitting the samples further, was a question of considering the precision of the sample splitter versus the even distribution on the tray, as mentioned above.
In addition to the counting of >300 specimens per sample of the 1000-125µm fraction, an additional 100-200 specimens of the 125-63µm fraction were counted. Although the biostratigraphically significant groups were expected in the larger fraction, the counting of the 125-63µm fraction was done to obtain a more complete picture of the assemblage and thus a better understanding of paleoecological and paleoenvironmental aspects. Considering the number of counted microfossils, the minimum number of counted specimens as suggested by Fatela & Taborda (2002) being 300 in order to incorporate species that account for as little as 3% of the assemblage, the numbers in this study exceed this by far. Thus, a minimization of errors caused by missed specimens is given here.

5.5 Scanning Electron Microscope Imaging

Planktic foraminifera were analyzed and photographed using a JEOL JCM-6000Plus Benchtop SEM with the associated software. Ahead of the scanning, stubs with foraminifera specimens were gold-sputtered with a DII-29030SCTR Smart Coater. Both coater and SEM have been kindly provided by Dr. Benjamin Sames. Further editing of the photographs and

creating of plates has been done using the open source softwares GIMP (GNU Image Manipulation Program) and Inkskape (vektor graphics editor).

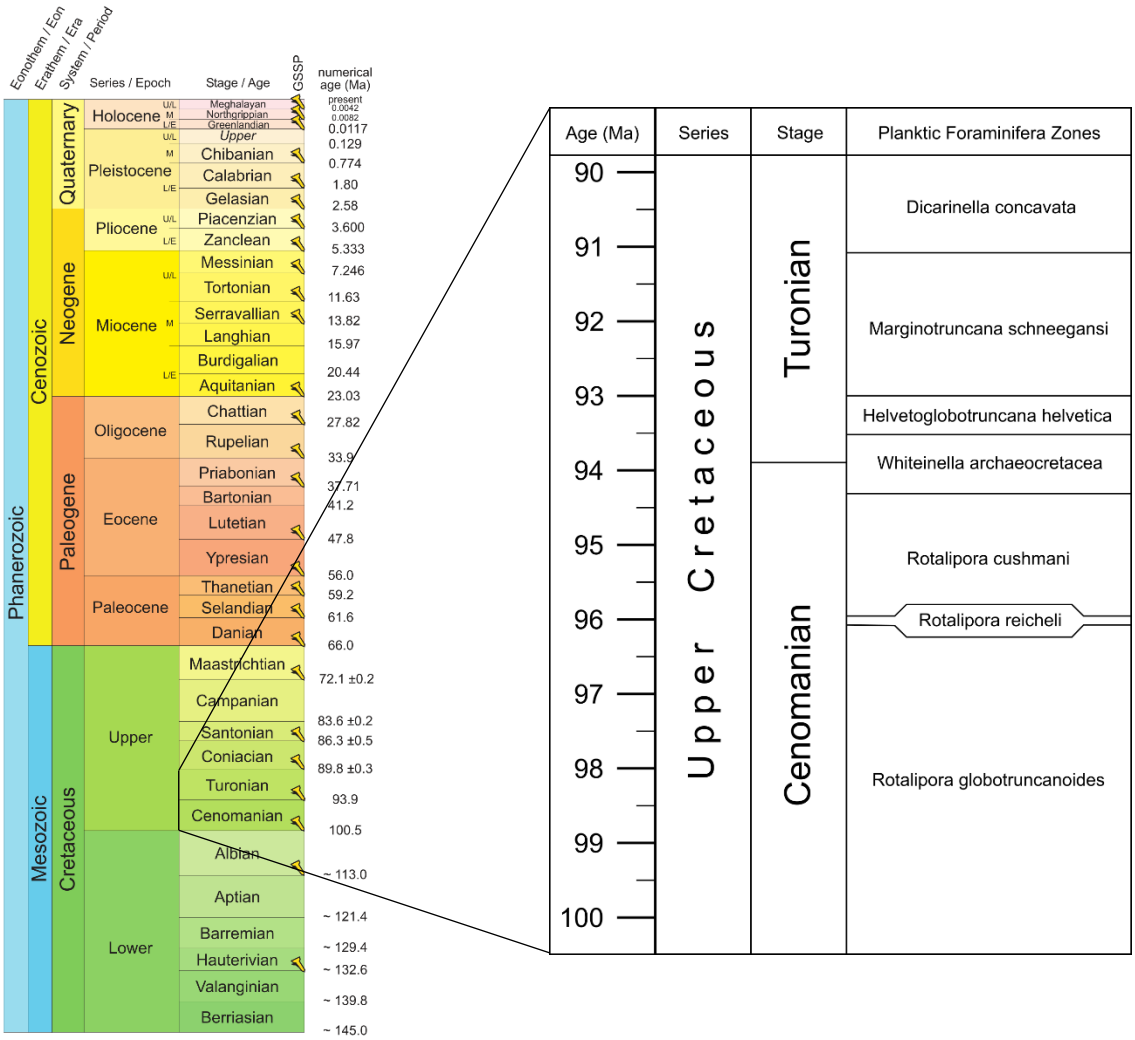

Figure 5 *Stratigraphical collumn, modified after the ISC (International Stratigraphic Chart) (left) (stratigraphy.org). Planktic foraminifera biostratigraphic zonation, modified after Mikrotax.org.*

5.6 Classification and Methodological References

Planktic foraminifera classifications were done primarily according to the guide included in Premoli Silva & Verga (2004), and with the additional aid of mikrotax.org. The taxonomic system was adapted from Premoli Silva & Verga (2004), and with few exceptions from mikrotax.org, which are mentioned in the taxonomic list in the appendix. The biostratigraphic zonation scheme has been adopted from mikrotax.org & Premoli-Silva &

Verga (2004). The scheme is given in fig. 5, with the addition of *Dicarinella algeriana* subzone (Soua, 2005) as a further subdivision of the *R. cushmani* zone. The ecological concepts of planktic foraminifera genera (chapter 6.3) has been adopted from Coccioni & Luciani (2004) and Hart (1999).

5.7 Geochemical Data ($CaCO_3$, TOC, $\delta^{13}C$)

In addition to the micropaleontological part of this study, geochemical data have been obtained. They include carbonate content ($CaCO_3$), total organic carbon (TOC) and stable carbon isotope $\delta^{13}C_{carb}$. The sample density for these measurements is higher, resulting in a total of 51 values along the section, from sample OK -2.40 to OK 39.00. All data included here was provided by Prof. Michael Wagreich. $CaCO_3$ and TOC values are given in percent. The values of $\delta^{13}C_{carb}$ are given in per-mille (‰) from VPDB (Vienna Pee Dee Belemnite) standard. The calculation is as follows:

$$\delta^{13}C_{sample} = \frac{^{13}C/^{12}C_{sample}}{^{13}C/^{12}C_{VPDB}} - 1$$

6. RESULTS

The microscopic analysis of the washed samples yielded a detailed picture of the biostratigraphic distribution of the present fossil microfauna. Of the 16 samples at hand, 12 could be used for biostratigraphic analysis. The remaining 4 samples (OK 5.00, OK 7.55, OK 10.40 and OK 25.00) are fossil barren and therefore only appear in the geochemical data analysis.

6.1 Preservation and Content

The general characteristics of the various samples differ quite strongly from another, and so does the state of preservation of microfossils contained. The section can be roughly subdivided by these characteristics. Firstly, the lower three Cenomanian samples have a (comparably) good preservation and are brown-grey in their macroscopic appearance. OK 0.00 is a significantly light-coloured sample that shows signs of dissolution and generally worse preservation than the ones below. Samples from 9.50 upwards are generally darker (darker grey), with more abiotic components and a worse state of preservation than the presumed-Cenomanian samples. The most significant ones to mention here are 9.50, 11.70, where large parts of the tests are red or black, with metallic shimmer. Apart from differences concerning colour and presence of abiotic components, there is a pattern of reoccurring (presumably) post-sedimentary dissolution throughout the profile, that is striking. The dissolution is displayed in partly dissolved specimens, where part of their shape is still recognizable and in a much stronger way in the "cornflake-shaped" components that do not allow any kind of association with remains of an organism. The latter is the case in the four samples excluded from the study. There are some, somewhat intermediate samples, do show signs of dissolution, but have been included, as the state of preservation allowed a counting to a degree acceptable for this study. These are particularly samples OK 0.00, 18.60 and 36.00. In almost all assemblages of the studied samples, planktic foraminifera make out the

vast majority of not only microfossils, but the whole sieved size fractions (1mm - 63µm). None of the washed samples yielded any significant amount in the >1mm fraction, if anything, it contained clumps, not properly dissolved by the applied method. The only exception to the predominance of planktic foraminifera in the assemblages in this section is OK 9.50, where Radiolaria prevail. Incidentally, the intervals below and above 9.50, namely 7.55 and 10.40 contain nodules and layers of SiO_2 within and inbetween the light-coloured, soft material. Benthic foraminifera do occur in almost all parts of the profile, though always making up only a minor component of the total assemblage.

6.2 Individuals Per Gram Sediment

For this data, the weight of sample material gathered in the >1mm sieve has been mathematically removed from the equation. No samples have yielded larger grains for that fraction, it was comprised solely clumps, not dissolved by the applied method. The weight of the >1mm data does not exceed 0,6%, except for samples 11.70 and 18.60. In these samples, the weight-percentage of either single larger grains, or aggregates not dissolved, in the >1mm fraction but also in the 1mm-125µm fraction make out a significant percentage of the weight. Thus, in these two samples, this error has been calculated and removed, and these samples have been subsequently marked in the individuals per gram data, as the new values are to be considered with care.

The ind/g sediment data shows a decline in total amount of foraminifera compared to the sample weight from the Cenomanian part of the section (-2.40 - 0.00) to the Turonian part from 9.50 onwards. Numbers in the lowest samples range from ~1000-4000 individuals per gram sample in the larger size fraction and ~12000-34000 in the smaller size fraction. At 9.50, planktic foraminifera go down to only about 30 individuals per gram in the larger and 1,6k in the smaller size fraction, which represents a reduction by a factor of ~150 and ~20 respectively. In this sample, not only total numbers of planktic foraminifera are highly decreased, but also the general numbers of microfossils per /g sample (radiolaria).

Table 1 *Samples studied for microfossils. The weight of the sample used for counting and its sieved fractions and percentages. Red numbers indicate corrected data.*

Sample	Weight [g]				Fraction weight [%]		
	Total	>1mm	>125µm	>63µm	>1mm	>125µm	>63µm
OK -2.40	37,861	0,01	0,70	2,64	0,03	1,86	6,98
OK -1.50	40,315	0	1,81	3,77	0	4,49	9,36
OK -0.70	43,646	0	1,18	1,96	0	2,71	4,49
OK 0.00	36,496	0	2,05	3,81	0	5,62	10,44
OK 9.50	64,988	0	0,10	0,41	0	0,15	0,63
OK 11.70	36,148	7,69	1,17	0,57	21,26	3,24	1,58
OK 13.50	41,28	0,22	0,44	0,47	0,54	1,07	1,14
OK 15.00	30,783	0,06	0,55	0,81	0,21	1,79	2,62
OK 16.00	39,773	0	0,31	0,34	0	0,78	0,84
OK 18.60	51,464	4,30	1,61	2,74	8,36	3,14	5,32
OK 20.30	42,31	0,03	0,31	0,57	0,09	0,74	1,34
OK 36.00	43,586	0,09	3,09	4,32	0,20	7,08	9,93

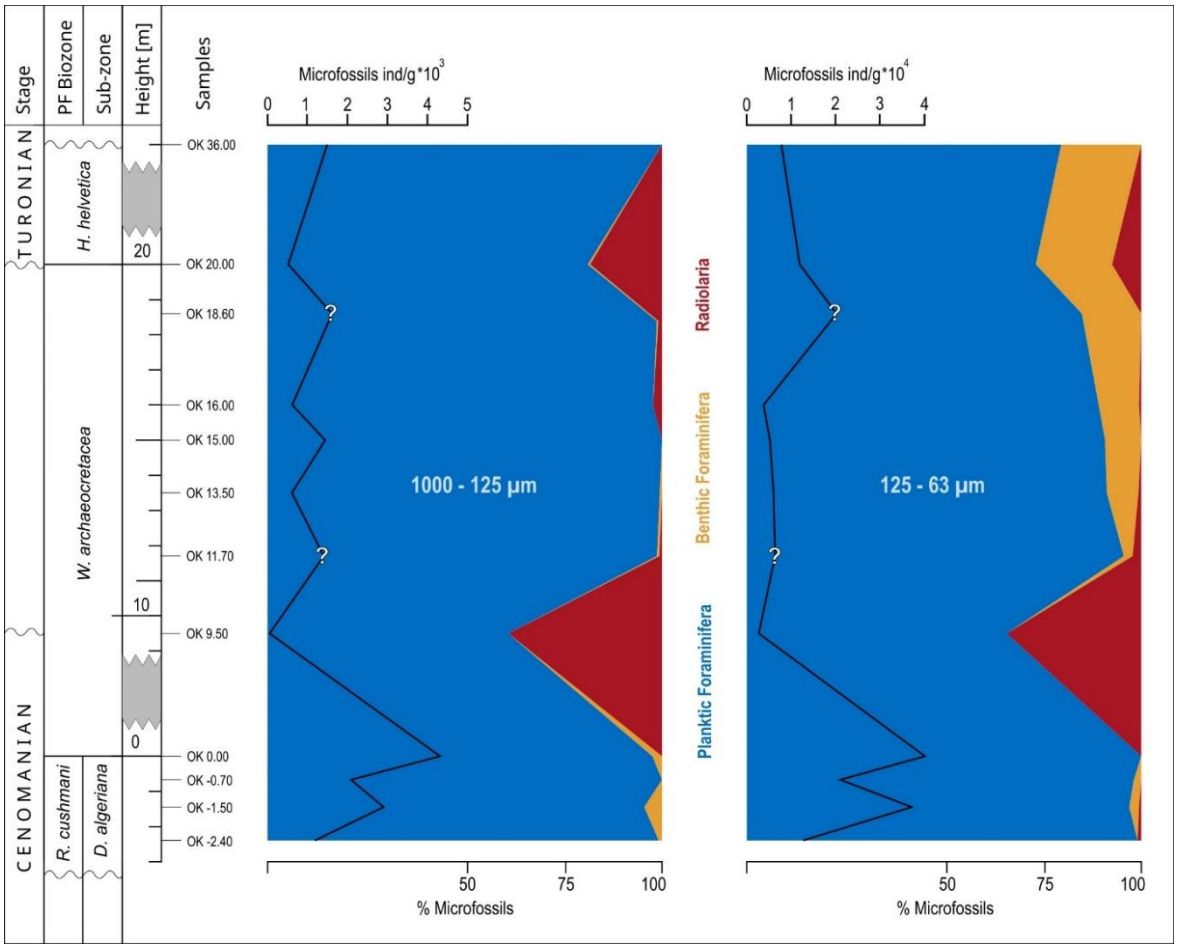

Figure 6 *Percentage of counted microfossils. Planktic foraminifera (blue), benthic foraminifera (yellow), radiolaria (red). Percentages are in relation to the counted fraction of >300 individuals.*

The numbers do not reach Cenomanian levels again in the smaller size fraction with around ~3000-8000 ind/g sediment from 11.70 - 36.00, while they continuously fluctuate between ~500 to ~1500 in the larger size fraction in this frame. A striking feature of this data is the magnitude of decline in individuals in the smaller size fraction compared to the larger size fraction. This is to be seen in the decline of the weight-percentage of this fraction compared to the total sample weight (see fig.8). As the data of the samples 11.70 and 18.60 is somewhat impaired, this slight peak at 18.60 is debatable (Fig. 8).

The planktic foraminifera assemblages in the larger size fraction (1mm-125µm) are generally dominated by the trochospiral genera *Muricohedbergella* and *Whiteinella* and the biserial *Heterohelix*, although the ratios change significantly with turnover and assemblage-changes along the profile. *Heterohelix* gains in numbers while *Muricohedbergella* become less significant. Keeled forms are generally low in numbers, although present throughout the profile. The exception here are the lowermost samples, where large keeled *Rotalipora* and the keeled *Praeglobotruncana* do constitute a significant percentage of the assemblage. Further upwards, in the middle part of the section, the double-keeled *Dicarinella* become more abundant. Considering the smaller size fraction (125-63µm), it is dominated almost exclusively by species of the genus *Heterohelix*, with the exception of OK 9.50, where Radiolaria constitute another major component of the assemblage. The other common group found in the smaller size fractions of the assemblages is *Muricohedbergella*, which are, due to the limited resolution of the light-microscope grouped together and not further differentiated at species niveau. The overall picture of the assemblages is shaped by dominance of groups with simple morphologies, but contrary trends are found as well in various occasions. The distribution of the major planktic foraminifera genera is described in the following.

6.3 Planktic Foraminifera: Biostratigraphic Zonation

Three planktic foraminifera biostratigraphic zones have been identified. The *Rotalipora cushmani* Total Range Zone (*Dicarinella algeriana* subzone) (OK -2.40, -1.50, -0.70), the *Whiteinella archaeocretacea* Partial Range Zone (OK 0.00) and the *Helvetoglobotruncana helvetica* Total Range Zone (OK 9.50, 11.70, 13.50, 15.00, 16.00, 18.60, 20.00, 36.00). The stratigraphic distribution of the most common genera of planktic foraminifera in both size

fractions occurring along the profile of this section are given in fig. 7. Most percentage dates given in this chapter, unless stated otherwise, will refer to the larger size fraction (1mm-125µm), as this fraction contains the biostratigraphically important groups. Most assemblages of the smaller size fraction are almost exclusively made up of *Heterohelix* and *Muricohedbergella* (as seen in fig. 8). Thus, not all percentage counts are displayed in fig. 8. The genera *Muricohedbergella, Macroglobigerinelloides* and *Clavihedbergella* are, for the most part, not further divided into their different species occurring in the studied section. This is due to their sizes and preservation states, that made it reasonable to combine them. The occurring species, however, are presumed and displayed in the plates and listed in the taxonomic list (Appendix, Taxonomic List). *Muricohedbergella* includes for the most part *Mh. delrioensis* and *Mh. planspira*, and some less common *Mh. flandrini*. *Macroglobigerinelloides* for the most part seems to be *Mg*. bentonensis. *Clavihedbergella* includes *C. amabilis*, *C. simplex* and possibly *C. simplicissima*. In the upper half of the section, some specimens strongly resembling what was identified as *Eohastigerinella subdigitata* by Gebhart et al. (2010), has been included in *Clavihedbergella* sp. here (compare Mikrotax.org; Gebhart et al. 2010). *Schackoina* includes *S. cenomana* and *S. multispinata*. *Heterohelix* includes *H. moremani*, *H. reussi* and *H. globulosa*. Rare, as well as not stratigraphically decisive species (concerning the studied section) are excluded from the general description of the zones and discussed separately in the following chapter 6.4. These include *Guembelitria, Schackoina* specifically.

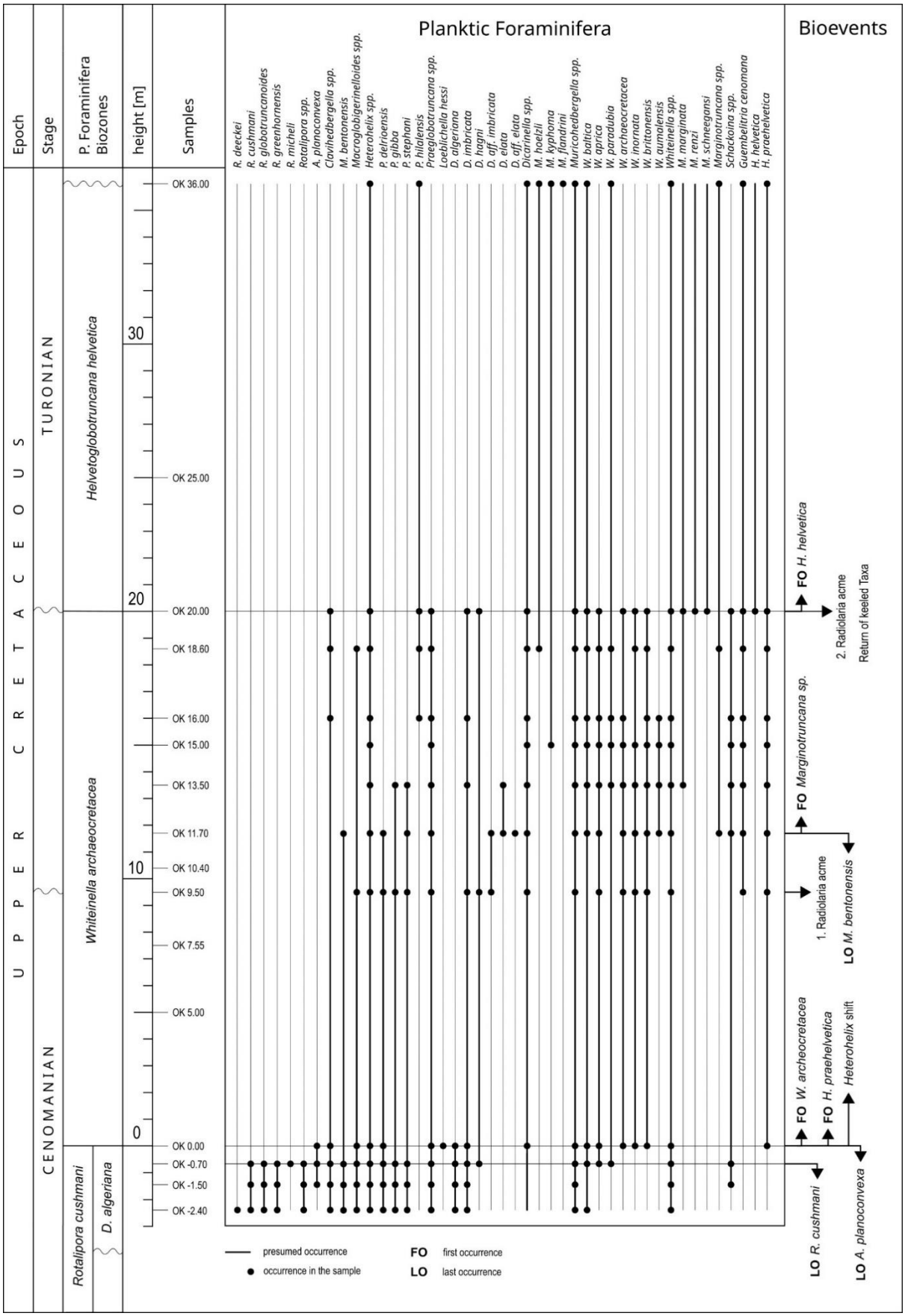

Figure 7 *Profile of the Oued Kharroub section. Occurrence of planktic foraminifera and associated bioevents. Wave-lines indicate uncertainty of boundary. Black dots indicate occurrence of the respective species/genus.*

6.3.1 *Rotalipora cushmani* Zone

OK -2.40, -1.50, -0.70

late Cenomanian

The lowest point in the studied section has been identified to lie in the late Cenomanian, in the *Rotalipora cushmani* Zone. The FO of the marker species defining this total range zone, the large, keeled *Rotalipora cushmani*, is already present in the lowest interval. Furthermore, the FO of *Dicarinella algeriana*, defining the beginning of the subzone (*D. algeriana* Zone, Premoli Silva & Verga 2004) within the *R. cushmani* zone, also lies in this lowest interval OK -2.40. This shows the lowest point in the section being already in the uppermost Cenomanian. The named zone includes in this section the samples OK -2.40, OK -1.50 and OK -0.70. OK -0.70 shows the LO of *R. cushmani* and the whole genus *Rotalipora*. This marks the end of the *R. cushmani* Zone and the extinction of the genus *Rotalipora*. No other species of *Rotalipora* could be found in samples of above lying strata. *R. deeckei* only occurs in the lowest sample at -2.40, whereas the other species of Rotalipora (*Thalmanninella*) *R. greenhornensis, R. globotruncanoides* and *R. micheli* last occur together with *R. cushmani* at -0.70. Apart from *D. algeriana*, *D. imbricata* occurs at the base of the section, and *D. hagni* first occurs at -0.70.

The general picture in this section of the profile shows an assemblage of high diversity. Especially so the keeled taxa from the genera *Rotalipora* and *Praeglobotruncana* in the lower part. Going upwards within this zone, there are obvious trends to be seen, where these genera decline (Fig. 8). The genera *Rotalipora* and *Praeglobobotruncana* consitute a major part of the assemblage in the size fraction 1mm-125µm in the lowest interval with ~25% and ~20% respectively. In the last interval of the zone (OK -0.70), foraminifera of the genus *Rotalipora* make out ~13% and *Praeglobotruncana* only ~5%. The numbers of the third keeled genus appearing in this zone, *Dicarinella*, remain low in the whole zone and below 5%. *Whiteinella*, as well as *Heterohelix* become more dominant within the zone. However, specimens of *Whiteinella* remain relatively small until further up in the section in the *H. helvetica* zone. All larger specimens in this zone belong to the genus *Rotalipora.* Especially *R. greenhornensis* is to be mentioned here as by far the most abundant species of the genus. It makes out ~16% of all counted PF. If one takes the smaller size fraction into account, the smaller genera like *Heterohelix* and *Muricohedbergella* are the most abundant groups. There are some juvenile forms not further classified on account of their small size and lack of

displaying characters necessary to divide them. While in the 1mm-125µm fraction, *Heterohelix* remains below 10%, they make up up to 50% in the 125-63µm fraction. Numbers of *Muricohedbergella* are high in the lowest interval OK -2.40 in the 125-63µm fraction with around 63% and decrease with simultaneously with the increase of *Heterohelix* to ~40% in the last interval of this zone. In the larger size fraction, *Muricohedbergella* goes from ~24% in the lowest sample to 33% in OK-0.70. Two more groups are very abundant in the *R. cushmani* zone. Although more so in the larger size fraction (see fig. 8). *Clavihedbergella* makes up around 12-14% throughout the zone. *Macroglobigerinelloides* constituting ~35% of planktic foraminifera in the lowest interval and ~17% in the uppermost interval of the zone. Both genera remain below 10% in the smaller size fraction. *Anaticinella* (*A. planoxonvexa*), remains absent or very rare throughout the *R. cushmani* zone.

6.3.2 *Whiteinella archaeocretacea* Zone

OK 0.00, 9.50, 11.70, 13.50, 15.00, 16.00, 18.60

late Cenomanian - early Turonian

The *W. archaeocretacea* Zone begins with the interval OK 0.00 just above the LO of *Rotalipora cushmani*. It constitutes the interval between the LO of *R. cushmani* and the FO of *H. helvetica.* The transition into this zone is accompanied by an apparent change in the assemblage. Although this sample is unfortunately impaired by partial dissolution, which may have slightly distorted general picture of percentual microfossil distribution, the changes are still obvious, and the absence of *Rotalipora cushmani* is clear. OK 0.00 contains the FO of *W. archeocretacea*. The following samples 5.00 and 7.55 could not be used due to complete lack of any microfossil remains. Apart from the extinction of *Rotalipora*, two other groups that constituted a major percentage of planktic foraminifers in the assemblages in the *R. cushmani* zone are here now strongly reduced in numbers or miss completely. *Macroglobigerinelloides* (mostly *Mg. bentonensis*), making out up to 20% of the assemblage in the *R. cushmani* zone dissappears in the *W. archaeocretacea* zone with the minor exceptions of single specimens further upwards. *Praeglobotruncana*, already strongly declined in the lower zone, stays low at about 2%. OK 0.00 contains the only occurrence of *Loeblichella hessi*. Furthermore, the FO of *H. praehelvetica* is found in this sample. The genus *Clavihedbergella* reaches a percentual maximum of 20% of the assemblage in OK 0.00. The dominating genera are, as in the underlying samples, *Muricohedbergella* and

Clavihedbergella, together constituting the majority of individuals in the sample. Also found in this sample is the LO of *A. planoconvexa.* The obvious faunal change displayed in this sample, as compared to the ones below, is in sizes, as well as morphotypes. Large, keeled taxa are absent, and even smaller keeled taxa like *Dicarinella* and *Praeglobotruncana* are very rare. Due to the in many cases poor preservation, some specimens remained unclassified and are listed only as *p. foram. indet*. The next sample, OK 9.50 generally differs quite clearly from lower parts (i.e. the base) of the section. The general appearance and distribution of microfossil groups represents an assemblage after a faunal turn-over. Many major foraminifera groups of the Cenomanian are strongly reduced or absent. The whole zone from this point on is continuously characterized by a high abundance of *Heterohelix* and generally low abundance of larger keeled species. Larger foraminifera for the most part belong to the genus *Whiteinella*.

In the samples 9.50, 11.70 and 13.50, *D. imbricata* var., *D. elata* as well as *H. praehelvetica* occur in higher numbers. 9.50 shows the FO of *D. elata*, as well as *D.* aff. *Imbricata* and *H. praehelvetica* somewhat resembling *H. Helvetica* (Plate 2). *H. praehelvetica* occurs synchronically in different shapes (morphotypes) with partly keeled ones as well as more rounded ones in 9.50, 11.70 and 13.50 respectively. Partly they occur in very large sizes. The strongly inflated chambers of *D. imbricata* var. are a characteristic feature of the samples 9.50, 11.70 and in part also 13.50, that do not occur again further upwards in the section. The inflation of chambers as well as the somewhat poorly developed keel (as in comparison to common *D. imbricata*), causes their general outline to resemble *Whiteinella* (see Plate 1 nr. 12) or *P. ovariensis*. Similarly, *D. imbricata* specimens show more inflated chambers in the last whorl. *D.* aff. *imbricata* does only occur in sample OK 9.50. OK 9.50 generally contains few foraminifera, as this sample is dominated by Radiolaria in both size fractions. In 11.70, the case is similar as in 9.50, with *D. elata* becoming more common, as are other dicarinellids. *D* aff. *elata* has its only occurrence in 11.70 (Plate 2, nr. 2). In OK 11.70, *Marginotruncana* first occurs in this section, although not identified at species level. In OK 13.50, the FO of *M. marginata* could be identified. Separate to the counting process, *M. schneegansi* and *M. renzi* could be identified as well, although only further upwards in the section (OK 20.00). In any case, *Marginotruncana* remains very rare throughout the section (< 1%), with a slight increase at 20.00. The two samples 9.50 and 11.70 thus represent a first return of keeled taxa. The abundance of *Dicarinella* and also *Praeglobotruncana* is significantly higher than in all following samples with 12%

Praeglobotruncana in OK 9.50 and 23% and 15% *Dicarinella* in OK 9.50 and OK 11.70 respectively. *Praeglobotruncana* and *Dicarinella* are always present in samples above although only in low numbers (<5% and <7% respectively). OK 9.50 in particular, but also OK 11.70 somewhat constitute an exception to the following samples of this zone. Mainly in as far as they include larger and more keeled taxa than the samples above. Mainly species of *Dicarinella* are to be highlighted here (*D. elata* and *D. imbricata* var.). The difference of the first two samples of this zone is also seen in the sizes of keeled genera. They occur in sometimes very large sizes (*D. elata* Plate 2*).* Further upwards in the zone, *D. elata* and *D. imbricata* var. do not appear anymore and other species of keeled genera occur in very small sizes only, up until OK 20.00. Especially the samples 15.00, 16.00 and 18.60 account for minimal abundance and size of the genera *Dicarinella, Praeglobotruncana Marginotruncana*. These samples show quite similar assemblages representing a stressed environment, where keeled genera are strongly reduced in numbers as well as size.

Considering the developments in the smaller sized groups, *Muricohedbergella* and *Heterohelix*, along the whole section and especially from 9.50 upwards, a shift in abundance is apparent. *Heterohelix* species experience a massive increase from 0.00 upwards ("*Heterohelix* shift"), compared to lower samples. *Muricohedbergella*, though still abundant and between 8-24% (1mm-125µm) and 9-25% (125-63µm), is overwhelmed by the numerous *Heterohelix*, that is mostly around 50% in the larger size fraction and from 65% up to 99% in the smaller size fraction. The two genera undergo a reversal in percentual abundance during the OAE-2. *Heterohelix* show the highest number in the 1mm-125µm fraction in OK 36.00, where they also occur in the largest sizes (see Plate 5 and fig. 8). *Muricohedbergella*, however, is significantly more abundant in the samples from 13.50 to 18.60, where larger, keeled species are highly reduced in sizes and numbers. Aside from these two very common, small planktic foraminifera genera, the larger non-keeled genus *Whiteinella* constitutes 11-29% of the planktic foraminifera of the assemblages and shows a major proliferation. Whiteinellids not only occur in high numbers but in great diversity. Seven different species (*W. archeocretacea, W. baltica, W. paradubia, W. aprica, W. inornata, W. aumalensis, W. brittonensis),* from whom most of them occur throughout the zone, could be identified. Species of this genus themselves vary strongly in morphotypes. A prime example for this is *W. archaeocretacea* (Fig. 3). *Clavihedbergella*, a very abundant genus at the base of the *W. archaeocretacea* zone of this section is completely absent in OK 9.50 and does only reappear in very low numbers in further-above samples (<1% in the

1mm-125µm fraction, <3% in the 125-63µm fraction) of the zone. A similar eclipse is recorded for *Macroglobigerinelloides*, which only occurs in two samples of this zone and in very low numbers. The LO of *Mg. bentonensis* occurs in 11.70. The LO of *Macroglobigerinelloides* in the counted fraction occurs in 18.60, however additional search in the sample residue yielded a specimen in 36.00, which could not be classified at species level.

6.3.3 *Helvetoglobotruncana helvetica* Zone

OK 20.00, 36.00

early to mid - Turonian

In OK 20.00, larger specimens of more complex morphotypes, the keeled genera *Dicarinella* and *Marginotruncana* reappear in larger sizes and higher abundance. However, not by far as abundant as keeled forms in the *R. cushmani* zone. In OK 20.00 the first occurrence of *H. helvetica* is recorded. Although *H. praehelvetica* is continuously present in the *W. archaeocretacea* zone, it is only at meter 20.00, that a specimen with a distinct keel at all chambers of the last whorl could be identified. This, however could only be achieved by additional search in sample residues after counting of 300 individual specimens left the presence of *H. helvetica* somewhat uncertain. Sample 20.00 also represents the second acme of Radiolaria, which, in the meters between were rather rare or absent. The uppermost sample of this section, OK 36.00, is unfortunately impaired due to dissolution. *H. helvetica* could not be identified here, but *H. praehelvetica* is present. The assemblage shows the largest forms of *Heterohelix*, which occur here partly in sizes similar to the largest whiteinellids (see plate 5.). In this sample the triserial *Guembelitria cenomana* also reaches its acme. In lower samples, this species occurs only in the 125-63µm fraction. Its FO there lies in 9.50 and then in further samples has an abundance at up to 11% (18.60), being absent in 15.00, until the peak in abundance is reached in 36.00 at ~22% in the 125-63µm and ~7% in the 1mm-125µm fraction.

The general picture of OK 36.00 is one resembling the part of the section between 15-18.60, with the exception, that keeled species are slightly more common. Mostly the identification on species level has been unsuccessful due to the state of preservation of this sample. OK 36.00 also yielded the FO of *Mh. flandrini*. Classifications and general abundance patterns

in this sample are to be treated with caution, as the dissolution certainly impaired these data. However, one can still see clearly that this sample is not displaying typical characteristics reported from assemblages that lie somewhere within the *H. helvetica* zone.

Figure 8 *(p.35) Profile of the Oued Kharroub section. Developments of percentual abundances (relative to the counted total of PF numbers) of the most common planktic foraminifera genera of both size fractions. Planktic foraminifera individuals per gram sediment & ratios of planktic to benthic foraminifera. Corrected data values are marked with a red questionmark.*

Stage
CENOMANIAN
TURONIAN
PF Biozone
R. cushmani
W. archaeocretacea
H. helvetica
Sub-zone
D. algeriana
Height [m]
0
10
20
Samples
OK -2.40
OK -1.50
OK -0.70
OK 0.00
OK 9.50
OK 11.70
OK 13.50
OK 15.00
OK 16.00
OK 18.60
OK 20.00
OK 36.00
Heterohelix
1000 - 125 µm
125 - 63 µm
Heterohelix shift
Muricohedbergella
Whiteinella
Rotalipora
Extinction of Rotalipora
Praeglobotruncana
Dicarinella
Clavihedbergella
Macroglobigerinelloides
Exit / Decline of Macroglobigerinelloides
Planktic Foraminifera [ind/g sediment]
P/B ratio (% P. Foram)
1000 - 125 µm
125 - 63 µm
corrected data

6.4 Planktic Foraminifera: Distribution of Indicative Species Along the Profile

As indicators for the environmental conditions in the ocean at the time, some species shall be specifically considered in this chapter. The scheme used here, after which to divide planktic foraminifer genera and species into groups according to their ecological properties is in accordance with Coccioni & Luciani, 2004 as well as Gebhart et al. 2010, among others and depicted in tab. 2. Planktic foraminifera genera from this section are divided into their favored dwelling-depths, below, around and above the thermocline (deep - intermediate - surface). The division of K-strategists and r-strategists, ecological terms referring to the reproductive behavior in response to the stability of the environment, is also reflecting a spectrum of water-chemical properties from oligotrophic (favoring K-strategists) to mesotrophic and eutrophic (r-strategists) respectively.

Table 2 *modified after Coccioni & Luciani, 2004. The genus Clavihedbergella[1] is here added to the group of surface dwellers and r-strategists according to the originial publication, where "Hb. simplex" is listed, a species synonymous with Clavihedbergella simplex, which is one of the species of this genus occurring in this section. C. amabilis is therefore added to this group as well, presumed on account of its similar morphology.*

Deep dwellers	Intermediate dwellers	Surface dwellers
Rotalipora	*Macroglobigerinelloides*	*Muricohedbergella*
Marginotruncana	*Heterohelix*	*Whiteinella*
Helvetoglobotruncana	*Schackoina*	*Clavihedbergella*[2]
	Dicarinella	
	Praeglobotruncana	

K-strategists	K-r-intermediates	r-strategists
Rotalipora	*Macroglobigerinelloides*	*Muricohedbergella*
Marginotruncana	*Dicarinella*	*Heterohelix*
Helvetoglobotruncana	*Praeglobotruncana*	*Schackoina*
	Whiteinella	*Guembelitria*
		Clavihedbergella

While the lower part of the section (*R. cushmani* zone) clearly shows a high diversity and quantity of deep dwelling K-strategists (e.g. *Rotalipora*) and also intermediate forms like *Praeglobotruncana* and *Dicarinella*, opportunistic species do constitute the majority of PF

[2] Falzoni & Petrizzo (2020) doubted the usefulness of hedbergellids with elongated chambers (i.e. *Clavihedbergella*), due to data implying they suffered from increased sea surface productivity and reduced thermal stratification and were mostly replaced by other groups. Nevertheless, it is included here, illustrating the diversity of hedbergellids (muricohedbergellids and clavihedbergellids) at the base of this section.

in here and in the whole section. As one goes upwards in the section, the contrast becomes more extreme, where almost no deep-dwellers and K-strategists respectively are present anymore. For the better part of the *H. helvetica* zone (9.50 upwards), the opportunistic *Heterohelix* dominate the assemblage. The only other groups making out high percentages are surface dwelling whiteinellids and muricohedbergellids, which possess simple morphology and are surface dwelling and adapted to eutrophic conditions. *Clavihedbergella* also accounts for this trend, although it disappears after the beginning of the *W. archaeocretacea* zone. At the beginning of the *H. helvetica* zone, the intermediate *Dicarinella* occurs in considerably high numbers, and also the type species itself *H. helvetica*, which can be assigned to similar preferences, is relatively abundant. However, as mentioned in chapter 6.1, they both become very rare and indeed smaller in size in the following samples 13.50 to 18.60. This part of the section is characterized by a strong decline of keeled, intermediate and deep dwelling K-strategists, where the only group proliferating in depths around the thermocline is the opportunistic *Heterohelix*. This trend is incised by a return in abundance of these taxa in 20.00. This "comeback" of keeled K-strategists (namely *Dicarinella* and *Marginotruncana*) in OK 20.00 is significant, however, the trend towards a real proliferation of K-strategists remains rather tentative. Especially given the assemblage in OK 36.00, where deep dwellers and K-strategists are again less prominent than in OK 20.00. The proliferation of *Heterohelix* does not end before the top sample of this section, where they also occur in the largest sizes (Fig.8).

Opportunists (mainly *Heterohelix*) and surface dwellers (mainly *Whiteinella* and *Muricohedbergella*) are clearly dominating the assemblages throughout the section. *Whiteinella* more so in the upper part of the *W. archeocretacea* zone, indicating slightly less-eutrophic conditions there. Less dominance of these genera is recorded in the samples assigned to the *R. cushmani* zone, but trends towards this type of assemblage can be seen starting from -0.70 already. The quantity of "disaster" species (Gebhart et al. 2010), known to be able to tolerate extreme conditions of eutrophia and oxygen deficiency (*Guembelitria, Schackoina*) remain very rare. *Guembelitria* only starts to thrive towards the uppermost part of the section, first exclusively in the smaller size fraction, with its peak in the top sample 36.00, the only sample where they also occur in the larger size fraction. This trend falls in line with the continuous proliferation of *Heterohelix,* which also shows peaks in size and diversity in 36.00. *Schackoina* is relatively stable in low numbers throughout the section and does not show varaiations that correlate with the trends of other, more abundant groups. Two

species of *Schackoina* (*S. cenomana, S. multispinata*) could be identified. *Clavihedbergella*, a surface-dwelling foraminifer also considered to prevail in eutrophic and/or dysoxic conditions is very prominent in the lower Cenomanian samples and then experiences an eclipse and only occurs very rarely in lower Turonian samples. Its use for paleoenvironmental reconstructions is however doubted (see chapter 7, Falzoni et al. 2020)

6.5 Radiolaria

Radiolaria are very rare in the lowermost Cenomanian samples, where they only occur in the smaller size fraction and with <1% of counted microfossils. They remain rare throughout the whole section and nearly exclusively occur in the smaller size fraction. This is, however, with two exceptions. In sample 9.50, the highest amount of Radiolaria is found (~35% of counted microfossils). It even exceeds the in this interval abundant *Heterohelix*, which usually dominate the assemblages here. The other sample with a significant amount of Radiolaria is 20.30, where they constitute roughly ~15% of all counted microfossils. Inbetween these two exceptional intervals concerning radiolaria, they do appear in slightly higher numbers than in the lowermost Cenomanian samples, but stay below 3% in both size fractions. The uppermost sample of this section 36.00 completely lacks radiolaria. Although further classification of radiolaria has not been done for this study, an obvious dominance of *Spumellaria* relative to *Nassellaria* could be observed. Percentages of relative abundances are given in fig.6.

6.6 Benthic Foraminifera

Benthic foraminifera occur in low numbers and low diversity throughout the whole section. Their highest abundance in the larger size fraction is in -1.50 with ~4,5%. Common genera here are *Ammodiscus* and *Gyroidinoides*. Further upwards, larger specimens of benthic foraminifera are found in most intervals (11.70, 13.50, 18.60, 20.30) (e.g. *Lenticulina*) but only very rarely (~0,2-0,5%). However, there is a trend towards smaller forms upwards in the section. From 11.70 they increase in numbers from ~2% (11.70) to ~20% (36.00). For the most part, these include very small mono- bi- and tri-serial forms (*Bicazammina*,

Praebulimina). These only appear from 11.70 upwards and are absent in lower intervals. The only interval in the section, that completely lacks any benthic foraminifera is 9.50. The planktic to benthic Foraminifera Ratio (P/B-ratio) is given in fig. 9, percentual abundance relative to all microfossils is given in fig. 6.

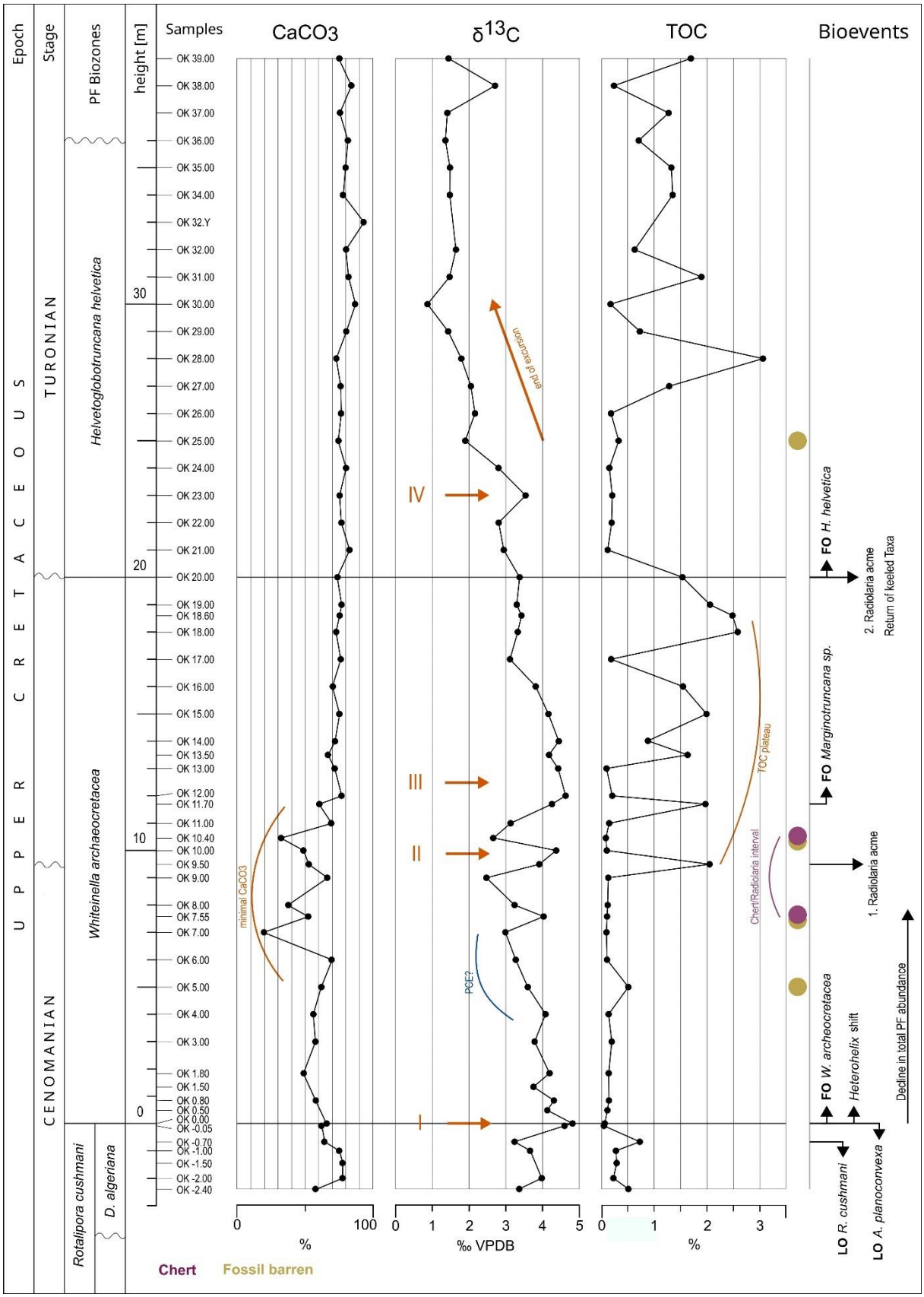

Figure 9 *Profile of the Oued Kharroub section. $CaCO_3$, $\delta^{13}C_{carb}$, TOC and bioevents along the whole section. Coloured dots indicate fossil barren (yellow) and chert (purple) layers. Numbers I-IV mark the carbon-isotope peaks.*

6.7 Geochemical Data

The geochemical data obtained from the Oued Kharroub samples include Carbonate content ($CaCO_3$), total organic carbon (TOC) and stable isotope $\delta^{13}C$.

6.7.1 Calcium Carbonate ($CaCO_3$):

The carbonate content of the samples along the section mostly lies between 70 and 80% (see fig. 9). However, the rough trend shows a trough between -0.70 and 11.70, as well as a very low value in the lowermost sample -2.40 of ~57%. After values decline from -0.70 upwards, there are some considerable minima, where carbonate values fall to ~19 to 40%. The lowest percentages are found in 7.00 and 10.40. Within the trough, some higher carbonate values are found in 6.00 and 9.00 close to 70%, therefore still lower than the average value of the upper part. The lower CaCO3 values between -0.70 and 11.70 are synchronic with the transition from *R. cushmani* zone to *H. helvetica* zone, represented by the *W. archeocretacea* zone, and thus surrounding the time of the C/T boundary. For the most part, the reduction of carbonate values in that timeframe is not very high, except for the few minima mentioned. Above meter 11.70, the carbonate values are fairly steady, and slightly increasing up to around 80-90%. The only value above 90% is 32.y, which represents the Thrombolite sample.

6.7.2 Total Organic Carbon:

The trend of total organic carbon content in this section shows an obvious delay compared to the CaCO3 trend. With the exception of a small peak at -0.70 (~0,7%), TOC values remain very low until meter 9.50, with small peaks at -0.70 and 5.00. From there on, several distinct peaks appear, with values in-between the peaks being very low. Minima are among others also represented by the light-coloured fossil barren samples 7.55 and 10.40, which also contain layers of chert. The peaks, with values from around 1,5 - 2,5% TOC, correlate with the aforementioned darker colour of these samples; namely 9.50, 11.70, 13.50, 15.00, 16.00, 18.60. The timeframe of higher TOC content is therefore clearly starting after the trough in the CaCO3 content curve. The highest TOC value (~3%) is at 28.00, a singular peak, above a part of the section with TOC values close to zero. Above that, values remain high relative to the lower part of the section, but unsteady. There seem to be two areas or timeframes,

where TOC values rise to considerable values. These are from 9.50 to 20.00 and 27.00 to 39.00.

6.7.3 $\delta^{13}C_{carb}$:

The $\delta^{13}C_{carb}$ values over the section display a positive excursion in form of a plateau of high values that reaches from 0.00 to 17.00 (Fig. 9). The values within that part of the section are not steadily high but rarely fall below 3‰. Three peaks are considerable within the named plateau. The first (I) is at 0.00 (4.81‰). 9.50 and 10.00 (II) (4.36‰) constitute a double peak, which is treated as one peak here. The third peak (III) is around 11.70-12.00 (4,62‰), where values remain high 1-2 meters above and at 11.70. Values stay at about 4‰ up to meter 14.00. A minor peak at 7.55 lies between peak 1 and 2. The whole *W. archaeocretacea* zone is characterized by high values (plateau). Within the plateau, a slight trough can be made out from 0.00 to 10.00. Samples 7.00, 9.00 and 10.40 show minimal values within the plateau. After the decline, the 4th, a little smaller peak at 23.00 (IV) could be observed. Above that point, values decline strongly, with one last sample showing an elevated value at 38.00. The plateau, especially the part between 0.00 and 12.00 mirrors the $CaCO_3$ trend along the section. $CaCO_3$ values are generally low where $\delta^{13}C_{carb}$ values are high. As the section begins with already elevated values, the onset of the excursion is not seen here. Values below the first peak suggest that the base of the section lies within the first increase of $\delta^{13}C$ values. Values return to being lower than at the base at 17.00, and after peak-IV again at 25.00. The extended plateau can therefore also be considered lasting from 0.00 to 23.00 encompassing the four detected peaks shown in fig.9.

PLATES

Plate 1

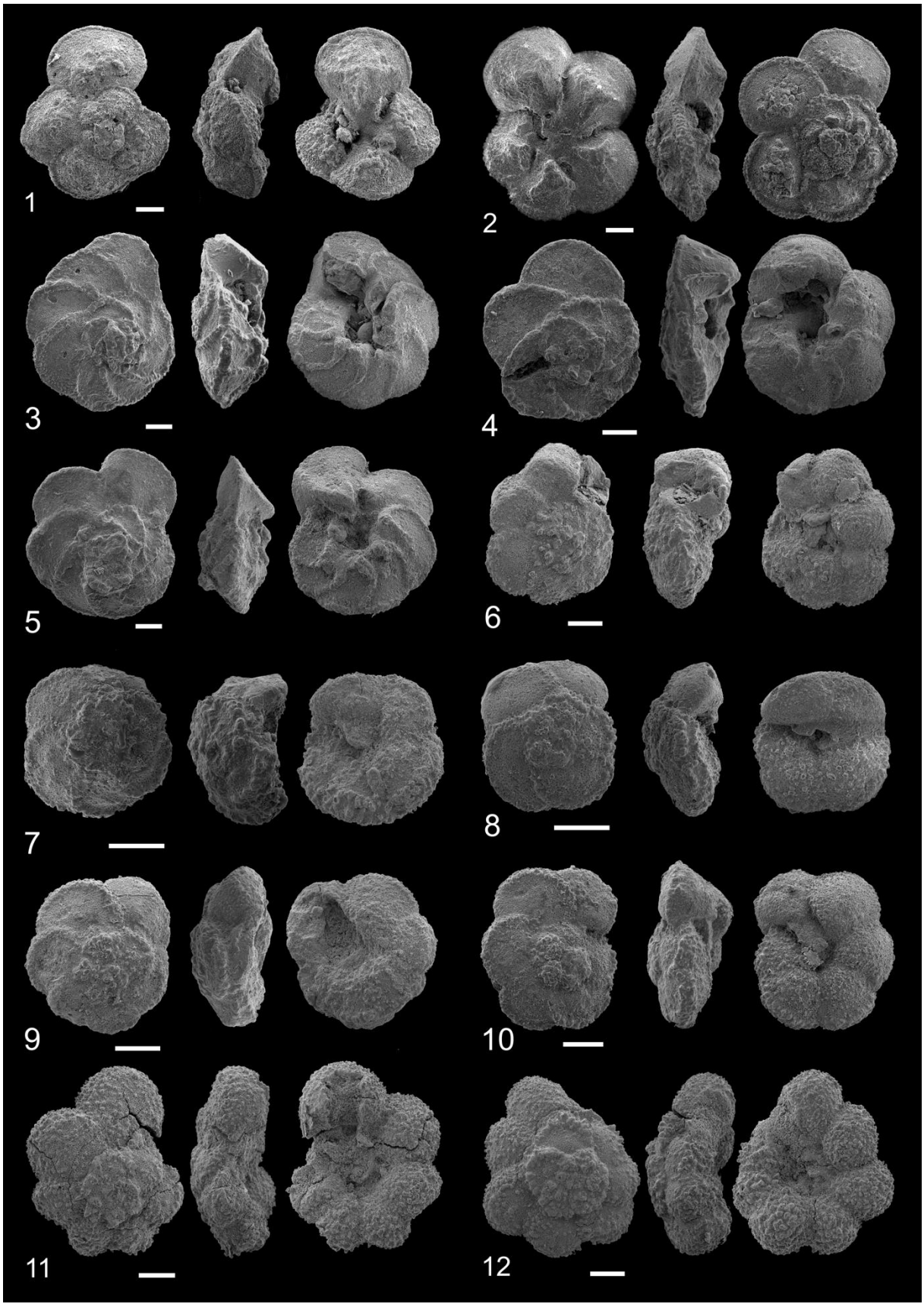

Figure 10 **Plate 1**, Scale bars = 100µm.

1. *Rotalipora cushmani* (Morrow, 1934) (OK -2.40); 2. *Rotalipora cushmani* (Morrow, 1934) (-2.40); 3. *Rotalipora greenhornensis* (Morrow, 1934) (OK -2.40); 4. *Rotalipora deeckei* (Franke, 1925) (OK -2.40); 5. *Rotalipora globotruncanoides* Sigal, 1948 (OK -1.50); *Rotalipora micheli* (Sacal & Debourle, 1957) (OK -0.70); 7. *Dicarinella algeriana* (Caron, 1966) (OK -1.50); 8. *Dicarinella algeriana* (Caron, 1966) (OK -0.70); 9. *Dicarinella imbricata* (Mornod, 1950) (OK -1.50); 10. *Dicarinella hagni* (Scheiberova, 1962) (OK -0.70); 11. *Dicarinella imbricata var.* (OK 9.50); 12. *Dicarinella aff. imbricata* (OK 9.50).

Remarks

(1, 2):

Two typical morphotypes of *R. cushmani* from the base of the section. Specimen 1 is slightly more convex in the edge view. Moreover, it only has 4 chambers in the last whorl compared to 5 chambers in specimen 2. Accessory apertures at the sutures on the umbilical view are seen in both specimens. Large grouped pustules located at the center of the chamber on the umbilical, as well as spiral side of the chambers are well preserved.

(9, 11, 12):

Dicarinella imbricata shows different morphotypes. (9) shows one from the Cenomanian part of the section, with a low to moderate coiling axis. (11) shows a variate form of *D. imbricata*, which occurs from 9.50 onwards. Chambers are inflated more strongly and the two keels diverging towards the next chamber in the edge view is less distinct, though still visible.

D. aff. *imbricata* (12) shows two keels on the first chambers, visible on the spiral side, while not displaying proper keels on all chambers of the last whorl, except for the first chamber of the last whorl, as seen in edge view, which shows a second keel. Thus, it resembles *D. imbricata* var. (11), but cannot be surely assigned to the species, as key characters are missing. As seen on the spiral view of the specimen, chambers of the last whorl are flattened on the spiral side and almost hemispherical on the umbilical side and slightly tilted. The general morphology and outline resemble the ones of non-keeled genera like *Whiteinella* or *H. praehelvetica*. Notice the large size of *D.* aff *imbricata*.

Plate 2

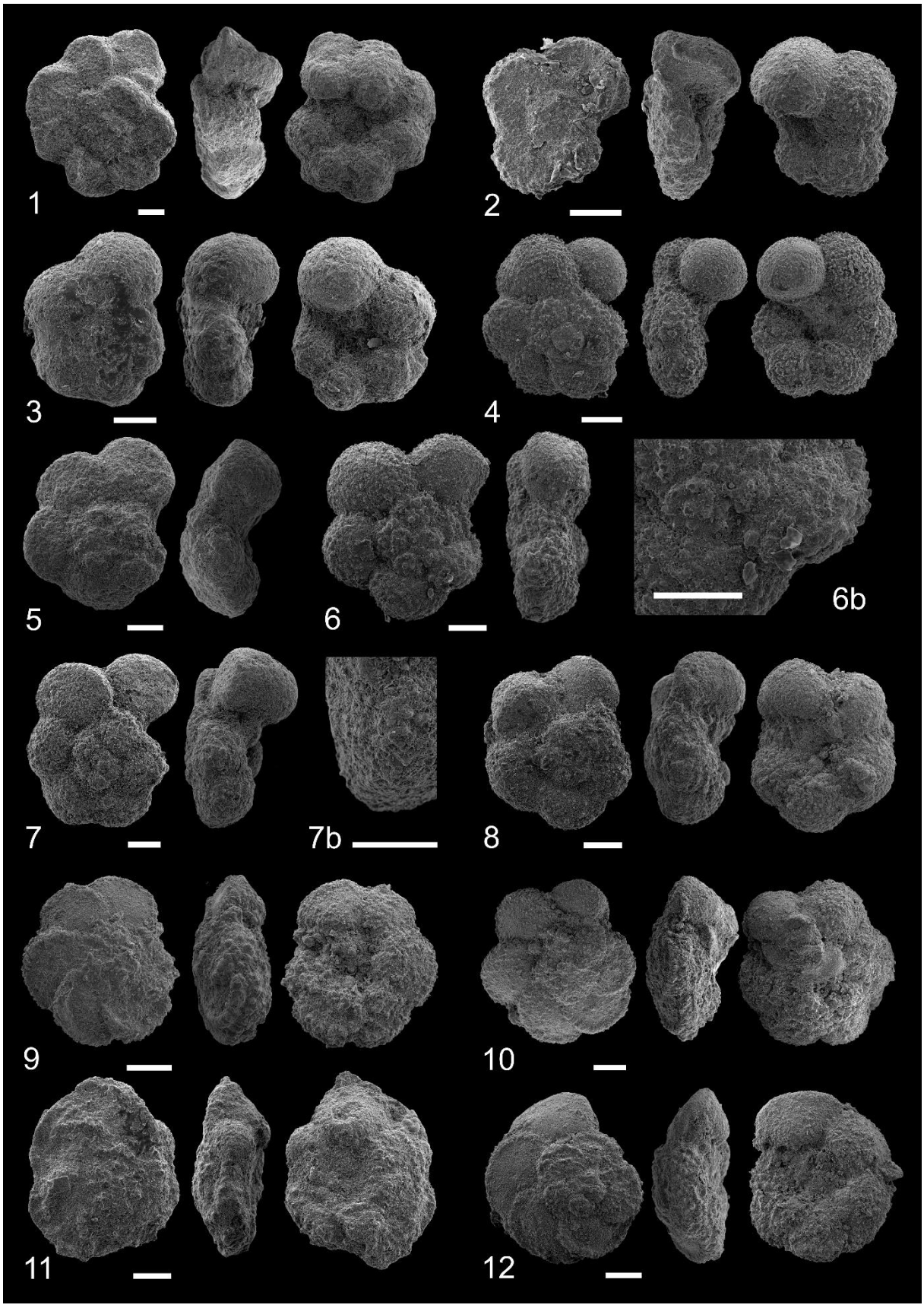

Figure 11 **Plate 2**, Scale bars = 100µm

1. *Dicarinella elata* Lamolda, 1977 (OK 11.70); 2. *Dicarinella* aff. *elata* (OK 11.70); 3. *Helvetoglobotruncana praehelvetica* (Trujillo, 1960) (OK 18.60); 4. *Helvetoglobotruncana praehelvetica* (OK 13.50); 5., 6. & 7. *Helvetoglobotruncana* sp. (OK 11.70), 8. *Helvetoglobotruncana* sp. (OK 11.70); 9. *Helvetoglobotruncana helvetica* (Bolli, 1945) (OK 20.00); 10. *Marginotruncana marginata* (Reuss, 1845) (OK 13.50); 11. *Marginotruncana renzi* (Gandolfi, 1942) (OK 20.00); 12. *Marginotruncana renzi* (OK 36.00); 13. *Marginotruncana schneegansi* (Sigal, 1952) (20.00)

Remarks

(1)

A very large specimen of *D. elata*. Sizes like this are typical for the species occurring here. There are however also many specimens, where the double keel is developed (or preserved) much more clearly. In those specimens, the angle in which the chambers dip from the spiral "plane" (see edge view), tend to be narrower.

(2)

This form only occurs at 11.70 and somewhat fits descriptions of *D. elata* in the literature. However, it has only 4 chambers in the last whorl, and is significantly smaller. It may represent a juvenile form of *D. elata*, which would fit the generally high abundance of the species in this sample, but the much faster chamber growth compared to specimen (1) rather points to a variation or different species altogether. Due to the affinity towards *D. elata* in the chamber shape it is therefore assigned as "*D*. aff. *elata*", but it cannot be placed within this species with certainty.

(3)

Morphotype of *H. praehelvetica* that is common throughout the section. Last chamber is not lowered in the manner typical for the other morphotype of the species. 5 chambers in the last whorl.

(4)

Morphotype of *H. praehelvetica* occurring from 9.50 onwards. General shape differs from (3) (*H. praehelvetica*). 6 chambers in the last whorl. Keel does occur in the first chambers

of the last whorl, but becomes less distinct in later chambers, especially, the last, slightly lowered chamber.

(5)
Specimen resembling *Falsotruncana (loeblichae, douglasi)* (Petrizzo et al. 2022), but lacking a second keel.

(6, 6b)
Transitional form of *Helvetoglobotruncana* with keel in the earlier chambers of the last whorl. General outline resembling *W. aprica* - type. Also resembling *Falsotruncana maslakovae* (Petrizzo et al. 2022) or *Falsotruncana douglasi* (Mikrotax.org), but lacking a distinct second keel in earlier chambers of the last whorl. Aperture extra-umbilical. Closeup displays distinct keel in first chambers of the last whorl.

(7, 7b)
Transitional form of *Helvetoglobotruncana* strongly resembling *H. helvetica*, but lacking keel throughout all chambers of the last whorl. Chambers are subrounded and hemispherical

(8)
H. helvetica type from 20.00, showing keel throughout the last whorl of chambers, as well as remnants of typical flaps extending throughout the wide umbilicus.

(10, 11)
Two morphotypes of *M. renzi*. (11) resembles morphotypes of *D. elata* (*D marianosi*) provided at mikrotax.org. However, the umbilical view shows elevated sutures, and slight ridges on the top of the umbilical side of the chambers.

Plate 3

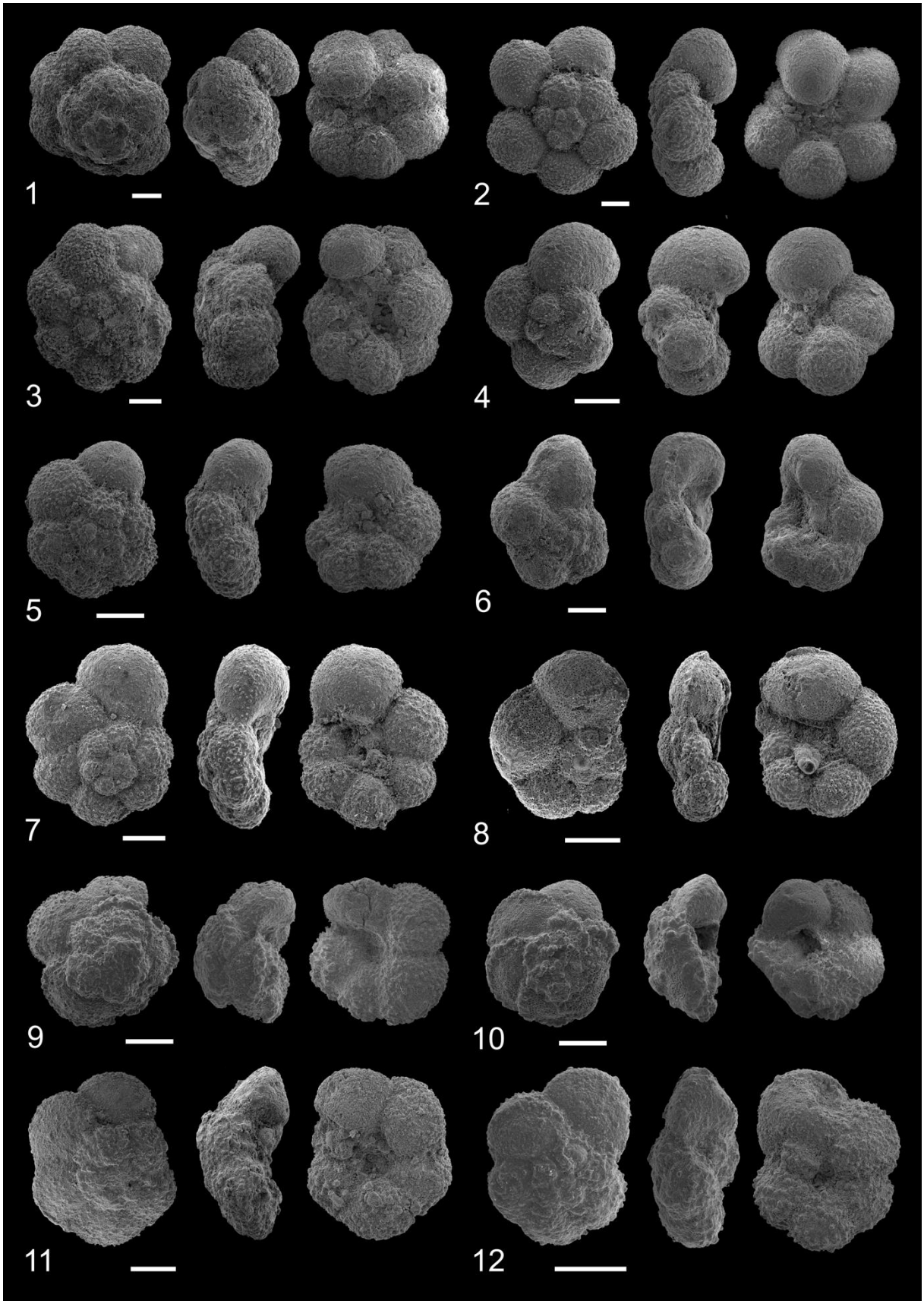

Figure 12 **Plate 3**, Scale bars = 100µm.

1. *Whiteinella paradubia* (Sigal, 1952) (OK 13.50); 2. *Whiteinella aprica* (Loeblich & Tappan, 1961) (OK 16.00); 3. *Whiteinella brittonensis* (Loeblich & Tappan, 1961) (OK 20.30); 4. *Whiteinella baltica* Douglas & Rankin, 1969 (OK 13.50); 5. *Whiteinella aumalensis* (Sigal, 1952) (OK 16.00); *Whiteinella inornata* (Bolli, 1957) (OK 18.60); 7. *Whiteinella archaeocretacea* Pessagno, 1967 (OK 16.00); 8. *Whiteinella archaeocretacea* (OK 0.00); 9. *Praeglobotruncana gibba* Klaus, 1960 (OK -2.40); 10. *Praeglobotruncana stephani* Gandolfi, 1942 (OK -0.70); 11. *Praeglobotruncana hilalensis* Barr, 1972 (OK 20.30); 12. *Praeglobotruncana delrioensis* Plummer, 1931 (OK -1.50).

Remarks

(7, 8):

Two specimens of *Whiteinella archaeocretacea*, a species, which becomes larger upwards the section. A thin keel on the last chamber somewhat extending towards the first chamber of the last whorl can be observed in specimens of the lowest occurrences of the species. Specimens of the upper part of the *W. archaeocretacea* zone show slightly higher coiling axis and more inflated chambers, but within the morphological variability displayed in Mikrotax.org, compiling various publications. Umbilicus is wide and shallow in both specimens. (7) shows a small lip at the umbilical aperture border.

Plate 4

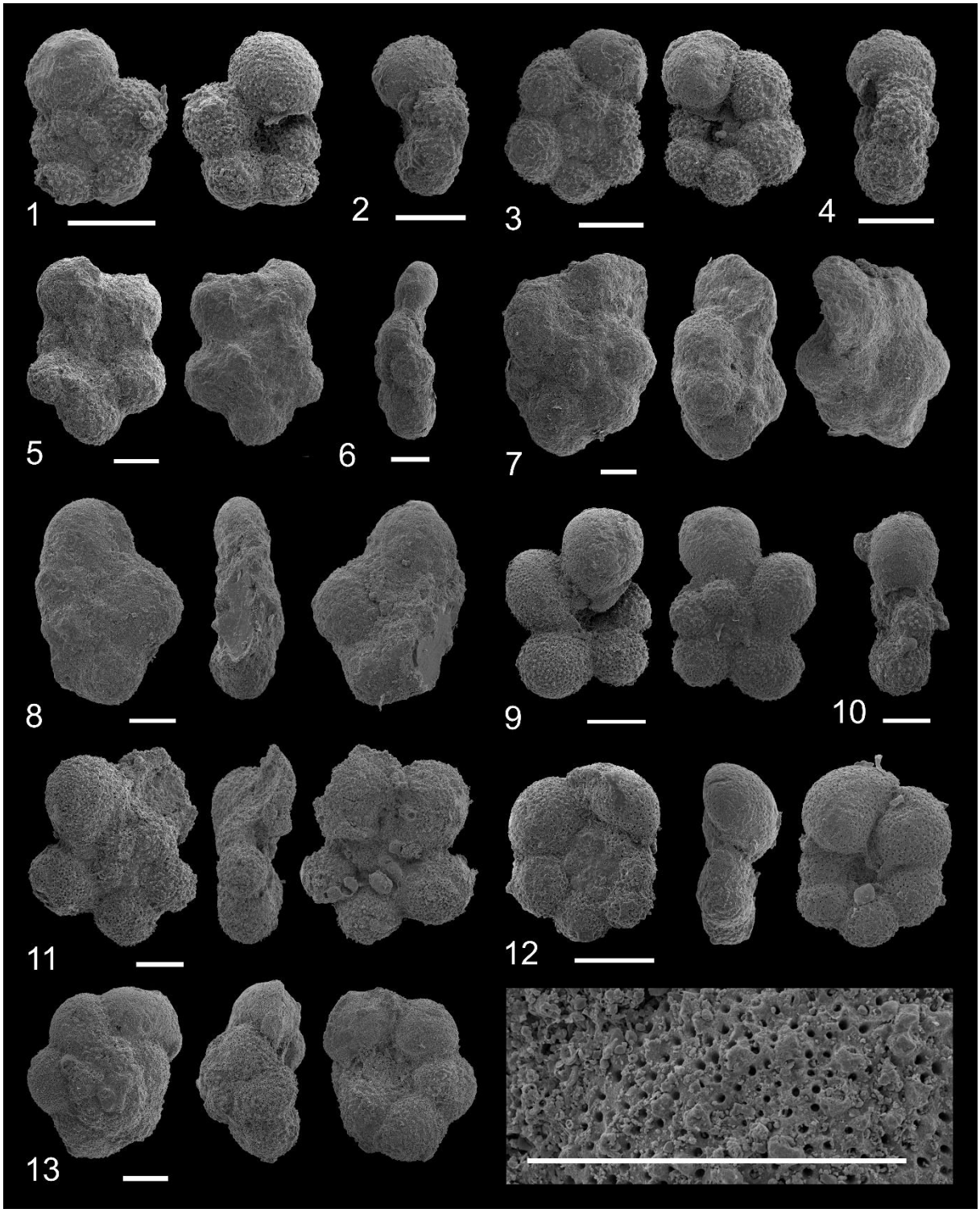

Figure 13 **Plate 4**, Scale bars = 100µm.

1. *Muricohedbergella delrioensis* (Carsey, 1926) (OK -2.40); 2. *Muricohedbergella delrioensis* (OK -1.50); 3. *Muricohedbergella planspira* (Tappan, 1940) (OK -0.70); 4. *Muricohedbergella planspira* (OK -1.50); 5. *Muricohedbergella hoelzli* (Hagn & Zeil, 1954) (OK 36.00); 6. *Muricohedbergella hoelzli* (OK 18.60); 7. *Muricohedbergella kyphoma* (Hasegawa, 1999) (OK 36.00); *Muricohedbergella flandrini* Porthault, 1970 (OK 36.00); 9. *Clavihedbergella amabilis* (Loeblich & Tappan, 1961) (OK -0.70); 10. *Clavihedbergella amabilis* (OK -0.70); 11. *Clavihedbergella sp*. (OK 0.00); 12. *Loeblichella hessi* Pessagno, 1962 (OK 0.00); 13. *Anaticinella planoconvexa* Longoria, 1973 & Closeup (right) (OK 0.00)

Remarks

(9, 10):
The typical morphotype of *Clavihedbergella* found in upper Cenomanian samples of the section (i.e. *R. cushmani* zone), that vanish above 0.00. Counted data does not differ species of *Clavihedbergella* in this study, yet it is worth mentioning that *C. amabilis* is the dominant species of this genus in the OK section.

(11):
This morphotype of *Clavihedbergella* only occurs with a single specimen in 0.00 and 16.00. It strongly resembles the specimen classified as *Eohastigerinella subdigitata* by Gebhart et al. 2010; and partly the ones displayed in Premoli Silva & Verga (2004), although chambers are less elongated. It shows affinity to *Clavihedbergella simplex* as described by Pessagno (1967) (mikrotax. org) and *Clavihedbergella subdigidata* specimens (mkrotax.org).

Plate 5

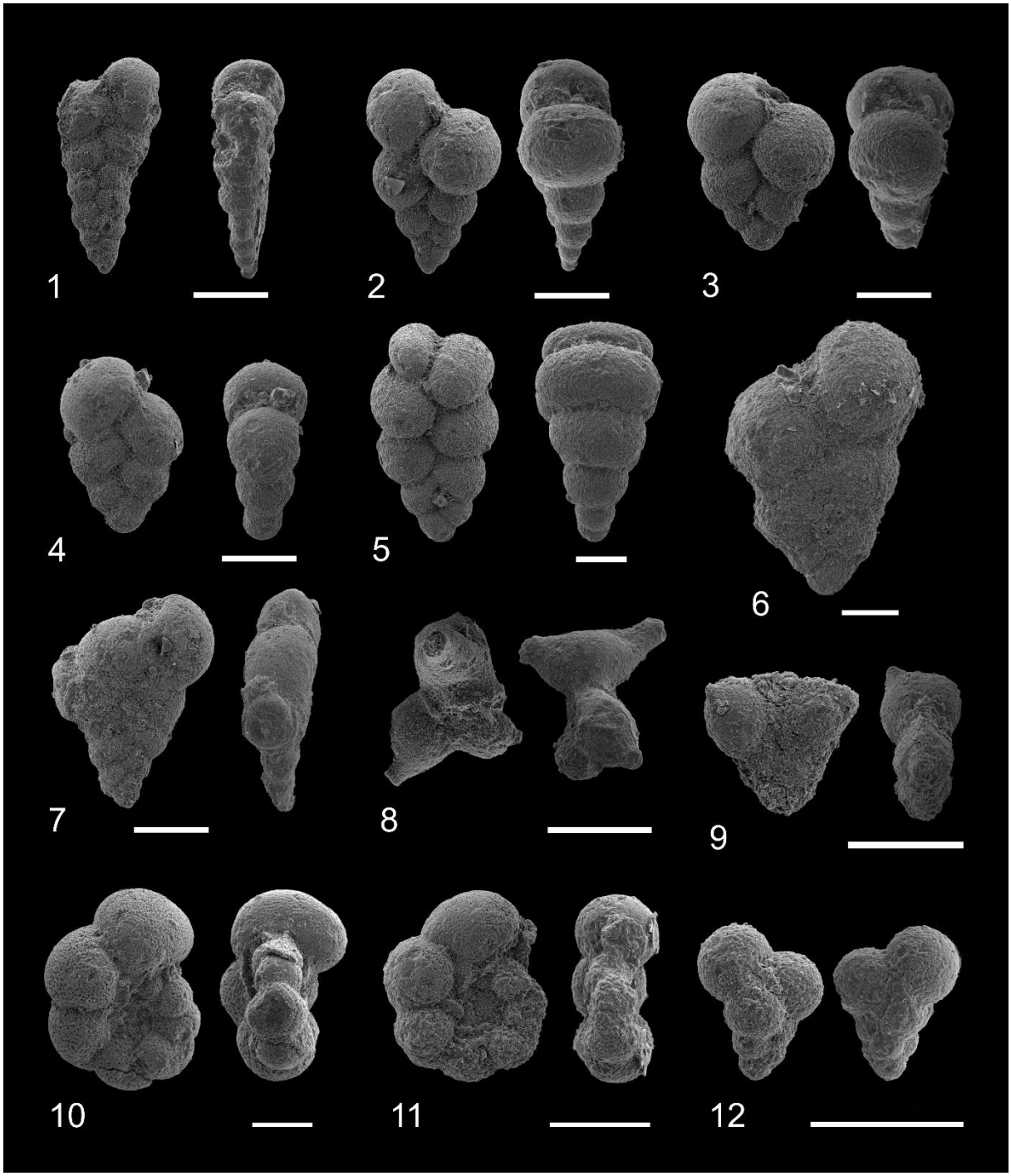

Figure 14 **Plate 5**, Scale bars = 100µm

1. *Heterohelix moremani* (Cushman, 1938) (OK -1.50); 2. *Heterohelix reussi* (Cushman, 1938) (OK 13.50); 3. *Heterohelix globulosa* (Cushman, 1938) (OK 16.00); 4. *Heterohelix* sp. (OK 20.30); 5. *Heterohelix* sp. (OK 16.00); 6. *Heterohelix* sp. (large) (OK 36.00); 7. *Pseudoguembelina costellifera* Masters 1976 (36.00); 8. *Schackoina multispinata* (Cushman & Wickenden, 1930) (OK 16.00); 9. *Schackoina cenomana* (Schacko, 1897) (OK 11.70); 10. *Macroglobigerinelloides bentonensis* (Morrow, 1934) (OK -1.50); *Macroglobigerinelloides sp*. (-0.70); *Guembelitria cenomana* Keller, 1935 (OK 11.70)

Remarks

(2,3)

H. reussi and *H. globulosa* are sometimes grouped together by authors as they are very similar. Here the classification criterion was the faster increase in chamber size of *H. globulosa* compared to *H. reussi*, resulting in a somewhat less elongated shape of the specimen.

(5)

This is a morphotype of *Heterohelix*, which only occurs in the uppermost part of the *W. archaeocretacea* zone and the *H. helvetica* zone. It is relatively large compared to other biserial foraminifera at this stage (16.00).

(6)

A specimen of *Heterohelix* (presumably *H. reussi*) from the uppermost sample, added to the plate to illustrate the immense growth in size of heterohelicids in the upper part of the section compared to the Cenomanian. However, the smaller specimens (<125µm) still make out the vast majority of heterohelicids.

7. DISCUSSION AND INTERPRETATION

7.1 General Remarks on Material and Section

The sequence of macroscopically similar dark grey calcareous marls and black shales in the studied section at Oued Kharroub are typical for the dark C/T-deposits of Tunisia, although the general TOC content in this section (< 3 %) is rather low compared to other C/T sections of Tunisia and the Bargou area, where a maximum of 13% can be reached (Lüning et. al 2004, Soua et al. 2009). The overall appearance of the section, apart from the different microfossil contents, suggests a rough division into three parts. The first being the three lowermost samples, slightly lighter grey in colour, also reflected in a low organic matter content (~ 0.3 - ~ 0.7 %). The second are samples that are much darker, also showing the highest TOC values with up to 3 %, and a high number of dark brown- and red metallic shiny components (probably pyrite). These fall with the exemption of OK 20.30, into the part of the section where $CaCO_3$ values are the lowest and radiolaria are significantly abundant. Two of these samples (7.55, 10.50), excluded from the microfossil study due to their being fossil barren, also contain layers or nodules of silica (Fig. 9). The occurrence of silica in these C/T-deposits is, as the increased content of organic matter, linked to eutrophic conditions, and oxygen depletion (Soua et al. 2011). The SiO_2 (chert) occurrences in this section at 7.55 and 10.40 are likely to originate from silica-secreting organisms. The highest abundance of Radiolaria occurs at 9.50, right between the two SiO_2 layers. 5.00 and 25.00 are similar to 7.55 and 10.40 in their appearance and lack of microfossils, but lack chert-layers. The dissolution in these samples seems to be independent from chert occurrences. The third kind are the majority of the samples from 11.70 upwards, black shales with comparably high TOC, but no silica accumulations, and few Radiolaria. Considering the fact, that the general composition and geochemical signals in the material do not suggest a major change until the uppermost sample OK 36.00, it is fair to assume that, the whole section represents the Bahloul Formation. A thickness of a little less than 40 m is not entirely uncommon for the Bahloul Formation in northern central Tunisia (Lüning et al. 2004).

However, it is uncertain how far the Bahloul Formation reaches into the Turonian compared to other OAE-2 sites (See chapter 7.2).

The general state of preservation could be described as "frosty" as meant by Sexton et al. 2006. There are, however, different stages to be seen in planktic foraminifera of this section (Fig. 15), where the lowermost, Cenomanian, samples show a better preservation than the ones further upwards in the section. The "frosty" appearance is common for planktic foraminifera from Cretaceous hemi-pelagic / pelagic deposits (Sexton et al. 2006), and the samples at hand do not represent an exception. Apart from the samples that are impaired to a higher degree by dissolution, the samples OK 9.50, and 11.70 stand out in their general appearance of being darker and foraminifer tests in these assemblages often contain metallic components and many tests are partly dissolved and very easily breakable. This phenomenon is not present further upwards and the number of metallic components (presumed Pyrite) and occurrence of metallic recrystallization in foraminifer tests decreases. This further shows that this part of the section differs quite significantly from the rest, which is also displayed in the geochemical data (see Fig. 9).

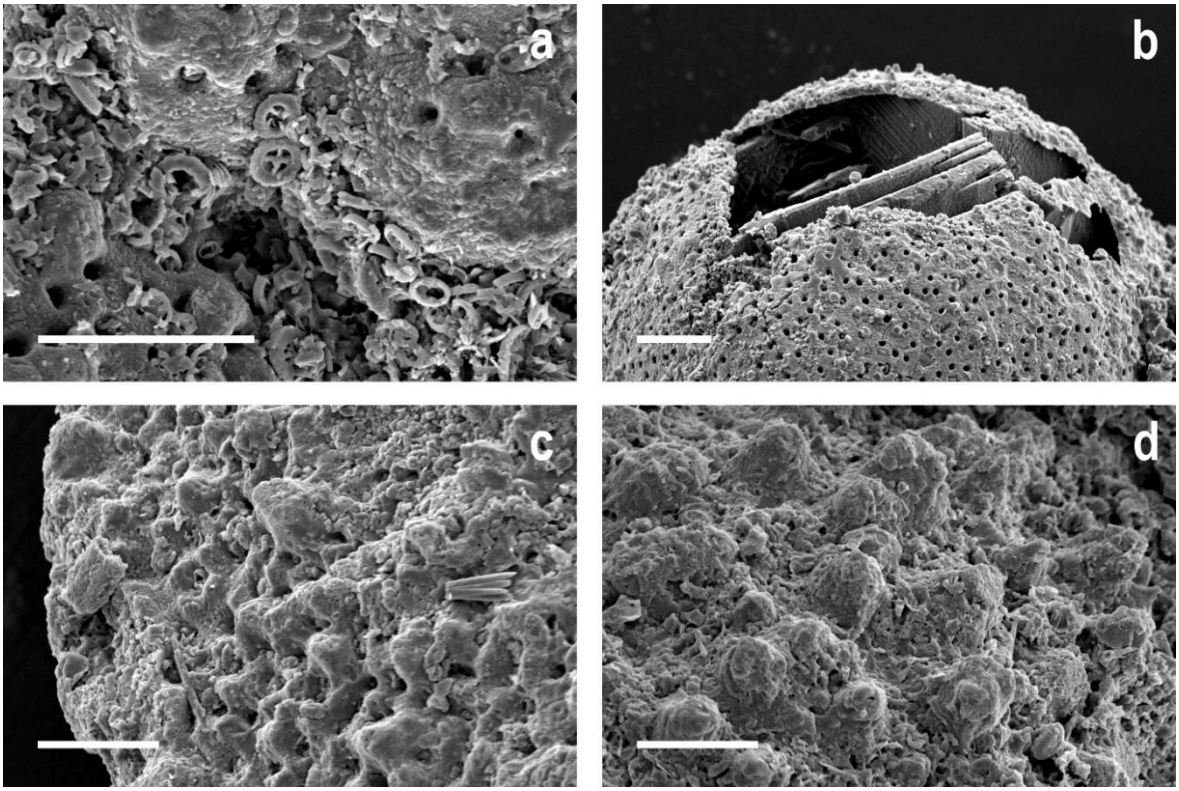

Figure 15 *Closeups of the test surfaces. Nannofossils (Prediscosphaera spp.) on W. archaeocretacea (OK 0.00) (a); partly broken test (OK 0.00) (b); R. cushmani (OK -2.40) (c) and W. aprica (OK 16.00) (d). Surface features are slightly better preserved on tests in assemblages of the base of the section than in samples further upwards. Scale bars = 20µm.*

Individual per gram data has been calculated but is in some of the samples not an ideal representation, due to the impaired preservation and secondary dissolution. Especially the counts for 0.00, 11.70 18.60 and 36.00 are to be mentioned here. The corrected data for 18.60 specifically, seems to be of little value, as the numbers do not fit the otherwise great similarity to 11.70. However, this only concerns total numbers per sediment and the general picture in percentages of these impaired samples do contain valuable information, even if its data may be slightly less accurate, as one cannot be sure, if undissolved clumps contain different microfossils in an evenly distributed manner.

7.2 Biostratigraphic Interpretation: Bioevents and Faunal Turnovers

Recorded bioevents in chronological order (from bottom to top):

1.	LO *R. cushmani*	-0.70
2.	Exit of *Mg. bentonensis (?)* - "eclipse of macroglobigerinelloids"	-0.70 - 11.70
3.	FO *W. archaoecretacea*	0.00
	FO *H. praehelvetica*	0.00
	LO *A. planoconvexa*	0.00
4.	*Heterohelix* shift	0.00
5.	1st Radiolaria acme;	9.50
	1st (slight) return of keeled taxa	9.50
	FO *D. elata, D.* aff. *imbricata*	9.50
6.	FO *Marginotruncana sp.*	11.70
7.	2nd Radiolaria acme	20.00
	2nd return of keeled taxa	20.00
	FO *H. helvetica*	20.00
	FO *Marginotruncana schneegansi & M. renzi*	20.00

7.2.1 Upper Cenomanian - *R. cushmani* zone

The lowest part of the section is situated in the uppermost Cenomanian in the *Dicarinella algeriana* subzone of the *Rotalipora cushmani* zone, as indicated by the presence of *R. cushmani* as well as *D. algeriana* in the lowermost sample OK -2.40. This suggests an approximate age, derived from the zonation scheme used in Premoli Silva & Verga, 2004, of roughly about 96-94 Ma, which spans the *Dicarinella algeriana* subzone. The scheme derived from *mikrotax.org* (Fig. 5) suggests a similar age. A typical feature of the end of this zone, as also observed in this section, is the eclipse of *Macroglobigerinelloides* (Scopelliti et al, 2003; Falzoni & Petrizzo, 2020; Coccioni & Luciani, 2004 i.a.), which occurs just at the end of the *R. cushmani* zone, synchronous to the extinction of *Rotalipora*. However, one specimen of *Macroglobigerinelloides* was found in the small size fraction, slightly delaying this eclipse respective to the LO of *R. cushmani*. The "*Rotalipora* crisis" (Coccioni & Luciani, 2004) that precedes their extinction is represented in the OK section. Although other accounts of planktic foraminifera assemblages just before the end of this zone describe a much less diverse and stress-characterized assemblage (Coccioni & Luciani, 2004, Zaghbib-Turki & Soua, 2013, Gebhart et al. 2010), considering the abundance of equilibrium genera like *Rotalipora* or *Praeglobotruncana*, which both make out large quantities of planktic foraminifera in this zone. The overall picture of this zone is very much in accordance with recent work on Tethyan OAE-2 assemblages (Zaghbib-Turki & Soua, 2013; Coccioni & Luciani, 2004, Gebhart et al. 2010). The immense abundance of *R. greenhornensis* compared to other species of the genus, seems to be a speciality of this section. Furthermore, its LO is usually stratigraphically lower than the one of *R. cushmani* (Falzoni et al. 2018), whereas it lies here in the same interval.

7.2.2 C/T-Transition - *W. archaeocretacea* zone

The beginning of the *Whiteinella archaeocretacea* zone is marked clearly by the abrupt extinction of the genus *Rotalipora* with its last occurrence in OK -0.70. The sample 0.00 shows the first appearance of *W. archaeocretacea*. Also *W. praehelvetica* first occurs at 0.00. Considering the exact Cenomanian-Turonian boundary, as for the biostratigraphic indications, the range of uncertainty remains rather large. This is due to the fact that the two subsequent samples (OK 5.00 and OK 7.55) could not be counted as they are even more affected by dissolution and completely lack any preserved microfossils. The LO of

Anaticinella planoconvexa, being the most commonly used indicator for the Cenomanian-Turonian boundary among planktic foraminifera (Caron et al. 2006) can therefore unfortunately not be reliably used, as is it likely that the C/T-boundary actually lies well above its last occurrence in OK 0.00. Moreover, the species *A. planoconvexa* is rather obscure and very rare in this section. However, it lies just below and thus roughly coincides with the onset of the proliferation of *Heterohelix* in the *W. archaeocretacea* zone, which is a well-documented feature in OAE-2 sites (Caron et al. 2006; Robaszynski et al. 2010; Zaghbib-Turki & Soua, 2013 i.a.). *Macroglobigerinelloides* is absent in the intervals above -0.70, but reoccurs in 11.70, though only with one single counted specimen.
The LO of *Mg. bentonensis* is usually suggested to be within the lower part of the *W. archaeocretacea* zone (Zhagbib-Turki & Soua, 2013; Falzoni & Petrizzo, 2020). Falzoni & Petrizzo (2020) recorded the timeframe of the *Globigerinelloides* eclipse (i.e. *Macroglobigerinelloides* eclipse) to contain the C/T-boundary, which supports the hypothesis, that in the present section this occurs before 9.50 or 11.70 respectively. Isotope data, however, points to a later C/T boundary, considering similar Tunisian sections (see 7.3.3). Furthermore, the LO of *Mg. bentonensis* has been found to be a rather reliable marker for the uppermost Cenomanian (Falzoni et al. 2018). *Mg. bentonensis*, as the whole genus, is absent with the exception of one specimen in the smaller size fraction, suggesting that this is near the local LO of *Macroglobigerinelloides* (Fig. 8). The genus only occurs very rarely afterwards with one specimen each in 9.50 and 11.70 before another eclipse of the genus takes place until 18.60. Given this ambiguous signal, it cannot be reliably used as a marker for the C/T-boundary in this section.

The increasing abundance of *Heterohelix* during the OAE 2 is typically referred to as "*Heterohelix* shift", or "*Heterohelix* dominated assemblage" (Caron et al. 2006), a change in the assemblages that is also associated with a proliferation of *Whiteinella*. In the section, this is documented quite well, not only in numbers but also reflected in species diversity (Fig. 7). The onset of the "*Heterohelix* shift" is placed here at 0.00. The percentages of *Heterohelix* and *Whiteinella* genera show an obvious and significant increase between the samples OK 0.00 and OK 9.50. It is therefore set here form 0.00 onwards, where a stronger increase begins (Fig. 8). It is however noteworthy, how developments differ between the smaller and larger size fractions (Fig. 8). In higher levels of the section, *Heterohelix* is of great dominance in numbers, however, this is impaired at 9.50 by the high abundance of Radiolaria. The abundance of *Heterohelix* specimens increases further up in the larger size

fraction but reaches its peak with almost 100% in the smaller size fraction. The *Heterohelix* shift is apparent throughout the *W. archaeocretacea* zone, together with the proliferation of *Whiteinella* and the diversification of *Dicarinella*, this development in the assemblages is in accordance with the characterization given by Premoli-Silva & Verga (2004). Also coinciding with the rise of heterohelicids is the decline of *Muricohedbergella,* and even before that, the eclipse of *Clavihedbergella* and *Macroglobigerinelloides*. Both of these genera, which inhabit surface waters like heterohelicids, seem to have been replaced by them as it were. *Muricohedbergella* to a lesser degree, as it remains present and quite numerous throughout the early Turonian, as is typical for the zone.

The FO of *Marginotruncana* is reported from different sources to be well below the FO of *H. helvetica* (Falzoni & Petrizzo, 2020), however the proliferation of the genus does not occur within the *W. archaeocretacea* zone, as it remains very rare. Its FO in 11.70 is coinciding with the occurrence of other keeled forms, mainly of the genus *Dicarinella*, which constitutes a peculiar bioevent within the *W. archaeocretacea* zone. The diversification and abundance of *Dicarinella* lasting only a few meters, before the assemblage becomes almost completely dominated by *Whiteinella, Muricohedbergella* and *Heterohelix*. *H. praehelvetica* morphotypes found in this part strongly resemble *H. helvetica* but lack some the definite characters (imperforate, pustulose keel on the penultimate and earlier chambers, relative elevation of earlier chambers on the spiral side) as defined by Huber & Petrizzo (2014). It is worth mentioning that the morphotype of *H. praehelvetica* which has its first occurrence in 9.50 differs quite significantly from the one that is already present at 0.00 (last chamber lowered, more chambers in the last whorl, earlier chambers elevated in respect to outer chambers on the spiral side; see plate 2, nr. 3 & 4 - and related descriptions) and throughout the section. The occurrence of the *H. praehelvetica* occurring from 9.50 onwards could serve as an important secondary biomarker within the *W. archaeocretacea* zone, as it marks a point in this section where planktic foraminifera assemblages show a significant change compared to lower ones. The FO of this species therefore may vary significantly, depending on which morphotype one refers to.

Caron et al. (2006), have stated that the FO of *H. helvetica* coincides with the reestablishment of keeled genera, namely *Praeglobotruncana, Dicarinella* and early *Marginotruncana*. This development could be observed in the sample 9.50, however dicarinellids and *Praeglobotruncana* decline again a few meters above, and the lack of proliferation of keeled

marginotruncanids (Zagbhib-Turki & Soua, 2013) as well as the high abundance of OAE-2 interval-typical dominance of *Whiteinella*, *Muricohedbergella* and *Heterohelix* suggest that even though this short "comeback" of keeled genera occurs, it is still well within the *W. archaeocretacea zone*. It is quite noteworthy that the first resurgence of keeled genera as well as the second, which is synchronous to the FO of *H. helvetica*, are both coinciding with a radiolaria acme (1st and 2nd radiolaria acme, fig. 7 & fig. 9). Furthermore, this part of the section sees two forms that only occur in 9.50 (*D.* aff. *imbricata*) and 11.70 (*D.* aff. *elata*) respectively. Considering the upper part of the *W. archaeocretacea* zone (15.00-18.60), planktic foraminifera assemblages remain relatively similar and lack specific biostratigraphic signals.

7.2.3 Radiolaria Peaks

Considering the major radiolaria peak at 9.50 (fig. 6 & 9), comparisons and correlations with other data seemed viable, as one major peak is quite common in OAE-2 sections (Petrizzo et al. 2022, Petrizzo et al. 2021, Gebhart et al. 2010, Moez et al. 2012 i.a.) and correlates with the other faunal events (i.e. PF). The radiolaria peaks found in other OAE-2 locations typically lie in the lower half of the *W. archaeocretacea* zone (Petrizzo et al. 2021, Petrizzo et al. 2022, Moez et al. 2012, Gebhart et al. 2010) and, just like in the present section, are major components of the assemblages for a short interval during the OAE-2. The major peaks of radiolaria in these sections lying at - or well below - the C/T boundary, within the main phase of environmental perturbation, resemble the data of this section quite well. Although the exact positions vary, the first radiolaria acme at 9.50 is expectedly lying in the lower part of the W. archaeocretacea zone and therefore assigned late Cenomanian age, presumably close to the C/T-boundary. The second, slightly smaller acme of radiolaria can be roughly traced in other sections where secondary peaks do occur (e.g. Petrizzo et al. 2021) just below the FO of H. helvetica. In consideration of the correlations with other OAE-2-level radiolaria occurrences, the C/T boundary in this section can be expected to lie between the two radiolaria acmes.

7.2.4 FO *H. helvetica*

Huber & Petrizzo (2014) concluded in their work about the genus *Helvetoglobotruncana*, that due to its rarity and morphological variability at the base of the *H. helvetica* zone, its use as biostratigraphic marker is questionable and that, on the contrary, their extinction is

very abrupt and seems to be a valuable bioevent. The problems concerning the beginning of the zone can be confirmed hereby in this section. The FO of *H. helvetica* is quite obscure given the morphological similarities of *H. praehelvetica* and transitional or morphologically similar forms (see plate 2). Only detailed investigation with the SEM can yield insight to whether all definitive characters to the species are present. Given Huber & Petrizzo's definition of *H. helvetica*, including the presence of a well-developed keel to the last (lowered) chamber, *H. helvetica* could not be found in 9.50 and 11.70, where many of the transitional forms appear. Still, the faunal assemblage in 9.50 and the following 2 - 4 meters in the section did yield a remarkable return of keeled taxa.

D. elata, has been stratigraphically restricted to a short range, that lies completely within the *H. helvetica* zone as observed in different localities in the past (according to Premoli-Silva & Verga, 2004 and Mikrotax.com). Falzoni & Petrizzo (2020) have stated its occurrence to be ecologically controlled and diachronous. Falzoni et al. (2018) reported various sites where *D. elata* occurs well below the FO of *H. helvetica*, questioning its association with the beginning of the *H. helvetica* zone and thus its use as secondary marker species. In the studied section, *D. elata* occurs only within the interval 11.70 - 13.50, along with *D.* aff. *elata*, just above 9.50, where large specimens of *D.* aff *imbricata*, *D. imbricata* occur. This short return of keeled taxa in the present secition, which is most significantly represented in 11.70, is dominated by dicarinellids, the largest specimens being *D. elata*. Given the shortness of this interval and the returning back to OAE-controlled fauna in the meters above, one is inclined to attribute this occurrence of *D. elata* to a short change in environmental conditions, rather than the major return of keeled taxa that coincides with the beginning of the *H. helvetica* zone, recorded in other OAE-2 sections. Therefore, the findings of this part of the section are in accordance to the conclusion concerning the lack of synchronicity of the occurrence of *D. elata* by Falzoni et al. (2018).

H. helvetica is also diachronous, and occurs earlier in lower latitude sites (Caron et al. 2006). As *H. helvetica* is known to be very rare at the base of the zone (Huber & Petrizzo (2014), it is quite possible that it already occurs in these mentioned samples, where keeled planktic foraminifera first re-occur in the section after the extinction of rotaliporids. The specimens in Plate 2 show different morphotypes, that are very similar to morphotypes of *H. helvetica* given in Huber & Petrizzo (2014) as well as the online database Mikrotax.org and Premoli Silva & Verga (2004). However, they do not show a distinct keel on all chambers of the last whorl. Furthermore, the general outline differs from *H. helvetica* found in literature today.

The different morphotypes of *H. helvetica* varying quite strongly does leave some uncertainty to the picture given here. However, extensive search for the species in the mentioned samples, beyond the 300 counted specimens, was unsuccessful, and even if very rare, it should have been found in this endeavor, if present. Based on the results of this study, it seems quite legitimate to question the usefulness of FO of *H. helvetica* as a biostratigraphic marker. However, the morphotypes of *H. helvetica*, differing strongly in their display of the key characters, as described by Huber & Petrizzo (2014), may be clear more or less, depending which ones can be observed in the respective locality. The FO of *H. Helvetica* in this section is to be seen with some concern, firstly because of its rarity, and secondly as the elevation of inner chambers in respect to outer ones on the spiral side, a key characteristic according to Huber & Petrizzo (2014) are slightly ambiguous due to preservation of the specimens. Given the specimens found, the other faunal and geochemical signals and the section at large, setting the beginning of the *H. Helvetica* zone at 20.00 nevertheless seems reasonable.

7.2.5 Early - mid - Turonian - *H. helvetica* zone and section Top

The beginning of the *H. helvetica* zone (20.00) marks a return of the keeled genera as typical for the beginning of this zone. The suggested age of this bioevent is 93,3 Ma (Caron et al. 2006) *Marginotruncana* occurs, although still in low numbers, with three different species. The diversification of *Marginotruncana* is an event attributed to the middle part of the *H. helvetica* zone (Premoli-Silva & Verga, 2004). This could not be observed in the present section. As the only other sample from this zone (36.00), is strongly impaired by bad preservation, interpretation remains unclear. However, even if species of this sample could only be classified at genus level, a proper proliferation of larger marginotruncanids can be ruled out. This result suggests, that the uppermost sample may still be placed within the lower part of the *H. helvetica* zone.

The obvious characteristic, which could be observed in this uppermost sample and which, again, is in accordance with characterizations given by Premoli-Silva & Verga (2004), is the diversification and further proliferation Heterohelicids. *H. helvetica* could not be identified in this uppermost sample, but on account of the lack of occurrence of marker species for the next zone, it has been attributed to the *H. helvetica* zone. Occurrence of *Mh. flandrini*, whose stratigraphic range begins in the *M. sigali* zone (Premoli-Silva & Verga, 2004) is a

noteworthy feature. There also have been found specimens resembling *Archaeoglobigerina cretacea* in the sample residues. A faint double keel on the last chamber as well as the general outline could hint towards *A. cretacea*, however, the preservation did not allow a certain conclusion concerning the classification and thus the biostratigraphic position concerning this uppermost sample of the section. There is no real indication of a reestablishment of stable environmental conditions, as to be expected after the ending of the OAE-2 in 36.00.

The faunal turnover in the OK section can be clearly observed from 0.00 to 20.00 as in comparison with the typical turnover one would expect from a black shale C/T-locality. The end of the turnover in association with the FO of *H. helvetica*, accompanied with stabilization of environmental conditions, however, cannot be entirely confirmed here. The return of keeled taxa at 20.00 is significant, but OK 36.00 shows an ambivalent picture, given the abundance of *Heterohelix*, the *G. cenomana* acme and the lack of diversification and proliferation of the genus *Marginotruncana*, which may have had environmental restrictions in this particular section. In other OAE-2 sections of Tunisia, the proliferation of *Guembelitria* appears much earlier, in the *D. algeriana* subzone (Zaghbib-Turki & Soua, 2013). According to the biostratigraphical concept of mikrotax.org, the LO of *G. cenomana* lies within the *W. archaeocretacea* zone, which would contradict the scheme created for this section. However, Premoli-Silva & Verga (2004) set the stratigraphical range of the species up to the late Coniacian (upper *D. concavata* zone). Its acme at 36.00, being a "disaster-species" of the OAE-2, however does raise questions concerning the top of the section in relation to the end of OAE-2. The percentual gain of *H. helvetica* respective to *H. praehelvetica* as a feature of assemblages' evolution within the *H. helvetica* zone (Huber & Petrizzo, 2014), does not occur in the OK section; however, this may be a result of too low sample resolution. *H. helvetica* never becomes more frequent here, as it in fact could not be identified in the top sample.

Benthic foraminifera grow in numbers over the upper 20 meters of the section, even though only in the smaller size fraction (see fig. 8). The most common benthic foraminifera in this size fraction are rather small and infaunal forms tolerant of suboxic conditions such as *Praebulimina* (Petrizzo et al. 2022) and *Bicazammina*.

7.3 The OAE II at Oued Kharroub

7.3.1 Microfauna and Paleoenvironment

Based on the relative abundance of planktic foraminifera groups, the assemblage at the bottom of this section (-2.40) is interpreted as still representing one that reflects relatively stable conditions with a rather large abundance of deep dwelling species with complex morphotypes. The high abundance and diversity of oligotrophic, deep dwelling *Rotalipora* and intermediate forms like *Praeglobotruncana* and *Dicarinella* suggest rather stable conditions throughout the water column and no widespread oxygen minimum zone. In this part of the section, the opportunistic *Heterohelix* is rather rare compared to the upper part, which fits the given interpretation. Surface dwelling *Muricohedbergella*, a typical r-strategist is highly abundant, and could hint towards slightly eutrophic surface waters. In this timeframe, at the end of the Cenomanian, there is also benthos present. Although not in significant numbers, some large specimens of benthic foraminifera at the base of the section suggest, that no completely anoxic conditions at the sediment-water surface were present. The P/B-ratio (Fig. 8) is one characteristic for a pelagic setting, far off the coast (Leckie, 1987). This ratio stays roughly the same until benthic foraminifera in the smaller size fraction begin to grow in numbers in the upper third of the section. As this rise of BF is represented by very small elongated, assumed infaunal forms (e.g. *Praebulimina*), oxygen deficiency in the deep water may still be present to some extent at this point.

The general picture given by the assemblages is typical for the deep-water shelf environment attributed to the Bahloul Formation (Lüning et al. 2004). In accordance to the observations made by Coccioni & Luciani (2004) in the OAE-2 section in Italy, the conditions at the base of the section, apparently preceding the peak-stressed conditions of the OAE-2, are stable enough to allow a high diversity and abundance of planktic foraminifera species (see ind/g sediment, fig. 8). Indicators for a more oxygen deficient and eutrophic environment like radiolaria (Ben Fadhel et al. 2012) and typical "disaster-species" like *Guembelitria* and *Schackoina* (Gebhart et al, 2010) are very rare in this part, which differs from some other OAE-2 sections, where *Guembelitria* starts to thrive already in the uppermost *R. cushmani* zone (Zaghbib-Turki & Soua, 2013). The relative decline of the species of the genera *Rotalipora*, *Praeglobotruncana* and *Dicarinella* is seen along these lowest samples, hinting towards the onset of the OAE-2.

The stark contrast in conditions, reflected by the extinction of the genus *Rotalipora*, the disappearance of the intermediate *Macroglobigerinelloides* as well as *Clavihedbergella* and the onset of the proliferation of *Heterohelix* at meter 0.00 leads to an assemblage (see chapter 6) not only differing in species distribution, but also in reduced foraminifera sizes. OK 0.00 lacks larger keeled species, but also *Whiteinella*, which occur in larger sizes further up in the section (especially 13.50 upwards), are rather small. It is the planktic foraminifera assemblage, together with these observations, that suggest an incision in the environmental conditions at that point in time in this section, as expected for the OAE-2.

The microfossil assemblages are typical for a downward expansion of the OMZ, which affects deeper dwelling K-strategists like rotaliporids, who are more sensitive to environmental changes first (Leckie, 1987). The conditions reflected in this sample and in the following ones, do not turn back to pre-OAE-conditions entirely until the top. One key sign in the assemblages are the keeled genera, which, after the extinction of *Rotalipora*, never quite recover in numbers until the top of the section. Another good example yielded by the present assemblages is *Heterohelix*, which, after its proliferation in the *W. archaeocretacea* zone, dominates the assemblages, and does so also in the uppermost sample 36.00, where it even occurs in its largest sizes. *Heterohelix* being an important indicator for a stressed marine environment in depths around and above the thermocline, its dominance in the assemblages, accounts for conditions that are continuously severely stressed. The thriving of surface dwellers such as *Whiteinella* are in accordance with that and are typical (as mentioned in chapter 7.1) for the severe environmental crisis of the short interval around the C/T-boundary. *Whiteinella* is defined as intermediate form by Coccioni et al. (2005) concerning affinity towards oligotrophy, and their proliferation in the upper half of the *W. archaeocretacea* zone points towards slight relaxation in surface waters concerning eutrophy. The high abundance of surface dwellers compared to deeper dwelling PF can also be an indication for shallow marine environments, where no deeper habitat exists. This, however, can be ruled out for the section at hand, as it is well within the global transgression phase recorded for this timeframe, and the basal sample reflects deep-water environment (Lüning et al. 2004).

The OAE-2 in this section is also reflected in the total abundances of planktic foraminifera per gram sediment. The massive decline in these values from 0.00 to 9.50 is characteristic for an environment, where conditions preclude higher abundances. The ind/gram curve

correlates with the TOC content and the plateau of $\delta^{13}C_{carb}$, as seen in fig. 9 and fig.17. Another phenomenon in the assemblages after the onset of the OAE concerns the test sizes. Although the middle part of the *W. archaeocretacea* zone constitutes an exceptional interval, generally, keeled taxa occur in smaller sizes in the upper *W. archaeocretacea* part and also in 0.00. This development is generally known as dwarfism, caused by environmental stress, i.e. oxygen deficiency and eutrophy. Smaller genera being most abundant in numbers is typical for an OAE assemblage.

A peculiar feature of the section is the synchronicity of radiolaria occurrence with keeled genera returns (9.50, 20.00). Although in the first case, the radiolaria acme is slightly below this level. Radiolaria are known to "replace" PF in assemblages at the most severely stressed intervals of OAE-2 sections (Gebhart et al. 2010). Their occurrence is described as characteristic for the OAE-2 "Bonarelli-"level as for the radiolarian tolerance of eutrophic water conditions (Scopelliti et al. 2004). Indeed, the 1st Radiolaria acme is significant in this section. Its coinciding with abundant occurrence of large *D. imbricata* and *D.* aff *imbricata* especially, seems contradictory. It can be argued that this peculiarity is due to a short upward reduction of the OMZ, allowing these larger deep dwellers to prevail. If one considers the fossil-barren samples 7.55 and 10.40, where chert was also found, the interval from 7.55 to 10.40 may constitute the most severe time-interval of the Oceanic Anoxic Event in this section. The mentioned inflation of chambers extending beyond the usual morphospace of *Dicarinella*, may have been an adaption to the stressed conditions, which allowed this specific form to prevail, and maybe migrate further upwards in the water column. However, larger *D. elata* and *D. imbricata* are also found in this timeframe of the section (e.g. 11.70), constituting a somewhat ambiguous signal concerning ecological developments along the OAE-2 in the Oued Kharroub section.

Generally, the expansion of the OMZ and anoxia in deeper waters is well recorded in the microfaunal assemblages of Oued Kharroub. One can assume that after the short appearance of keeled genera in the middle part of the *W. archaeocretacea* zone, conditions must have remained unfavorable for K-strategists / equilibium-genera. The OAE-2 typical disaster species of *Schackoina* show no acme and in fact remain very rare. Coccioni et al. (2005) argue, that the presence of species with elongated chambers and their evolution in general is controlled not only by oxygen availability but also by variations in nutrient availability. The OK section may have had a severe oxygen crisis in the lower water-column, but trophic

conditions which were more oligotrophic compared to other Tethyan OAE-2 sites. This is, as mentioned above, very much supported by the great abundance of large *Whiteinella* throughout the upper *W. archaeocretacea* zone and also further into the *H. helvetica* zone. The *Guembelitria* acme in the uppermost sample constitutes an unusual feature, as it is well above the OAE-2 level and even 16 m above the FO of *H. helvetica*. It may have constituted a local, paleoceanographic phenomenon, that may be an extension of the oxygen crisis for this locality.

7.3.2 TOC, Carbonate versus Silica

TOC contents in this section remain relatively low compared to other Tunisian sites as stated in chapter 7.1 (Lüning et al. 2004). The plateau of high TOC values from 9.50 to 18.60 is clearly delayed as compared with the $\delta^{13}C_{carb}$ signal, as also recorded by Lüning et al. (2004). TOC and $\delta^{13}C_{carb}$ values do not correlate well throughout the section, and TOC even shows some high values well above the stable isotope excursion (Fig. 9), which may be the result of local environmental phenomena, that occurred after the globally recorded increased OM burial, as mentioned in 7.3.1. The correlation of TOC and planktic foraminifera total abundance (per gram sediment) shows a clear trend (Fig. 17). The high value that is far away from the trendline represents the sample 18.60, which as mentioned in chapters 5 and 6 is corrected, and as seen in this graph does not fit with the general trend. The cluster on the left side represents the most part of the *W. archaeocretacea* zone, where increase TOC values coincide with a significant reduction in planktic foraminifera, and all planktonics numbers for that matter. As for the elevated TOC values towards the top of the section (28.00, 31.00), they cannot be correlated with developments in microfaunal assemblages, as these samples were not included in that part of the study. Considering the $\delta^{13}C_{carb}$ signal, these values may be a result of a local phenomena, rather than the global OAE-2 frame. It is noteworthy, how elevated TOC values are not reflected in reduction of carbonate percentages in the sample. $CaCO_3$ rather correlates with the stable isotope values, and even stronger with the occurrence of chert layers and the radiolaria acme.

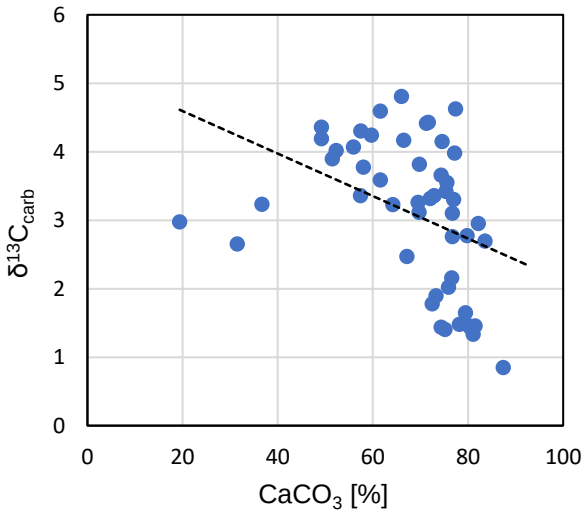

Figure 16 *Correlation diagram showing carbonate content and isotope data correlation. The black dotted line indicates the trend.*

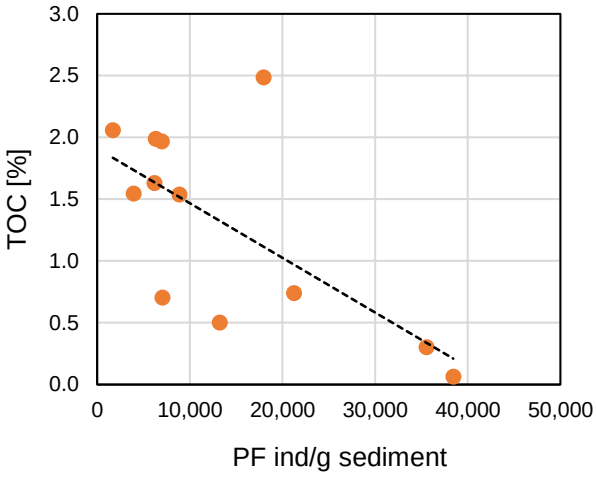

Figure 17 *Diagram showing the correlation of total organic carbon and the total abundance of planktic foraminifera in the assemblages. Samples with high TOC tend to have lower amount of planktic foraminifera per gram sediment.*

7.3.3 Stable carbon isotope correlation

The $\delta^{13}C_{carb}$ peaks, of which usually the first is observed in the upper part of the *R. cushmani* zone and the second in the lower part of the *W. archaeocretacea* zone, still lying in the upper Cenomanian (~93,91 and ~93,86 Ma in the type section Pueblo, USA) (El-Sabbagh et al. 2011), are here slightly more obscure. The first peak (I, fig. 9) at 0.00 after the increase of $\delta^{13}C_{carb}$ values in this section could be correlated to the first peak in Pueblo. Unfortunately, there are no values from further below in the section, but given the biostratigraphic signals of planktic foraminifera, one can assume, that the first peak here, which lies within the frame of the event, is to be seen as the first in comparison of the different sections given by El-Sabbagh et al. (2011), namely Pueblo and three different north-African sites in Morocco and Egypt. It also correlates well with the description given by Soua et al. (2022), in which data from various Tunisian localities have been combined, for their peak "a", which is placed

right above the LO of *R. cushmani*. The minor peak within the trough around 7.55 precedes the major peaks within the $\delta^{13}C_{carb}$ -plateau (Peak II and III, fig. 9). They correspond to the Peak "b" and peak "c" respectively of Soua et al. (2022). The decline of values and the end of this plateau fits the foraminiferal signals roughly, although real stable equilibrium conditions cannot be assumed in this section until the uppermost part of the zone. The decline from the plateau in this sample (upwards from peak III) therefore precedes the biotic signal considering the end of the OAE 2. Zagrarni et al. (2008) defined 4 peaks for the OAE-2 excursion at Oued Bahloul. At Oued Bahloul, this peak coincides roughly with the FO of *H. helvetica*. In the OK section, the 4th peak, which is the last peak, with lower value than the first three and just before values decline significantly. In the OK section this excursion lies three meters above the FO of *H. helvetica*. At the Guern Halfaya section in Tunisia (Soua et al. 2022), the FO of *H. helvetica* lies even further apart from this fourth peak "d". Despite minor differences, the isotopic signal of the present section can be correlated quite well with other Tunisian OAE-2 sites.

Considering the C/T-boundary, the stable isotope signal suggests a later position in the section than the biotic signal. This is, however, if one considers other Tunisian sections mentioned above as comparable in this respect. The boundary definitions do differ but generally are placed between peak 3 and 4, in the upper *W. archaeocretacea* zone (Salmi-Laouar et al. 2018, Zagrarni et al. 2008, Falzoni et al. 2018 i.a.). This would point to a position somewhere between 13.00 and 20.00 m for the C/T boundary. However, further investigations are needed to narrow down this frame of uncertainty.

7.3.4 Indications for the Plenus Cold Event

Although not recorded in the faunal analysis of this section because of lack of microfossil content in the samples between 0.00 and 9.50, the carbon-isotope data of the present section shows a trough, resembling the P-CIE (Plenus Carbon Isotope Excursion) recorded in various European sections (Falzoni & Petrizzo 2021). The two $\delta^{13}C_{carb}$ troughs between peak 1 and 2 in the OK section (OK4.00 - 7.00 and OK 7.00 - 9.00) lie roughly in the expected timeframe of the PCE (see Petrizzo et al. 2021, Falzoni & Petrizzo, 2021) but are less distinct. Furthermore, as argued by Soua et al. (2022), the PCE records differ from Tunisian locations in the LAD of R. cushmani, which lies within the P-CIE in e.g. Eastbourne (UK), Clot Chevalier (FR) (Falzoni & Petrizzo, 2021), but lies below the first carbon-isotope peak

in Tunisian records, as is the case in the section of this study. Correlations with PCE-sites concerning the behavior of faunal changes within PF do not seem viable, as the patterns differ significantly from the one in the present section (e.g. delayed increase of abundance of *Dicarinella*), and is also partly impossible due to the mentioned fossil-barren intervals in the relevant part of the section. Connor et al. (2019) argued the PCE to be diachronous, and it may have occurred later in the lower latitudes of the Tethyan realm. Given the ambiguous signal in the OK section, and somewhat lack of data for PCE correlation, no certain conclusions can be made for the presence of the PCE here, as further studies are needed.

Table 3 *Phases of the OAE-2 along the Oued Kharroub section*

1	*-2.40 - 0.00*	relatively stable conditions in deeper water column, high numbers and diversity of keeled genera, low TOC, $\delta^{13}C_{carb}$ - increase, rare benthos, extinction of *Rotalipora* at the end of the phase
2	*0.00 - 9.50*	expansion of OMZ and extinction / eclipse of keeled genera, significant decrease in total microfossil numbers, proliferation of *Heterohelix*, radiolaria become a major component of micorfauna (1st radiolaria acme, chert occurrences), peak of environmental stress, eutrophia and anoxia in large parts of the water column, benthos disappears
3	*9.50 - 13.50*	highly stressed environment in the upper water collum, TOC peaks, $\delta^{13}C_{carb}$ peaks 2 & 3, slight return of larger keeled taxa (*Dicarinella*) possibly allowed by short upward reduction of OMZ, proliferation of *Whiteinella*, minimum microfossil content /g sediment, pyrite occurrences, minimal $CaCO_3$
4	*13.50 - 20.00*	further prevailing of stressed environment, keeled taxa strongly reduced in size and numbers, *Whiteinella* and *Heterohelix* dominate, TOC plateau with maximum at 18.60; rise of *Guembelitria*, overall stressed environment with slight relaxation concerning eutrophia, oxygen depletion in bottom waters precludes larger benthos but small opportunistic BF increase
5	*20.00 - 36.00*	partial stabilization of conditions, return of keeled taxa, also larger in sizes, but still percentually relatively low, 2nd radiolaria acme, further proliferation and increase in size of *Heterohelix*, *Guembelitria* acme at 36.00, *Whiteinella* remain dominant, environmental conditions prevent the proliferation of larger K-strategists, small infaunal BF acme at the section top

8. CONCLUSIONS

The investigations of the Oued Kharroub section in Tunisia have yielded valuable insights into developments and changes in microfaunal assemblages along the Oceanic Anoxic Event 2 in the Late Cretaceous. Three planktic foraminifera biozones have been established along a ~38m profile. The base of the section represents the uppermost Cenomanian *Rotalipora cushmani* zone (*Dicarinella algeriana* subzone) characterized by an equilibrium fauna expressed by a high diversity and abundance of keeled planktic foraminifera genera, e.g. the large *Rotalipora*. General ratios of planktic to benthic foraminifera, as well as the abundance of rotaliporids suggest a deep-water shelf facies far off the coast with moderately to well mixed, oxygenated waters. A sudden extinction of rotaliporids, together with the disappearance of *Clavihedbergella* and *Macroglobigerinelloides* as well as the beginning of a positive $\delta^{13}C_{carb}$ excursion with the first peak at 0.00 marks the onset of the OAE-2 and the upper boundary of the *R. cushmani* zone in this section. The following *W. archaeocretacea* zone spans over 20 meters and is characterized by microfossil assemblages reflecting a highly stressed ocean environment spanning from the deep to surface waters. The rise of the opportunistic biserial planktic foraminifera *Heterohelix*, termed "*Heterohelix* shift" is recorded for the better part of the section, as they do not decrease in diversity or numbers until the top of the section. A reversal of percentual abundance of the r-strategists, *Heterohelix* with respect to *Muricohedbergella,* takes place during beginning of the *Heterohelix* shift.

A somewhat ambiguous phase in the section assemblage is recorded in the middle of the *W. archaeocretacea* zone, where a Radiolaria acme and peak TOC content coincides with a low-diversity and low numbers of planktic foraminifera, of which large specimens of *Dicarinella* dominate. Above this part, a short but significant rise of large keeled species (mainly *D. imbricata* and *D. elata*) occurs, which may represent a slight relaxation of the stressed environmental conditions in the lower water-column, where these large keeled genera dwell. An upward movement of the OMZ, where the upper water-column is dominated by radiolaria and *Heterohelix* could explain these observations. A proliferation of the large surface dwelling *Whiteinella* as well as the aforementioned *Heterohelix*

characterizes the following meters of the section. This part of the section is deemed to represent slightly less-eutrophic conditions than the lower part of the *W. archaeocretacea* zone with radiolaria-rich- and chert-intervals, mainly on account of the predominant, large *Whiteinella*.

The FO of *Helvetoglobotruncana helvetica,* coincides with a return of keeled taxa such as *Dicarinella* and *Marginotruncana* as well as a second radiolaria acme, just above the last TOC peak of the OAE-2. It is slightly below this point, that the $\delta^{13}C_{carb}$ positive-exkursion-plateau ends. PF assemblage characteristics, however, suggest an ongoing environmental crisis, that precludes the proliferation of large *Marginotruncana,* contradicting the typical development of this zone. The results from the *W. archaeocretacea* zone containing a temporary return of keeled taxa including transitional forms of *H. praehelvetica-H. helvetica*, represents a new finding, possibly special to this section, that raises questions about the FO of *H. helvetica* as a reliable biomarker and its characterizing accompaniment of resurging keeled taxa as there are two such short events concerning keeled taxa. Furthermore, the occurrence of *D. elata* is not necessarily associated with the beginning of the *H. helvetica* zone, and may be linked to environmental variations, as suggested before in other OAE-2 studies. Four stable carbon isotope peaks could be correlated with other localities, and are deemed OAE-typical. The constraints concerning the identification of the C/T boundary are slightly ambiguous and require further study to narrow down the frame of uncertainty.

In conclusion, the OAE-2 event at Oued Kharroub shows a complex faunal development with temporary resurgences of large keeled planktic foraminifera. A continuously hypoxic environment, that favors surface dwelling planktics and r-strategists over deep dwelling K-strategists is characteristic for the section. A peak in environmental stress is recorded middle part of the *W. archaeocretacea* zone on account of geochemical data and planktic foraminifera assemblages. Minor developments in ocean chemistry however allowed paleoecological niches to be taken over by K-strategists, if only for short durations. The local basin morphology seems to have allowed the water column to repeatedly become oxygen deficient, conditions that prevailed until deposition of the uppermost sample of the Oued Kharroub section.

REFERENCES

Literature

ARTHUR, M. A., BRUMSACK, H. J., JENKYNS, H. C., & SCHLANGER, S. O. (1990). Stratigraphy, geochemistry, and paleoceanography of organic carbon-rich Cretaceous sequences. In *Cretaceous resources, events and rhythms* (pp. 75-119). Springer, Dordrecht.

BOLLI, H. M., SAUNDERS, J. B., & PERCH-NIELSEN, K. (Eds.). (1989). Plankton stratigraphy: volume 1, planktic foraminifera, calcareous nannofossils and calpionellids (Vol. 1). CUP Archive.

BEN FADHEL, M., AMRI, A., BEN YOUSEF, M., LAYEB, MOHSEN, SOUA M., & ZOUAGHI, T. (2012). *Radiolarian age constraints of Mid-Cretaceous black shales in northern Tunisia*. INTECH Open Access Publisher.

BOCCALETTI, M., CELLO, G., LENTINI, F., NICOLICH, R., & TORTOCICI, L. (1989). Structural evolution of the Pelagian block and eastern Tunisia.

BOUDHAGER-FADEL, M.K. (2015). Biostratigraphic and Geological Significance of Planktonic Foraminifera. (updated second edition) UCL Press, University College London.

CARON, M., DALL'AGNOLO, S., ACCARIE, H., BARRERA, E., KAUFFMANN, E. G., AMÉDRO, F., & ROBASZYNSKI, F. (2006). High-resolution stratigraphy of the Cenomanian–Turonian boundary interval at Pueblo (USA) and wadi Bahloul (Tunisia): stable isotope and bio-events correlation. *Geobios*, *39*(2), 171-200.

CARPENTER, W. B. (1862). Introduction to the Study of the Foraminifera: By William B. Carpenter, Assisted by William K. Parker and T. Rupert Jones. Publ. for the Ray Society (Vol. 22). Hardwicke.

COCCIONI, R. (1989). Stratigraphy and mineralogy of the Selli Level (Early Aptian) at the base of the Marne a Fucoidi in the Umbrian-Marchean Apennines (Italy). In *Cretaceous of the Western Tethys. 3^< rd> International Cretaceous Symposium* (pp. 563-584). Schweizerbart.

COCCIONI, R., & LUCIANI, V. (2004). Planktonic foraminifera and environmental changes across the Bonarelli Event (OAE2, latest Cenomanian) in its type area: a high-

resolution study from the Tethyan reference Bottaccione section (Gubbio, Central Italy). *The Journal of Foraminiferal Research*, *34*(2), 109-129.

COCCIONI, R., & LUCIANI, V. (2005). Planktonic foraminifers across the Bonarelli Event (OAE2, latest Cenomanian): the Italian record. *Palaeogeography, Palaeoclimatology, Palaeoecology*, *224*(1-3), 167-185.

FALZONI, F., PETRIZZO, M. R., CARON, M., LECKIE, R. M., & ELDERBAK, K. (2018). Age and synchronicity of planktonic foraminiferal bioevents across the Cenomanian–Turonian boundary interval (Late Cretaceous). *Newsletters on Stratigraphy*, *51*(3), 343-380.

FALZONI, F., & PETRIZZO, M. R. (2020). Patterns of planktonic foraminiferal extinctions and eclipses during Oceanic Anoxic Event 2 at Eastbourne (SE England) and other mid-low latitude locations. *Cretaceous Research*, *116*, 104593.

FALZONI, F., & PETRIZZO, M. R. (2022). Evidence for changes in sea-surface circulation patterns and~ 20° equatorward expansion of the Boreal bioprovince during a cold snap of Oceanic Anoxic Event 2 (Late Cretaceous). *Global and Planetary Change*, *208*, 103678.

GALE A.S., MUTTERLOSE J., BATENBURG, S., GRADSTEIN, F.M., AGTERBERG, F.P., OGG, J.G., PETRIZZO M.R. (2020). Chapter 27 - The Cretaceous Period, Editor(s): Felix M. Gradstein, James G. Ogg, Mark D. Schmitz, Gabi M. Ogg; Geologic Time Scale 2020, Elsevier, 2020, Pages 1023-1086

GEBHARDT, H., FRIEDRICH, O., SCHENK, B., FOX, L., HART, M., & WAGREICH, M. (2010). Paleoceanographic changes at the northern Tethyan margin during the Cenomanian–Turonian Oceanic Anoxic Event (OAE-2). *Marine Micropaleontology*, *77*(1-2), 25-45.

HAQ, B. U. (2014). Cretaceous eustasy revisited. *Global and Planetary change*, *113*, 44-58.

HAQ, B. U., & BOERSMA, A. (Eds.). (1998). Introduction to marine micropaleontology. Elsevier.

HART, M.B. (1999). The evolution and biodiversity of Cretaceous planktonic Foraminiferida,
Geobios, Volume 32, Issue 2, 1999, Pages 247-255, ISSN 0016-6995

JENKYNS, H. C., DICKINSON, A. J., RUHL, M., & VAN DEN BOORN, S. H. (2017). Basalt-seawater interaction, the Plenus Cold Event, enhanced weathering and geochemical

change: deconstructing Oceanic Anoxic Event 2 (Cenomanian–Turonian, Late Cretaceous). *Sedimentology*, *64*(1), 16-43.

JONES, R. W. (2014). Foraminifera and their Applications. Cambridge University Press.

KENNEDY, W. J., WALASZCZYK, I., & COBBAN, W. A. (2005). The global boundary stratotype section and point for the base of the Turonian stage of the Cretaceous: Pueblo, Colorado, USA. Episodes Journal of International Geoscience, 28(2), 93-104.

LÜNING, S., KOLONIC, S., BELHADJ, E. M., BELHADJ, Z., COTA, L., BARIC, G., & WAGNER, T. (2004). Integrated depositional model for the Cenomanian–Turonian organic-rich strata in North Africa. *Earth-Science Reviews*, *64*(1-2), 51-117.

MCGOWRAN, B. (2005). Biostratigraphy: microfossils and geological time (No. 551.7 MCG)

NEDERBRAGT, A. J., & FIORENTINO, A. (1999). Stratigraphy and palaeoceanography of the Cenomanian-Turonian boundary event in Oued Mellegue, north-western Tunisia. *Cretaceous Research*, *20*(1), 47-62.

O'CONNOR, L. K., JENKYNS, H. C., ROBINSON, S. A., REMMELZWAAL, S. R., BATENBURG, S. J., PARKINSON, I. J., & GALE, A. S. (2020). A re-evaluation of the Plenus Cold Event, and the links between CO2, temperature, and seawater chemistry during OAE 2. *Paleoceanography and Paleoclimatology*, *35*(4), e2019PA003631.

OHKOUCHI, N., KURODA, J., & TAIRA, A. (2015). The origin of Cretaceous black shales: a change in the surface ocean ecosystem and its triggers. *Proceedings of the Japan Academy, Series B*, *91*(7), 273-291.

PETRIZZO, M. R., WATKINS, D. K., MACLEOD, K. G., HASEGAWA, T., HUBER, B. T., BATENBURG, S. J., & KATO, T. (2021). Exploring the paleoceanographic changes registered by planktonic foraminifera across the Cenomanian-Turonian boundary interval and Oceanic Anoxic Event 2 at southern high latitudes in the Mentelle Basin (SE Indian Ocean). *Global and Planetary Change*, *206*, 103595.

PETRIZZO, M. R., AMAGLIO, G., WATKINS, D. K., MACLEOD, K. G., HUBER, B. T., HASEGAWA, T., & WOLFGRING, E. (2022). Biotic and paleoceanographic changes across the Late Cretaceous Oceanic Anoxic Event 2 in the southern high latitudes (IODP sites U1513 and U1516, SE Indian Ocean). Paleoceanography and Paleoclimatology, 37, e2022PA004474.

REOLID, M., SÁNCHEZ-QUIÑÓNEZ, C. A., ALEGRET, L., & MOLINA, E. (2015). Palaeoenvironmental turnover across the Cenomanian-Turonian transition in Oued

Bahloul, Tunisia: foraminifera and geochemical proxies. *Palaeogeography, Palaeoclimatology, Palaeoecology*, *417*, 491-510.

ROBASZYNSKI, F., & CARON, M. C. (1979). Atlas of mid-Cretaceous planktonic foraminifera (Boreal Sea and Tethys). *Cahiers de Micropaléontologie*, *1*, 1-185.

ROBASZYNSKI, F., ZAGRARNI, M. F., CARON, M., & AMÉDRO, F. (2010). The global bio-events at the Cenomanian-Turonian transition in the reduced Bahloul Formation of Bou Ghanem (central Tunisia). *Cretaceous Research*, *31*(1), 1-15.

SALMI-LAOUAR, S., FERRÉ, B., CHAABANE, K., LAOUAR, R., BOYCE, A. J., & FALLICK, A. E. (2018). The oceanic anoxic event 2 at Es Souabaa (Tebessa, NE Algeria): bio-events and stable isotope study. *Arabian Journal of Geosciences*, *11*(8), 1-18.

SCHLANGER S.O. & JENKYNS H.C. (1976). Cretaceous Anoxic Events: Causes and Consequences. Geologie en Mijnbouw, Volume 55 (3-4), p. 179-184.

SCHLANGER, S.O., ARTHUR, M.A., JENKYNS, H.C., SCHOLLE, P.A. (1987). The Cenomanian-Turonian oceanic anoxic event: I. Stratigraphy and distribution of organic-rich beds and the marine δ 13C excursion. In: Brooks J, Fleet AJ (eds) Marine and petroleum source rocks, vol 26. Geol Soc London spec Publ, Bath, pp 371–399

SCOPELLITI, G., BELLANCA, A., COCCIONI, R., LUCIANI, V., NERI, R., BAUDIN, F., CHIARI, M. & MARCUCCI, M. (2004). High-resolution geochemical and biotic records of the Tethyan 'Bonarelli Level'(OAE2, latest Cenomanian) from the Calabianca–Guidaloca composite section, northwestern Sicily, Italy. *Palaeogeography, Palaeoclimatology, Palaeoecology*, *208*(3-4), 293-317.

SOUA, M., ECHIHI, O., HERKAT, M., ZAGHBIB-TURKI, D., SMAOUI, J., JEMIA, H. F. B., & BELGHAJI, H. (2009). Structural context of the paleogeography of the Cenomanian-Turonian anoxic event in the eastern Atlas basins of the Maghreb. *Comptes Rendus Geoscience*, *341*(12), 1029-1037.

SOUA, M., EL ASMI, A. M., ZAGHBIB-TURKI, D. (2022): The Cenomanian-Turonian Boundary Event (CTBE) as recorded in the northern margin of Africa: palaeoceanography of the Oceanic Anoxic Event (OAE-2), North-Central Tunisia, International Geology Review.

SOUA, M., ZAGHBIB-TURKI, D., BEN JEMIA, H., SMAOUI, J., & BOUKADI, A. (2011). Geochemical Record of the Cenomanian-Turonian Anoxic Event in Tunisia: Is it Correlative and Isochronous to the Biotic Signal?. *Acta Geologica Sinica-English Edition*, *85*(6), 1310-1335.

SOUA, M. (2013). Siliceous and organic-rich sedimentation during the Cenomanian–Turonian Oceanic Anoxic Event (OAE2) on the northern margin of Africa: an evidence from the Bargou area, Tunisia. *Arabian Journal of Geosciences*, *6*(5), 1537-1557.

SOUA, M., El ASMI, A. M., & ZAGHBIB-TURKI, D. (2022). The Cenomanian–Turonian Boundary Event (CTBE) as recorded in the northern margin of Africa: palaeoceanography of the Oceanic Anoxic Event (OAE-2), North-Central Tunisia. *International Geology Review*, 1-23.

TAKASHIMA, R., NISHI, H., HAYASHI, K., OKADA, H., KAWAHATA, H., YAMANAKA, T., ... & MAMPUKU, M. (2009). Litho-, bio-and chemostratigraphy across the Cenomanian/Turonian boundary (OAE 2) in the Vocontian Basin of southeastern France. *Palaeogeography, Palaeoclimatology, Palaeoecology*, *273*(1-2), 61-74.

TOUIR, J., MECHI, C., & ALI, H. H. (2017). Changes in carbonate sedimentation and faunal assemblages in the Tunisian carbonate platform around the Cenomanian-Turonian boundary. *Journal of African Earth Sciences*, *129*, 527-541.

WIGNALL, P. (1994). Black shales. Oxford University Press, Oxford OX2 6DP.

ZAGRARNI, M. F., NEGRA, M. H., & HANINI, A. (2008). Cenomanian–Turonian facies and sequence stratigraphy, Bahloul formation, Tunisia. *Sedimentary Geology*, *204*(1-2), 18-35.

ZHANG, Z., FANG, N., GAO, L., GUI, B., & CUI, M. (2008). Cretaceous black shale and the oceanic red beds: Process and mechanisms of oceanic anoxic events and oxic environment. *Frontiers of Earth Science in China*, *2*(1), 41-48.

Internet

https://mikrotax.org

https://foraminifera.eu

https://stratigraphy.org

https://earth.google.com

https://scotese.com

APPENDIX

Table A Counted Planktic Foraminifera in the 1000 - 125 µm fraction

Sample	PLANKTIC FORAMINIFERA																																										
	Guembelitria cenomana	*Heterohelix spp.*	*Pseudoguembelina costellifera*	*Macroglobigerinelloides spp.*	*Mg. bentonensis*	*Clavihedbergella spp.*	*Muricohedbergella spp.*	*Mh. kyphoma*	*Mh. Hoelzli*	*Praeglobotruncana spp.*	*P. delrioensis*	*P. hilalensis*	*P. gibba*	*P. stephani*	*Hv. helvetica*	*Hv. Praehelvetica*	*Whiteinella spp.*	*W. aprica*	*W. archaeocretacea*	*W. aumalensis*	*W. baltica*	*W. brittonensis*	*W. inornata*	*W. paradubia*	*Rotalipora spp.*	*R. cushmani*	*R. deeckei*	*R. greenhornensis*	*R. globotruncanoides*	*R. micheli*	*Anaticinella planoconvexa*	*Dicarinella spp.*	*D. algeriana*	*D. elata*	*D. aff. elata*	*D. hagni*	*D. imbricata*	*D. aff. Imbricata*	*Marginotruncana spp.*	*M. marginata*	*M. renzi*	*Loeblichella hessi*	*Schackoina spp.*	*S. multispinata*	*P. Foram indet.*
36.00	19	144	1	1	0	0	57	1	2	2	0	2	0	0	0	8	35	0	0	0	3	0	0	2	0	0	0	0	0	0	0	3	0	0	0	0	0	0	6	0	1	0	0	0	13
20.00	0	151	0	0	0	1	28	0	0	3	0	2	0	0	5	1	37	13	6	0	19	8	3	0	0	0	0	0	0	0	0	12	0	0	0	2	2	0	3	2	0	0	3	2	0
18.60	0	268	0	1	0	3	42	0	2	0	0	2	0	5	0	8	51	9	0	0	8	9	3	1	0	0	0	0	0	0	0	4	0	0	0	0	0	0	1	0	0	0	0	0	0
16.00	0	225	0	0	0	3	66	0	0	3	0	1	0	0	0	14	24	8	8	6	3	18	0	1	0	0	0	0	0	0	0	3	0	0	0	0	2	0	1	0	0	0	0	1	0
15.00	0	192	0	0	0	0	86	1	0	1	0	0	0	0	0	7	33	6	7	1	14	10	2	7	0	0	0	0	0	0	0	1	0	0	0	1	0	0	0	0	0	0	0	0	1
13.50	0	200	0	0	0	0	61	0	0	9	0	0	1	18	0	11	50	1	3	1	7	11	3	3	0	0	0	0	0	0	0	18	0	1	0	2	4	0	0	1	0	0	1	0	0
11.70	0	154	0	0	1	0	27	0	0	1	0	0	0	1	0	21	41	2	5	1	9	2	7	0	0	0	0	0	0	0	0	34	0	6	3	6	4	0	3	0	0	0	0	0	0
9.50	0	43	0	1	0	0	26	0	0	13	4	0	3	9	0	18	21	1	3	0	0	2	1	0	0	0	0	0	0	0	0	43	0	0	0	3	7	28	0	0	0	0	0	0	0
0.00	0	25	0	0	0	69	114	0	0	7	0	0	0	0	0	2	39	3	9	0	6	2	7	0	0	0	0	0	0	0	1	2	2	0	0	0	5	0	0	0	0	9	0	0	20
-0.70	0	34	0	33	33	54	126	0	0	1	7	0	1	10	0	0	12	5	0	0	6	0	0	1	10	3	0	33	1	1	2	0	2	0	0	1	1	0	0	0	0	0	0	0	0
-1.50	0	31	0	74	55	82	169	0	0	42	22	0	17	43	0	0	1	0	0	0	0	0	0	0	19	9	0	33	1	0	1	0	17	0	0	0	8	0	0	0	0	0	0	0	0
-2.40	0	9	0	23	13	47	90	0	0	27	24	0	5	19	0	0	4	0	0	0	2	0	0	0	19	4	3	58	8	0	0	0	13	0	0	0	5	0	0	0	0	0	0	0	0

Table B Counted Planktic Foraminifera in the 125 - 63 µm fraction

Sample	PLANKTIC FORAMINIFERA																																											
	Guembelitria cenomana	*Heterohelix spp.*	*Pseudoguembeline costellifera*	*Macroglobigerinelloides spp.*	*Mg. bentonensis*	*Clavihedbergella spp.*	*Muricohedbergella spp.*	*Mh. kyphoma*	*Mh. Hoelzli*	*Praeglobotruncana spp.*	*P. delrioensis*	*P. hilalensis*	*P. gibba*	*P. stephani*	*Hv. helvetica*	*Hv. Praehelvetica*	*Whiteinella spp.*	*W. aprica*	*W. archaeocretacea*	*W. aumalensis*	*W. baltica*	*W. brittonensis*	*W. inornata*	*W. paradubia*	*Rotalipora spp.*	*R. cushmani*	*R. deeckei*	*R. greenhornensis*	*R. globotruncanoides*	*R. micheli*	*Anaticinella planoconvexa*	*Dicarinella spp.*	*D. algeriana*	*D. elata*	*D. aff. elata*	*D. hagni*	*D. imbricata*	*Marginotruncana spp.*	*M. marginata*	*M. renzi*	*Loeblichella hessi*	*Schackoina spp.*	*S. multispinata*	P. Foram indet.
36.00	25	78	0	0	0	1	11	0	0	0	0	0	0	0	0	0	0	0	0	0	0	0	0	0	0	0	0	0	0	0	0	0	0	0	0	0	0	0	0	1	0	13
20.30	3	73	0	0	0	0	21	0	0	0	0	0	0	0	0	0	0	0	0	0	0	0	0	0	0	0	0	0	0	0	0	0	0	0	0	0	0	0	0	2	0	6
18.60	11	76	0	0	0	0	20	0	0	0	0	0	0	0	0	0	0	0	0	0	0	0	0	0	0	0	0	0	0	0	0	0	0	0	0	0	0	0	0	0	0	8
16.00	10	96	0	0	0	1	37	0	0	0	0	0	0	0	0	0	0	0	0	0	0	0	0	0	0	0	0	0	0	0	0	0	0	0	0	0	0	0	0	0	4	4
15.00	0	113	0	0	0	4	19	0	0	1	0	0	0	0	0	0	0	0	0	0	0	0	0	0	0	0	0	0	0	0	0	0	0	0	0	0	0	0	0	2	0	0
13.50	4	219	0	0	0	0	26	0	0	0	0	0	0	0	0	0	2	0	0	0	0	0	0	0	0	0	0	0	0	0	1	0	0	0	0	0	0	0	0	2	0	0
11.70	8	134	0	0	0	0	33	0	0	0	0	0	0	0	0	0	0	0	0	0	0	0	0	0	0	0	0	0	0	0	0	0	0	0	0	0	0	0	0	2	0	19
9.50	1	200	0	0	0	0	0	0	0	0	0	0	0	0	0	0	0	0	0	0	0	0	0	0	0	0	0	0	0	0	0	0	0	0	0	0	0	0	0	0	0	15
0.00	0	75	0	1	0	6	46	0	0	0	0	0	0	0	0	0	0	0	0	0	0	0	0	0	0	0	0	0	0	0	0	0	0	0	0	0	0	0	0	0	0	22
-0.70	0	97	0	9	0	16	83	0	0	0	0	0	0	0	0	0	3	0	0	0	0	0	0	0	1	0	0	0	0	0	0	0	0	0	0	0	0	0	0	1	0	14
-1.50	0	47	0	8	0	3	103	0	0	0	0	0	0	0	0	0	2	0	0	0	0	0	0	0	3	0	0	0	0	0	0	0	0	0	0	0	0	0	0	1	0	18
-2.40	0	36	0	5	0	0	72	0	0	0	0	0	0	0	0	0	0	0	0	0	0	0	0	0	0	0	1	0	0	0	0	0	0	0	0	0	0	0	0	0	0	5

Table D Counted microfossils,
1000 – 125 µm fraction

Sample	Total microfossil count	Planktic Foraminifera	Radolaria	Benthic Foraminifera	Ostracoda
OK 36.00	301	300	0	*1*	0
OK 20.30	373	303	68	*2*	0
OK 18.60	321	317	3	*1*	0
OK 16.00	401	387	9	*6*	0
OK 15.00	370	370	0	*0*	0
OK 13.50	411	406	0	*3*	2
OK 11.70	332	328	2	*2*	0
OK 9.50	370	226	144	*0*	0
OK 0.00	329	322	0	*7*	0
OK -0.70	378	377	0	*1*	0
OK -1.50	653	624	0	*29*	0
OK -2.40	376	373	0	*3*	0

Table C Counted microfossils,
125 – 63 µm fraction

Sample	Total microfossil count	Planktic Foraminifera	Radiolaria	Benthic Foraminifera	Ostracoda
OK 36.00	158	129	0	29	0
OK 20.30	141	105	10	26	0
OK 18.60	134	115	0	19	0
OK 16.00	170	152	1	17	0
OK 15.00	153	139	0	14	0
OK 13.50	278	254	2	22	0
OK 11.70	204	196	4	4	0
OK 9.50	323	216	104	0	0
OK 0.00	153	150	0	0	0
OK -0.70	227	224	0	4	0
OK -1.50	188	185	1	4	0
OK -2.40	120	119	1	0	0

Table E Samples, Splitting & Counting

	Sample Weight [g]					Fraction [%]		Subsample Fraction		Subsample Weight [g]		Tray Split		Fraction Counted [g]	
Sample	total	>1mm	corrected[3]	>125	>63	>125	>63	>125µm	>63µm	>125µm	>63µm	>125µm	>63µm	>125µm	>63µm
OK -2.40	37,86	0,01	37,85	0,703	2,643	1,86%	6,98%	1/2	0,25	0,3515	0,6608	3/4*1/45	1/8*1/25*1/5	0,0059	0,00066
OK -1.50	40,32	0	40,32	1,81	3,774	4,49%	9,36%	1/2	0,13	0,9050	0,4718	1/2*1/45	1/8*1/25*1/5	0,0101	0,00047
OK -0.70	43,65	0	43,65	1,184	1,958	2,71%	4,49%	1/4	0,25	0,2960	0,4895	3/4*1/45	1/8*1/25*1/5	0,0049	0,00049
OK 0.00	36,50	0	36,50	2,051	3,811	5,62%	10,44%	1/8	0,13	0,2564	0,4764	3/4*1/45	1/8*1/30*1/5	0,0043	0,00040
OK 9.50	64,99	0	64,99	0,1	0,408	0,15%	0,63%	1	1,00	0,1000	0,4080	4*1/30	1/2*1/30*1/9	0,0133	0,00076
OK 11.70	36,15	7,686	28,46	1,171	0,572	4,11%	2,01%	1/2	1,00	0,5855	0,5720	4*1/45	1*1/30*1/9	0,0098	0,00064
OK 13.50	41,28	0,223	41,06	0,44	0,471	1,07%	1,15%	1	1,00	0,4400	0,4710	3/4*1/45	1/2*1/30*3/45	0,0073	0,00052
OK 15.00	30,78	0,064	30,72	0,55	0,807	1,79%	2,63%	1/2	0,50	0,2750	0,4035	3/4*1/45	1/2*1/30*1/9	0,0046	0,00075
OK 16.00	39,77	0	39,77	0,312	0,335	0,78%	0,84%	1	1,00	0,3120	0,3350	3/4*1/45	1/2*1/30*3/45	0,0052	0,00037
OK 18.60	51,46	4,301	47,16	1,614	2,74	3,42%	5,81%	1/4	0,13	0,4035	0,3425	4*1/45	1/15*1/9	0,0067	0,00038
OK 20.30	42,31	0,036	42,27	0,314	0,565	0,74%	1,34%	1	0,50	0,3140	0,2825	3/4*1/45	1/4*1/30*3/45	0,0052	0,00016
OK 36.00	43,59	0,086	43,50	3,086	4,326	7,09%	9,94%	1/8	0,06	0,3858	0,2704	1/3*1/9	1/15*1/9	0,0143	0,00200

Table F Counted specimens & numbers per gram sediment

	PLANKTIC FORAMINIFERA				BENTHIC FORAMINIFERA				RADIOLARIA			
	# counted		# per gram sediment		# counted		# per gram sediment		# counted		# per gram sediment	
	>125µm	>63µm	>125µm	>63µm	>125µm	>63µm	>125µm	>63µm	>125µm	>63µm	>125µm	>63µm
OK -2.40	373	114	1183	12047	3	0	10	0	0	1	0	106
OK -1.50	624	165	2786	32742	29	4	129	794	0	1	0	198
OK -0.70	377	209	2073	19154	0	4	5	367	0	0	0	0
OK 0.00	322	131	4235	34459	7	0	92	0	0	0	0	0
OK 9.50	226	201	26	1670	0	0	0	0	144	104	17	864
OK 11.70	328	177	1383	5597	2	4	8	126	2	4	8	126
OK 13.50	406	254	593	5568	3	22	4	482	0	2	0	44
OK 15.00	370	139	1445	4887	0	14	0	492	0	0	0	0
OK 16.00	387	148	582	3349	6	17	9	385	9	1	14	23
OK 18.60	317	107	1613	16335	1	19	5	2 901	3	0	15	0
OK 20.30	303	99	430	8431	2	26	3	2 214	68	10	97	852
OK 36.00	300	115	1490	5710	1	29	5	1 440	0	0	0	0

[3] Corrected values represent total sample weight minus the > 1mm sieve fraction, which only constitutes undissolved clumps of sediment.

Table G $CaCO_3$, TOC & Stable Isotope data

Sample	Section*m	CaCO3[%]	TOC %	δ13C (VPDB)
OK -2.40	-2,40	57,4	0,502	3,36
OK -2	-2,00	77,2	0,227	3,98
OK -1.5	-1,00	77,5	0,301	
OK -1.00		74,4	0,281	3,66
OK -0.70	-0,70	64,2	0,739	3,23
OK -0.05	-0,05	61,6	0,045	4,59
OK 0.00	0,00	66,0	0,063	4,81
OK 0.50	0,50		0,115	4,12
OK 0.80	0,80	57,5	0,140	4,30
	1,50			3,75
OK 1.80	1,80	49,2	0,153	4,19
OK 3.00	3,00	58,0	0,194	3,78
OK 4.00	4,00	55,9	0,133	4,07
OK 5.00	5,00	61,6	0,504	3,59
OK 6.00	6,00	69,5	0,106	3,26
OK 7.00	7,00	19,4	0,087	2,97
OK 7.55	7,55	52,3	0,099	4,02
OK 8.00	8,00	36,7	0,115	3,23
OK 9.00	9,00	67,2	0,122	2,47
OK 9.50	9,50	51,5	2,059	3,90
OK 10.00	10,00	49,2	0,124	4,36
OK 10.40	10,40	31,5	0,081	2,65
OK 11.00	11,00	69,7	0,131	3,12
OK 11.70	11,70	59,7	1,968	4,24
OK 12.00	12,00	77,4	0,205	4,62
OK 13.00	13,00	71,3	0,086	4,41
OK 13.50	13,50	66,5	1,630	4,17
OK 14.00	14,00	71,7	0,875	4,43
OK 15.00	15,00	74,6	1,989	4,15
OK 16.00	16,00	69,8	1,544	3,81
OK 17.00	17,00	76,7	0,174	3,10
OK 18.00	18,00	72,1	2,585	3,32
OK 18.6	18,60	75,4	2,485	3,42
OK 19.00	19,00	77,0	2,059	3,30
OK 20	20,00	72,9	1,537	3,36
OK 21.00	21,00	82,2	0,110	2,95
OK 22.00	22,00	76,7	0,194	2,76
OK 23	23,00	75,6	0,201	3,55
OK 24.00	24,00	79,8	0,150	2,77
OK 25.00	25,00	73,3	0,320	1,90
OK 26.00	26,00	76,6	0,173	2,16
OK 27.00	27,00	75,9	1,278	2,02
OK 28.00	28,00	72,5	3,059	1,78
OK 29.00	29,00	80,4	0,725	1,44
OK 30.00	30,00	87,4	0,172	0,85
OK 31.00	31,00	81,5	1,894	1,46
OK 32.00	32,00	79,5	0,629	1,65
OK 32.Y		92,8		
OK 34.00	34,00	78,2	1,351	1,48
OK 35.00	35,00	79,6	1,327	1,48
OK 36.00	36,00	81,1	0,704	1,34
OK 37.00	37,00	75,2	1,272	1,41
OK 37.80	37,80	83,6	0,230	2,69
OK 39.00	39,00	74,4	1,699	1,44

Taxonomic List

Taxonomic list of all species found in the samples and included in this work. Classified, as well as presumed species included in a Genus that have not been classified further than to the genus-niveau, are mentioned. If Genus + spp. is not mentioned, it includes the listed species.

Class

Foraminifera Lee 1990

Order

Globogerinida Lancaster, 1885

Superfamily

Globigerinoidea Carpenter, Parker and Jones, 1862

Family

Hedbergellidae Loeblich and Tappan, 1961

Genus

Clavihedbergella Banner and Blow, 1959

- *Clavihedbergella* spp.: includes *C. amabilis* (Loeblich & Tappan, 1961); *C. simplex*[4] (Morrow, 1934); and possibly *C. simplicissima* (Magne & Sigal, 1954)

Muricohedbergella Huber and Leckie 2011

- *Muricohedbergella* spp[5].: includes *Mh. delrioensis (*Carsey, 1926); *Mh. planspira* (Tappan, 1940); *Mh.* sp.; *Mh. flandrini* (Porthault 1970)
- *Muricohedbergella hoelzli* (Hagn & Zeil, 1954)
- *Muricohedbergella kyphoma* (Hasegawa, 1999)
- *Muricohedbergella flandrini* (Porthault, 1970)

Loeblichella Pessagno, 1967

- *Loeblichella hessi* (Pessagno, 1962)

Whiteinella Pessagno, 1967

- *Whiteinella aprica* (Loeblich & Tappan, 1961)

[4] Here, the classification scheme used deviates from Premoli-Silva & Verga (2004), as this species is there ascribed to Muricohedbergella (Muricohedbergella simplex).

[5] This genus not only includes the named species as represented in Premoli-Silva & Verga (2004), but also a variety of morphotypes and possibly other species of the genus, which are summarized in the mikrotax.org database under the genus *Muricohedbergella*.

- *Whiteinella archaeocretacea* Pessagno, 1967
- *Whiteinella aumalensis* (Sigal, 1952)
- *Whiteinella baltica* Douglas & Rankin, 1969
- *Whiteinella brittonensis* (Loeblich & Tappan, 1961)
- *Whiteinella inornata* (Bolli, 1957)
- *Whiteinella paradubia* (Sigal, 1952)

Rotaliporidae Sigal, 1958

Anaticinella Eicher, 1973

- *Anaticinella planoconvexa* (Longoria, 1973)

Rotalipora[6] Brotzen 1942

- *Rotalipora cushmani* (Morrow, 1934)
- *Rotalipora deeckei* (Franke, 1925)
- *Rotalipora globotruncanoides* Sigal 1948
- *Rotalipora greenhornensis* (Morrow, 1934)
- *Rotalipora micheli* (Sacal & Debourle, 1957)

Globotruncanellidae Maslakovae, 1964

Dicarinella Porthault 1970

- *Dicarinella algeriana*[7] (Caron, 1966)
- *Dicarinella elata*[8] Lamolda, 1977
- *Dicarinella hagni* (Scheibnerova, 1962)
- *Dicarinella imbricata* (Mornod, 1950)

Helvetoglobotruncana Reiss 1957

- *Helvetoglobotruncana helvetica* Bolli, 1945
- *Helvetoglobotruncana praehelvetica*[9] Trujillo, 1960

Praeglobotruncana Bermudez 1952

- *Praeglobotruncana delrioensis* Plummer, 1931
- *Praeglobotruncana gibba* Klaus, 1960
- *Praeglobotruncana hilalensis* Barr, 1972

---

[6] *R. deeckei*, *R. globotruncanoides* and *R. greenhornensis* are classified under the genus *Thalmanninella* Sigal, 1948 in recent publications (see mikrotax.org). The present classification scheme of the Rotalipora is adopted from Premoli Silva & Verga (2004).

[7] Synonym: *Praeglobotruncana algeriana* (Caron, 1966) Falzioni et al., 2016 (Mikrotax.org)

[8] Synonym: *Dicarinella marianosi* (former *Marginotruncana marianosi*); two different morphotypes of this species have been recorded here. One resembling the D. elata in Premoli-Silva & Verga (2004) and one resembling D. marianosi (Mikrotax.org).

[9] This classification of *H. praehelvetica* is according to mikrotax.org. Synonym: *Whiteinella praehelvetica* (Trujillo, 1960) (e.g. Premoli Silva & Verga 2004)

- *Praeglobotruncana stephani* Gandolfi, 1942

Globotruncanidae Brotzen, 1942

Marginotruncana Hofker 1956

- *Marginotruncana* spp.:
- *Marginotruncana marginata* (Reuss 1845)
- *Marginotruncana Renzi* (Gandolfi, 1942)
- *Marginotruncana schneegansi* (Sigal, 1952)

Planomalinoidea Bolli, Loeblich and Tappan, 1957

Schackoinidae Pokórny, 1958

Schackoina Thalmann 1932

- *Schackoina* spp.: includes *S. bicornis* Reichel, 1948; *S. cenomana* (Schacko 1897); *S. multispinata* (Cushman & Wickenden 1930)

Macroglobigerinelloides Verga & Premoli Silva (2004)

- *Macroglobigerinelloides spp.: Macroglobigerinelloides bentonensis* (Morrow, 1934)

Heterohelicida Fursenko, 1958

Heterhohelicoidea Cushman, 1927

Guembelitriidae Montanaro Gallitelli, 1957

Guembelitria Cushman 1940

- *Guembelitria cenomana* Keller, 1935

Heterohelicidae Cushman 1927

Heterohelix[10] Ehrenberg 1843

- *Heterohelix* spp.: includes *H. moremani* (Cushman, 1938), *H. reussi* (Cushman, 1938) and *H. globulosa* (Cushman, 1938).

Pseudoguembelina Broennimann & Brown, 1953

- Pseudoguembelina costellifera Masters, 1976

[10] The genus *Heterohelix* is here used according to Premoli Silva & Verga, 2004. All species of the genus *Heterohelix* here are classified under the genus *Planoheterohelix* (see Mikrotax.org)

Figure Index

Table Index